12-14-2021 9:00 AM

Investigating The Role Of PKC And Its Mechanisms In Regulation Of IGF-I Bioavailability In Fetal Growth Restriction

Allan W. Chen, *The University of Western Ontario*

Supervisor: Gupta, Madhulika B, *Children's Health Research Institute*

A thesis submitted in partial fulfillment of the requirements for the Master of Science degree in Biochemistry

Abstract

Fetal growth restriction (FGR) is associated with decreased nutrient availability and reduced insulin-like growth factor (IGF)-I bioavailability via increased IGF binding protein (IGFBP)-1 phosphorylation. While protein kinase C (PKC) is implicated in IGFBP-1 hyperphosphorylation in nutrient deprivation, the mechanisms remain unclear. I hypothesized that the interaction of PKCα with protein kinase CK2β and activation of PKCα under leucine deprivation (L0) mediate fetal hepatic IGFBP-1 hyperphosphorylation. Parallel Reaction Monitoring Mass Spectrometry (PRM-MS) followed by PKCα knockdown demonstrated the PKCα isoform interacts with IGFBP-1 and CK2β under L0. Pharmacological PKCα activation with phorbol 12-myristate 13-acetate (PMA) increased whereas inhibition with bisindolylmaleimide II (Bis II) decreased IGFBP-1 phosphorylation (Ser101/119/169, Ser98+101 and Ser169+174), respectively. Furthermore, PMA mimicked L0-induced PKCα translocation and IGFBP-1 expression. PKCα expression was increased in baboon fetal liver in FGR, providing biological relevance *in vivo*. In summary, I report a novel nutrient-sensitive mechanism for PKCα in mediating IGFBP-1 hyperphosphorylation in FGR.

A version of this thesis has been accepted for publication with permission for reproduction requested from Elsevier.

Chen, A.W., Biggar, K., Nygard, K., Singal, S.S., Zhao, T., Li, C., Nathanielsz, P.W., Jansson, T., Gupta M.B., (2021) IGFBP-1 hyperphosphorylation in response to nutrient deprivation is mediated by activation of protein kinase Cα (PKCα). *Mol Cell Endo*, 536, 111400. https://doi.org/10.1016/j.mce.2021.111400.

Keywords

Placental Insufficiency, Protein Interaction, Protein Kinase CK2, HepG2 cells, Baboon

Summary for Lay Audience

Fetal growth restriction (FGR) affects approximately 5-10% of all pregnancies and occurs when the fetus fails to reach its growth potential in the uterus. The most common cause of FGR is placental insufficiency, a pathological condition where the placenta fails to adequately supply oxygen and nutrients to the developing fetus. FGR is the second most common cause of perinatal mortality and is responsible for 30% of stillbirths. Additionally, FGR may negatively affect physical and neurological development of the infant resulting in increased risk of metabolic, cardiac and neurological disorders which may not resolve in adulthood.

Fetal growth is primarily mediated by fetal liver secreted insulin-like growth factor I (IGF-I), a peptide hormone which is bound by insulin-like growth factor binding proteins (IGFBPs) which extends the half-life of IGF-I in circulation and mediates its functions. IGFBP-1 is additionally secreted by the fetal liver and is predominantly expressed during pregnancy where it serves its primary role of binding to and inhibiting IGF-I regulated fetal growth. Phosphorylation of IGFBP-1 increases its binding affinity for IGF-I resulting in greater inhibition of IGF-I mediated actions. In FGR, IGFBP-1 phosphorylation is increased and IGF-I bioavailability is reduced which are associated with decreased fetal nutrient provision. We have previously utilized the hepatoblastoma derived HepG2 cell line deprived of leucine as a model for the nutritionally deprived fetal liver to induce IGFBP-1 phosphorylation. However, the roles of the kinases which mediate the phosphorylation of IGFBP-1 in this model have not yet been elucidated.

In this study, we hypothesized that leucine deprivation (L0) activates protein kinase C (PKC) in a nutrient sensitive manner and induces its interaction with the putative IGFBP-1 kinase, protein kinase CK2 which results in increased IGFBP-1 phosphorylation. I found that PKC interacts with IGFBP-1 and CK2 in L0 and that PKC is activated in L0. Additionally, I demonstrate that PKC mediates IGFBP-1 phosphorylation in L0. To establish translational relevance, I further demonstrated global maternal nutrient restriction induces PKC expression within the fetal liver which is associated with increased IGFBP-1 phosphorylation.

Co-Authorship Statement

All chapters and figures were primarily prepared by me, Allan W. Chen and reviewed by Dr. Madhulika B Gupta. Dr. Kyle Biggar of the Institute of Biochemistry at Carleton University performed mass spectrometry experiments (Chapter 3, Section 3.1 and 3.4). Baboon samples were obtained from the Southwest National Primate Research Center (in collaboration with Dr. Peter W. Nathanielsz, Texas Biomedical Research Institute) (Chapter 3, Section 3.7). Karen Nygard of Biotron Integrated Microscopy, University of Western Ontario, was consulted in immunohistochemistry, dual immunofluorescence and proximity ligation assay image acquisition and automated quantification processes of microscopy images (Chapter 3, Section 3.3, 3.5 and 3.7). Bhawani Jain performed immunohistochemistry straining (Chapter 3, Section 3.7).

Acknowledgments

I would like to being my acknowledgements and gratitude regarding the completion of this thesis to my supervisor, Dr. Madhulika B. Gupta specifically for her direction, encouragement, and patience over the course of my MSc project. We had shared a plethora of productive discourse which led to the direction and completion of this project.

Next, I extend my gratitude to the members of the Gupta lab during my time there. To Pinki, Jenica, Chloe, Violet and Tiffany – thank you all for the companionship and special times we shared together at the bench, desk, and lunchroom. Those will always be cherished memories!

Furthermore, thank you to my advisory committee, Drs. Eric Ball and Michael Boffa for their constructive criticism and support which led to substantiating my work and pushing me to create a better project overall. I further extend my gratitude to the Department of Paediatrics for their financial support and the Children's Health Research Institute (CHRI) for their administrative support. Additionally, thank you to all other scientists and trainees at CHRI for their company and well meaning during my time at CHRI.

Lastly, I extend the greatest of gratitude towards my support system both back home and in London. Thank you mom and dad for your continued support, encouragement, and love. To Cathy, thank you for always standing by my side during the entirety of my MSc and always supporting me no matter the circumstance, I love you!

Table of Contents

List of Tables

List of Figures

List of Abbreviations

AAR	amino acid response
AGA	average for gestational age
aPKC	atypical type protein kinase C
ATF4	activating transcription factor 4
BCAA	branched chain amino acids
BM	basal membrane
Bis II	bisindolylmaleimide II
CK2	protein kinase CK2
CM	cell media
cPKC	conventional protein kinase C
DAG	diacylglycerol
eiF2α	eukaryotic initiation factor 2 alpha
ERK	extracellular signal regulated kinase
FGR	fetal growth restriction
GCN2	general control nonderepressible 2
GD	gestational date
GH	growth hormone
IF	immunofluorescence
IGF	insulin-like growth factor

IGF-1R	type 1 insulin-like growth factor receptor
IGFBP	insulin-like growth factor binding protein
IHC	immunohistochemistry
IP	immunoprecipitation
IR	insulin receptor
IUGR	intrauterine growth restriction
L0	leucine deprivation (0 μM leucine)
L450	leucine supplementation (450 μM leucine)
MEK	mitogen activated protein kinase kinase
MNR	maternal nutrient restriction
mTOR	mechanistic target of rapamycin
MVM	microvillous membrane
nPKC	novel protein kinase c
PDK1	phosphoinositide-dependent kinase-1
PKA	protein kinase A
PKC	protein kinase C
PKG	protein kinase G
PKM	protein kinase M
PLA	proximity ligation assay
PMA	phorbol 12-myristate 13-acetate

PP2A	protein phosphatase 2A
RKIP	Raf kinase inhibitory protein
ROI	region of interest
Raf	rapidly accelerated fibrosarcoma
SGA	small for gestational age
TBB	4,5,6,7-tetrabromobenzotriazole

1 Background Information

1.1 Fetal Growth Restriction

Fetal Growth Restriction (FGR) also known as Intrauterine Growth Restriction (IUGR) has been described as a reduction of fetal growth from its expected biological potential, however, this description often converges with small for gestational age (SGA) fetuses as both are habitually defined with estimated fetal weight below the 10th percentile for gestational age [1]. This definition, however, does not discern between pathological FGR or healthy constitutionally small fetuses and distinguishing these processes is difficult. Epidemiological studies demonstrated a decline in neonatal deaths and newborn morbidities with increasing gestational age, suggestive that SGA babies delivered at appropriate term are likely to be constitutionally small and not pathologically FGR[2]. FGR demonstrates an increased risk for adverse pre- and postnatal events, including adult morbidities including metabolic and cardiac disorders [1,3,4]. FGR is a pathological consequence of maternal, fetal, and/or placental factors contributing to the restricted growth potential of an individual and as of yet, no succinct definition exists. The etiology of FGR is expansive and complicated with risk factors encompassing but not limited to fetal genetics [5], perinatal infection [6,7], interventional therapeutics [8], environmental pollution [9,10] and maternal health [11,12]. FGR affects 5-10% of all pregnancies and is associated with higher rates of neonatal mortality and morbidities [13,14]. Currently, FGR screening methods are lacking. Prenatal detection of FGR is difficult and is primarily based on maternal risk factors and clinical assessments of maternal features (e.g. serum biochemistry and uterine artery blood flow) in conjunction with sonographic screening of the fetus [15].

1.1.1 Regulation of Fetal Growth

Fetal growth is a complex and dynamic process regulated by various maternal, placental and fetal factors of both genetic and environmental origin in multidirectional interactions. The placenta is the site of exchange between mother and fetus and regulates fetal growth via growth-regulating hormones such as the insulin-like growth factors

(IGFs). Fetal provision can be regulated by fetal and placental endocrine signals to increase transport of maternal nutrients by growth of the placenta and activation of transport systems. Poor fetal growth is inundated with consequences both in prenatal and postnatal life in the form of increased mortality and morbidity.

1.1.2 Maternal and Placental Contributions in Fetal Growth

Primary maternal contributions to fetal growth encompass maternal genetics, the uterine environment and maternal nutritional intake [12]. Maternal uterine capacity is a key determinant of fetal size and is correlated with genetic maternal height and represents a potential capacity for fetal growth [16]. Furthermore, uterine blood flow must meet metabolic demands of the growing uterus, placenta, and fetus [17]. Over the course of pregnancy, total maternal blood volume [18] and cardiac output increases by ~40% [19] while uterine artery flow rate increases >3-fold [17].

1.1.2.1 Maternal Nutrient Intake and Fetal Growth

Effects on the placenta

The placenta is composed of both maternal and fetal tissues and serves as the site of exchange between mother and fetus and is a metabolically active organ sustained by uterine circulation, of which, the placenta extracts 40-60% of total glucose and oxygen [20]. Nutrient transfer between placenta and fetus occurs via passive diffusion, facilitated diffusion, active transport, endocytosis and exocytosis [12]. As fetal growth rate increases over the course of gestation, placental growth and fetoplacental transfer also increase to meet increasing fetal nutritional demands [21,22]. Maternal undernutrition results in reduction of placental weight and reduced placental function [23–25]. Nutritional deprivation that results in human FGR is associated with decreased vasculogenesis, angiogenesis and generates deficient placentas with reduced surface area for nutrient exchange [26–28]. Causative FGR factors resultant of maternal nutrient deficiency include downregulated placental nutrient transport prior to the onset of FGR [29,30].

Effects on the fetus

Maternal nutrient intake is a significant factor in normal fetal growth. During the second and third trimesters, increased caloric intake is necessary to accommodate fetoplacental growth [31]. Low protein intake during late pregnancy is correlated to reduced birth weight [32]. Furthermore, a Cochrane systematic review found that balanced protein-energy supplementation resulted in a 30% reduced risk of SGA neonates [33]. Overall, an assessment of complete maternal dietary intake (total energy, protein and carbohydrate) indicated that protein intake is positively correlated with birth weight and ponderal index (an assessment of birth weight and length) whilst carbohydrate overconsumption in early pregnancy is negatively correlated with ponderal index, suggesting that sufficient protein intake is necessary for symmetrical growth [34]. Ultimately, the major non-genetic factors determining fetal size is referred to as maternal constraint – a plethora of maternal and uteroplacental factors, including the uterine environment in limiting support of fetal growth by mediating hormonal signals, nutrient availability and metabolism which are dependent upon maternal nutrient intake [11].

Effects on the fetal liver

Nutritional insult during gestation results in organ dysfunction and abnormal development [35]. Maternal undernutrition during fetal development commonly results in decreased liver weight and liver fibrosis [36,37]. Reduced liver functions, such as impaired cholinesterase activity, antioxidant capacity, glucose metabolism and lipid metabolism also occur due to reduced maternal intake [36,38]. Although many of the metabolic and digestive functions of the liver are not critical during gestation, the liver remains sensitive to the levels of metabolic substrates and alters its protein synthesis accordingly [39,40]. The liver is also particularly significant as the primary secretor of plasma proteins and therefore changes in its protein secretion affects the fetal body [41,42].

1.2 Placental Insufficiency in FGR

The placenta supplies the fetus oxygen and nutrient rich blood through the umbilical vein directly to the fetal liver and to the fetal heart via the ductus venosus (Figure 1) [43]. Pathological placental dysfunction related FGR occurs primarily due to

deficient maternal uterine spiral remodeling, leading to decreased fetoplacental oxygen and nutrient transfer [44]. In these cases, placental and fetal adaptations are necessary to accommodate for deficient nutrient availability [45–49]. The placenta serves to integrate maternal metabolic hormones such as low circulating insulin, IGF-1, leptin and elevated cortisol [30,50] to alter expression and/or activity of nutrient transporters supplying fetal provision [51–53]. The fetal liver integrates maternal nutrient supply and physiologically responds by mediating umbilical blood flow from the liver to fetal cardiac circulation via ductus venosus shunting resulting in decreased liver size and function [36–38,54,55]. As such, maternal undernutrition may induce placental insufficiency, the principal cause of FGR and the pathobiological consequence is mediated by placental hormones which regulate fetoplacental nutrient transfer and ductus venosus shunting of maternal blood supply to maintain fetal cardiac function at the cost of fetal liver development and function [38,55–58].

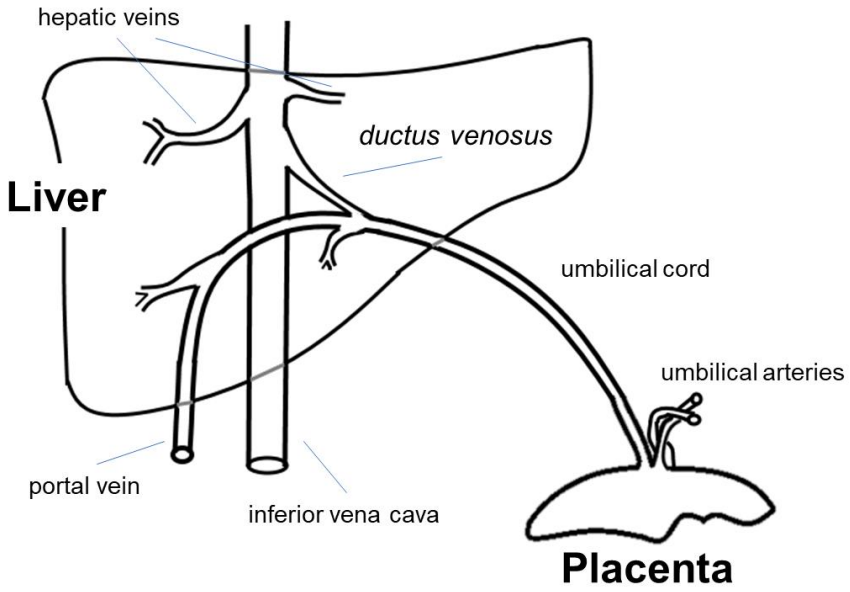

Figure 1. Anatomic scheme of placental blood supply to fetal liver through the umbilical cord with ductus venosus shunting.

1.2.1 Inadequate amino acid transfer in FGR due to placental insufficiency

The importance of adequate amino acid supply is facilitated by the fetal liver, which mediates cardiac circulation of amino acids to regulate fetal development via the ductus venosus [28,56]. Fetoplacental amino acid transfer is essential for fetal growth [51]. Fetal amino acid plasma concentration remains mostly constant over the course of pregnancy and is significantly higher than maternal concentration [59–62]. Fetal amino acids are supplied by the placenta through the umbilical cord, however, fetal amino acid concentration is determined by placental amino acid transfer [63,64]. In growth restricted fetuses, placental amino acid transfer is reduced [65] and amino acid concentration is significantly decreased in the umbilical artery and vein [66–68] with specifically decreased concentrations of essential branched chain amino acids (BCAAs) (valine, leucine and isoleucine) [62]. In animal models, decreased amino acid transfer occurs prior to the onset of FGR, emphasizing a causal role [29]. Several distinct systems of placental amino acid transporters have been described [69]. These transporters function within the syncytiotrophoblast of the human placenta at the microvillous (MVM; maternal facing) and basal (BM; fetal facing) membranes and transport amino acids against their concentration gradient [70]. Inadequate transplacental amino acid transfer leads to increased maternal amino acid concentration and decreased fetal amino acid concentration observed in FGR pregnancies [68,71]

Within FGR, significant reduction in transplacental flux and fetal turnover ratios of essential amino acids have been demonstrated [72–74]. Reduction in fetal amino acid concentrations in FGR cases may be attributed to the downregulation of expression and/or activity of specific transporters [29,73]. Na^+ dependent System A transporter which mediates small and neutral amino acid uptake has been demonstrated to exhibit decreased transport activity in FGR cases with respect to FGR severity [75–77]. Na^+ independent System L mediates transport of neutral amino acids with bulkier side chains such as leucine [69]. Although System L expression and activity at both the MVM and BM is not directly downregulated in early gestation FGR models [30], System L transport is

dependent upon exchange of non-essential amino acids supplied by System A for essential amino acids such as leucine [78] which may result in impaired System L transport and reduced BCAA concentration within fetal circulation [30,62]. In later gestation FGR models, cumulative effects of downregulated System A transport and reduced small, neutral amino acid concentrations results in a marked 84% reduction in System L transport [58].

Fetal growth is intimately linked to transplacental amino acid transport in both placental insufficiency induced FGR and in fetal overgrowth where transport is downregulated and upregulated, respectively [73,75,79–82]. Low leucine availability, in particular, has been implicated in FGR onset. Dichorionic average for gestational age (AGA) and FGR twin studies demonstrated significant reductions in BCAA concentrations in fetal plasma and in particular, a highly significant decrease in feto-maternal leucine ratio [83]. Likewise, significant reduction of leucine within fetal circulation has been identified in non-human primate models of FGR [49]. Teodoro et al. (2012) explored the distinct effects of leucine separate from isoleucine and valine in attenuating maternal protein deficiency induced growth restriction and concluded that leucine alone, apart from other BCAAs, is necessary for normal growth and organ mass in rat fetuses and supplementation of leucine is capable of restoring normal fetal growth [84].

1.2.2 Fetal Responses to Placental Insufficiency and Reduced Amino Acid Transport

Persistent placental insufficiency resulting in a declining nutrient deficit leads to an inability to maintain both fetal oxidative metabolism and placental function [85]. At this stage, concurrent down-regulation of active placental transport such as amino acid transporters and increasing fetal demands result in more widespread metabolic responses [48,86,87]. At advanced stages of malnutrition, fetal metabolic responses cumulate to the breakdown of endogenous muscle protein, failure to accumulate adipose stores and premature activation of hepatic gluconeogenesis [85,88]. Accordant to the degree and

severity of FGR, thyroid function at all levels is impaired [89,90] while corticotrophin releasing hormone and cortisol levels are significantly elevated [91,92].

Response of the Fetal Liver

Reduction in amino acid availability due to maternal undernutrition results in several biochemical fetal liver consequences. The proteomic liver profile of maternal nutrient restricted fetal liver demonstrates induction of cholesterol biosynthesis, inhibition of fatty acid oxidation and thyroid hormone metabolism [40]. Further metabolic effects include increases in BCAA oxidation and gluconeogenic capacity [39,93]. Reduction of general cell growth and proliferation kinase mechanistic target of rapamycin (mTOR) activity and increased amino acid response (AAR) pathway signaling is additionally observed in the fetal liver of maternal nutrient restriction [94]. Liver growth hormone (GH) and hepatocyte growth factor are induced in maternal nutrient restriction [95]. Additionally, the principal endocrine growth axis involving the metabolic and mitogenic peptides insulin, IGF-I and IGF-II is immediately downregulated upon critical placental insufficiency [96]. Fetal liver expression of fetal hepatic growth peptides IGF-I and IGF-II are reduced concomitant with the increase of their half-life extending carrier proteins [97]. Additionally, pro-apoptotic factors are upregulated [95,97].

1.3 The Insulin-like Growth Factor (IGF) Axis and Fetal Growth

The most important determinant of fetal growth is the IGF system [98]. The IGFs compose of two ligands, IGF-I and IGF-II and exist as single polypeptide chains which share similar amino acid sequence homology with proinsulin, however, primarily govern mitogenic roles instead of metabolic roles [99,100]. Baker et al. utilized embryonic null mutations in elegant mice studies to demonstrate the importance of the IGF system in fetal growth [101]. Deletion of *Igf1* or *Igf2* results in similar level of fetal growth restriction (60% of normal birth weight). In *Igf1* and *Igf2* knockouts, growth was further reduced (30% of normal birth weight) indicating both IGFs are critical in fetal growth and likely serve distinct roles. Deletion of the type 1 IGF receptor (IGF-1R) gene *Igf1r* alone with *Igf1* results in more severe growth restriction (45% of normal birth weight) than deletion

of *Igf1* or *Igf2* alone, suggesting that IGF-1R mediates growth via both IGF-I and IGF-II. Dual *Igf1r* and *Igf2* deletions resulted 30% of normal birth weight, further suggesting that the role of IGF-II is critically different than those of IGF-I. Although *Igf1* or *Igf2* deletions both result in similar fetal growth restricted phenotypes, a separate study observed placental hypoplasia only in *Igf2* deletions, suggesting that growth mediation in the fetus is highly dependent on IGF-I and that IGF-II has a function in placental development distinct from IGF-I [102].

Both IGFs are expressed in fetal tissues from pre-implantation to the final stages of tissue maturation prior to birth and are thought to primarily act in autocrine and paracrine fashion, with endocrine action occurring in the latter half of gestation [103–105]. Relatively, IGF-II concentrations are consistently higher than IGF-I concentrations within human fetal circulation (3-10 fold) [106]. Fetal serum concentrations of IGF-I and IGF-II increase with progressing gestation, however, the greatest rise is observed in IGF-I in late gestation [107–109]. IGF-I concentrations increase dramatically in the second and third trimesters as developmental changes in IGF expression become tissue specific and fetal liver dependent [109–111].

Initial findings regarding fetal plasma concentrations and *Igf2* mRNA abundance in fetal tissues lead to the hypothesis that IGF-II was the primary mediator of fetal growth [105,106,112,113]. However, Baker et al.'s studies on *Igf1* and *Igf2* null mutations in mouse embryos asserted that both IGF-I and IGF-II were necessary for normal fetal growth [101]. While IGF-II is more abundant than IGF-I during fetogenesis, only IGF-I plasma concentrations were found to be positively correlated with fetal size, length and birthweight [106,107,114,115]. IGF-II instead has been established as the primary growth factor mediating embryonic and placental development [116–119]. Additionally, two studies by DeChiara *et al.*,(1990, 1991) demonstrated that IGF-II while important for growth, is not necessary for producing viable offspring without severe defects unlike IGF-I [102,120]. During the exponential growth phase of the third trimester, IGF-I levels rise dramatically as the somatotropic axis begins to influence IGF-I production in the fetal liver [110,119,121]. Fetal IGF-I concentration increases exponentially from a mean of 15 ug/L to 70 ug/L while fetal IGF-II concentration rises linearly from a mean of 600 ug/L to 900 ug /L over

the course of 15 weeks to 40 weeks of gestation [109]. IGF-I as opposed to IGF-II, is the primary mediator of fetal growth in later gestation [104].

Maternal IGFs further affect fetal growth [122]. IGF-I and IGF-II are produced in several maternal tissues such as skeletal muscle, liver, adipose tissue and uterus [123–126]. Additionally, the placenta synthesizes substantial amounts of IGF-II but not IGF-I [127]. Maternal IGF-I consistently rises during the course of pregnancy while IGF-II concentrations remain relatively constant [128]. However, maternal IGFs do not cross the placental barrier in significant quantities [129], thus, the regulation of fetal growth by maternal IGFs are due to their effects on inducing placental development and modulating maternal metabolism and nutritional partitioning to sustain favourable maternal-fetal provision [122].

1.3.1 The IGF receptors and their functions

The IGFs are primarily mitogenic proteins that are highly conserved and structurally homologous to insulin [99,100]. Although structurally similar, the functions of the IGFs and insulin are divergent with the IGFs primarily serving mitogenic functions modulating cell growth and proliferation [130,131] and insulin primarily mediating glucose transport and the biosynthesis of glycogen and fat [132]. The IGFs exert their actions via their receptors. The type 2 IGF receptor binds with IGF-II with high affinity and serves primarily to clear IGF-II from circulation [133]. IGF-1R in contrast, is a tyrosine kinase with significant homology to the insulin receptor (IR) [134] and mediates the growth-promoting actions of both IGF-I and IGF-II [135].

The mature, functional form of IGF-1R has a membrane spanning heterotetrameric ($\alpha_2\beta_2$) structure formed from pre-formed dimers ($\alpha\beta$), all linked by disulfide bridges [131]. The $\alpha\beta$ pro-receptor is synthesized as a single chain and processed by proteolysis and glycosylation [136,137]. Ligand binding is mediated by the N-terminal extracellular α-subunits which are additionally conserved in the insulin receptor (IR) [134,138]. The α-subunit contains two homologous domains (L1 and L2) [139] separated by a cysteine-rich domain that mediates ligand binding [140]. The β-subunit contains extracellular, plasma membrane spanning and intracellular domains [141]. The intracellular

domain of the β-subunit is subdivided into three domains: a juxtamembrane domain, a tyrosine kinase domain and a C-terminal domain [142]. The juxtamembrane domain may mediate receptor internalization [143,144]. The tyrosine kinase domain contains a pseudosubstrate activation loop that contains critical Tyr residues 1131, 1135 and 1136 (with Tyr1131 occluding ATP binding) which are *trans*-phosphorylated by the dimeric subunit partner upon ligand binding and results in stabilization and catalytic competence of the tyrosine kinase domain [145]. After *trans*-phosphorylation of IGF-1Rβ Tyr residues, signal transduction molecules and adaptor proteins such as the Insulin Receptor Substrates (IRSs) and Shc proteins are able to bind to sites outside of the kinase domain and activate downstream signaling pathways [130].

1.3.2 Insulin-like growth factor binding proteins (IGFBPs)

Six IGFBPs (1-6) bind the IGFs with high affinity within the nanomolar range [146,147]. These proteins share an overall protein sequence homology of 50% and share conserved cysteine residues in the N and C-terminal domains [148]. The IGFs are primarily bound to IGFBPs within circulation thus prolonging the half-life of circulating IGFs [149], which is typically just 10-12 minutes [150]. IGFBP-3 is the most abundant IGFBP in circulation and predominantly forms a ~150 kDa ternary complex with the IGFs and an acid-labile subunit [151]. 75% of circulating IGFs are bound in this ~150 kDa ternary complex which prolongs the half-life of the IGFs to ~15 h [150]. No other IGFBP has such a stabilizing effect on prolonging the half-life of the IGFs [151]. The IGFBPs have several proposed functions with respect to both IGF-dependent and IGF-independent actions [130,152]. IGF-dependent functions include acting as carrier proteins, providing tissue specificity and modulating interactions between the IGFs and their receptors [146]. IGFBP-1 and IGFBP-2 contain Arg-Gly-Asp (RGD sequence) which serves as an integrin receptor sequence which binds to α5β1 integrin receptor which mediates cell migration [148,153]. IGFBP-3 has IGF-independent inhibitory actions on cell growth and DNA synthesis [154]. IGFBP-5 has been demonstrated to have some IGF-independent mitogenic properties [155].

1.3.3 IGFBP structure

The IGFBPs range from ~24 to 50 kDa and are conserved structurally, sharing similarities amongst their structured cysteine-rich, disulfide linked N- and C-terminal domains which contribute to IGF binding which are linked by a less structured and less conserved linker domain [147]. Both the N- and C-terminal domains of the IGFBPs share conserved IGF binding determinants, which are both necessary for high-affinity IGF binding [156,157]. Structural studies [158,159] determined key Val and Leu residues within the conserved N-domain that form a deep binding cleft which allows for IGF binding contributes to 1000-fold greater binding affinity than mutagenized IGFBP analogues [160–162]. The lesser conserved and predominantly unstructured linker region contains sites for post-translational modification and proteolysis, while additionally contributing to IGF-binding [147]. Isolated N- and C-terminal domains, without the linker region, demonstrate up to a 100-fold loss in binding affinity [163,164]. The linker regions of IGFBP-1, -3 and -5 permit phosphorylation [165].

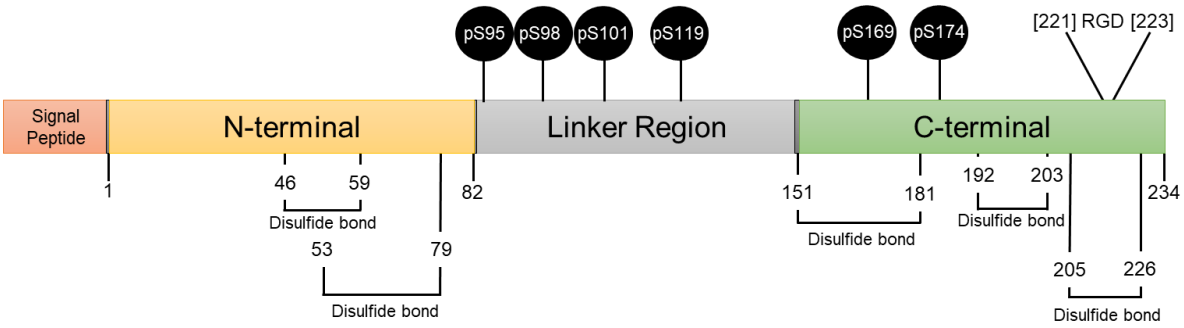

Figure 2. Schematic of IGFBP-1. Mature IGFBP-1 contains 234 residues and contains an N-terminal region, central linker region and C-terminal region. The N- and C-terminal domains are structured by disulfide bonds which are conserved amongst IGFBPs. The α5β1 integrin receptor binding RGD motif is located in the C-terminal. Phosphorylation sites are located within the linker region and C-terminal region.

1.3.4 IGFBP-1 regulates IGF-I bioavailability during pregnancy

During pregnancy, there are several sources of IGFBP-1 localized to different compartments. Fetal circulating IGFBP-1 is primarily secreted by the fetal liver [166] and is a potent inhibitor of the mitogenic actions of the IGFs both *in vitro* [167] and *in vivo* [168,169] thereby mediating fetal IGF-I bioavailability and thus directly regulating fetal growth [104]. An inverse correlation of fetal serum IGFBP-1 levels and birthweight has been observed, with marked increased levels of fetal IGFBP-1 in FGR [115,170]. Circulating IGFBP-1 is greatest during pregnancy [171] and maternal serum concentrations rise 25-fold over the course of gestation [172]. Maternal IGFBP-1 is primarily secreted from the endometrium by decidual cells into the placenta where it inhibits trophoblast invasion [122].

IGFBP-1 expression is largely regulated by the fetal environment [173,174]. A non-growth inducive environment such as low oxygen tension and low nutrient availability results in increased IGFBP-1 expression in both maternal and fetal compartments, which results in aberrant placental development and reduced fetal IGF-I bioavailability [12]. Fetal hepatic expression and circulating levels of IGFBP-1 are increased in FGR [175,176]. Fetal liver expression of IGFBP-1 has been extensively investigated in models. The expression and secretion of IGFBP-1 by the fetal liver in non-growth inducive environments are attributed to mTOR inhibition and the AAR upregulation [94,177–180]. In this way, nutritionally induced alterations in fetal liver IGFBP-1 expression entertains the duality of maternal constraint [11] and fetal programming [121] establishing IGFBP-1 as the regulatory protein which attenuates fetal growth if the environment is not conducive to sustaining the exponential growth phase during the third trimester.

1.3.5 IGFBP-1 phosphorylation and the regulation of IGF-I bioavailability

Phosphorylation of IGFBP-1 potently enhances its affinity for IGF-I [181,182] as well as its capacity to inhibit IGF-I dependent actions [183] such as cell proliferation, amino acid transport [184] and DNA synthesis [185,186] while also reducing its susceptibility to proteolysis [187].

Extensive work has characterized the extent of IGFBP-1 phosphorylation and its effects on its binding affinity towards IGF-I and IGF-I bioavailability. Phosphorylated IGFBP-1 derived from HepG2 cell conditioned media results in a 6-fold increase in affinity for IGF-I compared to non-phosphorylated IGFBP-1 [188]. Our lab further established an association between phosphorylated IGFBP-1 and decreased IGF-I bioactivity via IGF-1R autophosphorylation *in vitro* from several sources, including amniotic fluid derived from FGR pregnancies and conditioned HepG2 cell media [189–191]. Although non-phosphorylated IGFBP-1 binds both IGF-I and IGF-II with similar affinities, phosphorylation of IGFBP-1 increases its affinity towards IGF-I only [192].

We have demonstrated that IGFBP-1 is phosphorylated at six serine residues (Ser95, 98, 101, 119, 169 and 174) (Figure 2) [179,193]. Of these sites, Ser98, 101, 119 and 169 have been validated by alanine mutagenesis to mediate binding affinity and cause varied responses to IGF-I [190]. Previous stoichiometric analysis of IGFBP-1 phosphorylation sites in CHO cells demonstrated Ser101 as the major site of phosphorylation (70%) and Ser119 (5%) and Ser169 (25%) as minor sites of phosphorylation [181]. IGFBP-1 mutations Ser98Ala and Ser169Ala maintained potent inhibition of IGF-1R autophosphorylation in P6 cells although retained 42- and 34-fold reduced binding affinity towards IGF-I, respectively. Ser101Ala and Ser119Ala mutations, however, did not significantly inhibit IGF-1R autophosphorylation and demonstrated 89- and 99-fold respective decreases in IGFBP-1 to IGF-I binding affinity [190]. Thus, Ser101 and Ser119 have been demonstrated as potent inhibitory phosphorylation sites. However, the site and degree of IGFBP-1 phosphorylation rather than total amount of total IGFBP-1 or phosphorylated IGFBP-1forms mediates the functional effects of IGF-I bioactivity inhibition [194]. We have previously demonstrated a ~300-fold increase in binding affinity for IGF-I due to hypoxic stimulation with primarily Ser98 and Ser169 hyperphosphorylation compared to a ~30-fold increase in binding affinity for IGF-I from leucine deprivation which primarily induces Ser119 hyperphosphorylation [194]. The changes in IGF-I binding affinity were attributed to the degree of specific site hyperphosphorylation which varied between hypoxia and leucine

deprivation treatments where we demonstrated increased IGFBP-1 phosphopeptide peak intensity against an internal IGFBP-1 control peptide [194].

The linker region contains Ser98, Ser101 and Ser119 while the C-terminal domain contains Ser169 [189], indicating that both phosphorylation within the linker region and C-terminal domain may mediate increased IGFBP-1 affinity for IGF-I by distinct structural mechanisms. Our lab further characterized Ser101, Ser119 and Ser169 as upregulated phosphorylation sites in amniotic fluid [189], umbilical cord plasma [177] and primary fetal hepatocytes derived from a baboon model of FGR [177].

1.3.6 IGFBP-1 phosphorylation in FGR pregnancy

The phosphorylation status of IGFBP-1 in maternal and fetal compartments differ throughout gestation. Martina et al., (1997) examined gestational-age dependent phosphorylation of IGFBP-1 in several maternal and fetal compartments [195]. In early gestation, maternal serum contains primarily non-phosphorylated IGFBP-1 while non-pregnant maternal serum contains highly phosphorylated IGFBP-1. Maternal serum derived IGFBP-1 in amniotic fluid at this time, is also primarily non-phosphorylated. By mid-gestation, maternal serum contains all IGFBP-1 phosphoisoforms while amniotic fluid contains all but the most highly phosphorylated isoforms. In late gestation, maternal serum only contains the highly phosphorylated isoforms. Decidual IGFBP-1 production and phosphorylation status seems to be temporally and inversely regulated by local IGF-II levels which rises during normal pregnancy, resulting in predominance of non-phosphorylated IGFBP-1 [196]. The fetal liver however, consistently secretes highly phosphorylated IGFBP-1 over the course of pregnancy [195].

Elevated fetal IGFBP-1 levels which directly affects circulating fetal IGF-I bioactivity and therefore fetal growth [104] is additionally highly correlated with FGR. A causal relationship between increased IGFBP-1 and decreased birthweight in a mouse model overexpressing fetal liver IGFBP-1resulting in an 18% reduction in birthweight [197]. IGFBP-1 phosphorylation has not been extensively studied within the human fetal liver, in part, due to limited human fetal liver availability. Several models of FGR have instead been utilized for the better understanding of human fetal liver IGFBP-1

phosphorylation. Rat and animal models have been used previously, however, differences in IGFBP-1 primary structure between rat, mouse and human orthologs result in loss of specific IGFBP-1 phosphorylation sites and is therefore insufficient in studying human FGR [198]. A well established maternal nutrient restricted (MNR) baboon model of FGR [199,200] based on 30% caloric restriction reduces fetal essential amino acid levels, fetal weight and results in structural and functional changes in fetal organs [201,202] while being associated with increased IGFBP-1 expression within the fetal liver [97]. In respect to differentiation factors, fetal hepatocytes and human hepatocellular carcinoma HepG2 cells share close proteomic and transcriptomic resemblances [72,203,204]. HepG2 cells have been used extensively, primarily by our laboratory, as a model for fetal hepatocytes in the investigation of fetal IGFBP-1 phosphorylation [94,177–179,191,194].

The association of the degree of IGFBP-1 phosphorylation in maternal and fetal compartments and amniotic fluid in human pregnancies have been previously investigated though with contradictory results [177,182,186,189,190,196,205–210]. However, our team has demonstrated that the sites and degree of IGFBP-1 phosphorylation invariably affect binding affinity towards IGF-I and IGF-I bioactivity [190,194]. We further demonstrated that the phosphorylation status of IGFBP-1 in amniotic fluid is altered within FGR [211]. IGFBP-1 hyperphosphorylation in amniotic fluid and umbilical cord plasma [177] at sites which affect IGFBP-1 binding is elevated in FGR [189,210]. Furthermore, utilizing the well established MNR baboon model of FGR, our team has demonstrated increased IGFBP-1 phosphorylation at Ser98, Ser101, Ser119, Ser169 and Ser174 in FGR baboon fetal liver tissue during early and late gestation [94]. Within HepG2 cells, our group has demonstrated hypoxia and nutrient deprivation as determinant factors which induce IGFBP-1 phosphorylation [178,179,194,212].

1.4 Kinases regulating IGFBP-1 phosphorylation

Phosphorylation of IGFBP-1 at sites known to mediate IGF-I binding [190] occur are acidophilic Ser residues, containing either Asp or Glu residues following the phosphoacceptor [191]. These acidicophilic phosphorylation sites conform well to the protein kinase CK2 consensus site (S/T-x-x-D/E) [213] which has been previously

considered as and demonstrated *in vitro* to be the kinase phosphorylating IGFBP-1 [214,215]. Another kinase, Fam20C or otherwise known as the genuine "Golgi casein kinase" [216,217] has been identified to phosphorylate a similar acidophilic consensus sequence to CK2 (S-x-E/pS) and has also been demonstrated to phosphorylate IGFBP-1 *in vitro* by CRISPR knockdown [218]. However, Fam20C does not mediate the phosphorylation of the most important Ser98, Ser101 and Ser119 residues which mediate high affinity IGF-1 binding and inhibition of IGF-1R autophosphorylation [190,218] whereas CK2 has been demonstrated to mediate the phosphorylation of these distinct phosphorylation sites

Furthermore, IGFBP-1 contains consensus sequences for protein kinase A (PKA) and protein kinase C (PKC) [165]. PKA has been demonstrated to phosphorylate IGFBP-1 *in vitro* [186,214,215] and mediate IGFBP-1 transcription in decidual and endometrial cells [219], however, we recently demonstrated that PKA does not mediate IGFBP-1 phosphorylation in HepG2 cells [191]. PKC, on the other hand, has been implicated to regulate IGFBP-1 expression in several cell types [220,221]. Although PKC phosphorylates basic Ser/Thr residues, we have previously demonstrated inhibition or knockdown of PKC reduced IGFBP-1 phosphorylation at putative CK2 sites (Ser101, Ser119, Ser169) [191]

1.4.1 Protein Kinase CK2 – Structure and phosphorylation determinants

CK2 is ubiquitous in eukaryotic organisms and primarily exists as a tetrameric enzyme consisting of two catalytic subunits (α or α', in any combination) and two regulatory subunits (β), adopting a structure in which CK2β dimers form the core of the tetrameric enzyme [213].. CK2 phosphorylates Ser or Thr residues with a consensus sequence of S/T-x-x-D/E, though Pro, Lys or Arg at the +1 position are unfavourable [222]. Furthermore, CK2 phosphorylation sites may follow hierarchal phosphorylation, which allows for Ser phosphoacceptors outside of the canonical consensus sequence to be phosphorylated if adjacent pSer residues occur at the +1 and +3 positions [223]. However, these phosphorylation determinants are not quintessential for CK2 phosphorylation of a substrate [222,224].

1.4.1.1 CK2 phosphorylation of IGFBP-1 and involvement in FGR

IGFBP-1 has been demonstrated to be phosphorylated by CK2 in HepG2 [215] and endometrial stromal cells [214]. Our lab has demonstrated complete CK2 holoenzyme silencing and independent CK2 subunit silencing decreasing IGFBP-1 phosphorylation in HepG2 cells [177]. Accordant with increases in IGFBP-1 phosphorylation in FGR and models of FGR, CK2 activity is increased concomitantly [94,177,180,191].

1.4.2 Protein Kinase C – Initial Discovery

Cyclic nucleotide dependent kinases PKA and protein kinase G (PKG) were discovered in the 1960s and 1970s, respectively and had paved the way to the discovery of PKC [225,226]. Analysis of mammalian PKG from rat brain tissue led to the discovery of an active Mg^{2+} dependent enzyme termed protein kinase M (PKM), which could only be detected upon repeated freeze and thaw cycles, leading to the idea that PKM may be a proteolyzed active form of believed to be proteolytically cleaved from PKG by a Ca^{2+}-dependent protease based on their previous work [227,228]. However, brain PKG activity was curiously low thus the unknown parent protein of PKG was termed "proenzyme" (PKC). Comparatively, PKM readily phosphorylated protamine and H1 histone and protamine whereas the proenzyme recognized protamine but failed to phosphorylate H1 histone. A two-step reaction assay measuring Ca^{2+} dependence and kinase activity for Ca^{2+}-dependent protease with proenzyme resulted in the first mechanistic discovery of PKC where kinase activity was detected in both cytosolic and particulate fraction and that particulate fraction "Ca^{2+}-dependent protease" was not an enzyme as its mechanism activated proenzyme instantaneously [229]. Proenzyme was renamed to "protein kinase C" as Ca^{2+} was regarded as its critical regulator. The initial discovery of active PKC within the particulate fraction led to the discovery of the enzyme's true nature of being phospholipid dependent. Neutral lipids, glycolipids and phospholipids were extracted from tissue and separated by column chromatography. PKC activity was determined to be activated by neutral and glycolipid fractions and diacylglycerol (DAG) was determined as the second messenger which activated PKC [230].

1.4.2.1 Structure and Regulation of PKC

PKC comprises of a family of related Ser/Thr kinases involved in several signal transduction pathways [231]. The PKC family of kinases contain highly conserved, C-terminal catalytic domains, a regulatory N-terminal domain that maintains the enzyme in an inactive conformation via an autoinhibitory pseudosubstrate and membrane targeting modules known as C1 and C2. Based on the N-terminal domain structure, PKC isoforms are categorized into subfamilies known as conventional (cPKC), novel (nPKC) and atypical (aPKC) isoform based on their co-factor requirements. cPKC isoforms bind both DAG and Ca^{2+}, whereas nPKCs bind only DAG and aPKCs require neither DAG or Ca^{2+} for activity. The C1 domain mediates DAG/phorbol ester binding while the C2 domain binds Ca^{2+}. The C3 and C4 domains form the ATP and substrate-binding lobes of the kinase core [232].

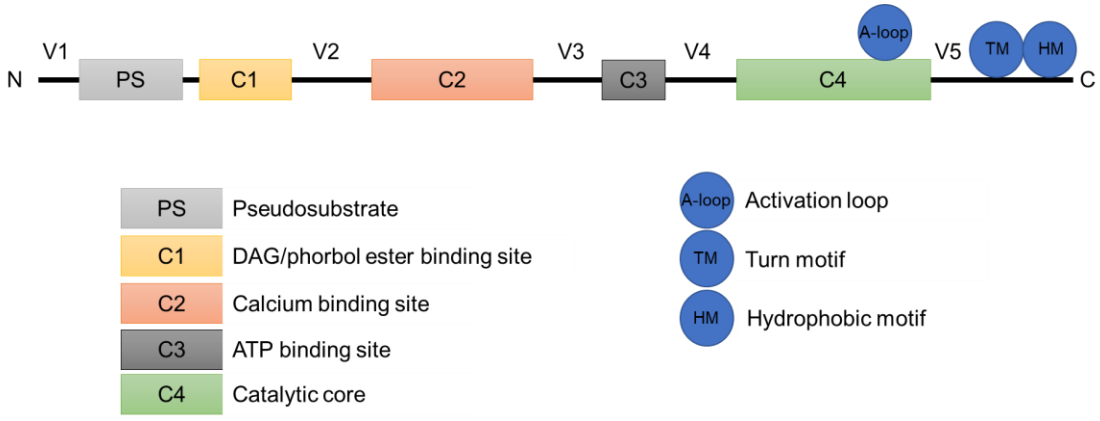

Figure 3. General schematic of conventional PKC isozymes. The length and relative sizes of cPKC isoforms are variable. Variable regions (V1-V5) represent poorly conserved sequences separating the highly conserved pseudosubstrate and C1-C4 domains. The novel PKC isoforms lack the C2 domain whereas the atypical PKC isoforms lack the C2 domain and contain a C2-like domain preceding the pseudosubstrate.

Numerous phosphorylations occur shortly after the biosynthesis of all PKC izozymes to yield a stable, autoinhibited (by the pseudosubstrate) enzyme ready to be activated by second messengers Ca^{2+} and DAG [233]. Phosphoinositide-dependent kinase

(PDK1) phosphorylates the conserved activation loop which triggers phosphorylation of the turn motif and hydrophobic motif resulting in the adoption of the stable, autoinhibited conformation [234]. Activation of cPKC requires translocation from the cytosol to membrane compartments [235]. Membrane translocation is critically dependent upon cytosolic Ca^{2+} concentrations which at basal conditions, is insufficient to active cPKC and require a stimulus to induce cytosolic mobilization of Ca^{2+} which results in the translocation of the enzyme to a membrane compartment for attachment [236]. Attachment to a membrane compartment following influx of cytosolic Ca^{2+} is further facilitated by DAG, which allows the penetration of PKC into the membrane bilayer [237]. Combination of both high cytosolic Ca^{2+} concentration affording initial translocation and DAG mediated membrane penetration facilitates activation of PKC [238].

1.4.2.2 PKC in FGR and Nutrient Sensitive Regulation of PKC

Evidence of PKC involvement in FGR is limited. Sugden and Langdown (2001) examined placental insufficiency induced changes in the placental PKC isoform profile and demonstrated increased expression of "pro-apoptotic" nPKC isoforms -δ and -ε and reduced expression of "anti-apoptotic" cPKC isoforms -α, -βI and -βII [239]. Upregulated activity of PKCα, PKCε and expression of PKCβ, PKCβII and PKCδ within the cardiac muscle of FGR offspring has also been demonstrated, though does not implicate involvement of PKC in the development of FGR [240].

PKC expression and its activity are regulated by nutrient availability. Importantly, nutrient sensitive regulation of PKC isoforms are differentially regulated based on tissue and cell type. Leucine stimulates PKC autophosphorylation and subcellular redistribution in skeletal muscle [241] and PKC activity in chicken hepatocytes [242]. Low protein diets however, inhibit PKC activity in pancreatic islets [243,244] while amino acid deprivation in MCF-7 cells induce PKC expression [245]. Furthermore, several PKC isozymes integrate signals from the nutrient sensitive kinase mTOR, which may indicate a non-direct nutrient sensitive function for PKC [246–248]. PKC upregulation is additionally intimately linked with attenuating nutrient transport in nutrient excess environments, possibly representing a feedback mechanism for regulating bodyweight [249–252].

1.4.2.3 Involvement of PKC in mediating IGFBP-1 phosphorylation

Conserved amino acid sequences in all six IGFBPs have previously elected PKC as a possible kinase responsible for their direct phosphorylation [165]. However, the basic requirements of PKC consensus sequences exclude the possibility of direct PKC phosphorylation at IGFBP-1 at sites which mediate IGF-I binding [190,232]. PKC activation has been previously demonstrated to induce IGFBP-1 expression in endometrial carcinoma cells and HepG2 cells [220,221]. Our previous work demonstrated a supporting role for PKC in mediating IGFBP-1 phosphorylation at Ser101, Ser119 and Ser169 [191]. While PKC contributes to IGFBP-1 phosphorylation, the specific isoform(s) involved, and their respective role and mechanisms have not yet been elucidated.

1.5 Rationale, objective and hypothesis

1.5.1 Rationale: Amino acid availability dramatically affects cellular signaling in several protein networks, resulting in altered protein expression. Cellular responses to amino acid restriction include an increase in IGFBP-1 phosphorylation which is a key constituent to FGR [71,178,193]. IGF-I bioavailability is the vital determinant of fetal growth and the phosphorylation of IGFBP-1 at several sites significantly increases its binding affinity for IGF-I thus considerably reducing IGF-I bioactivity [104,111,190]. The key signaling mechanisms resultant of amino acid restriction and IGFBP-1 phosphorylation have been explored *in vitro* and *in vivo* [94,178,180]. Furthermore, previous studies have demonstrated the involvement of multiple kinases regulating IGFBP-1 phosphorylation under leucine deprivation [191]. However, the role of an apparent supporting kinase, PKC, has not been thoroughly investigated and the mechanisms involved in which it mediates the phosphorylation of IGFBP-1 in leucine deprivation have not been elucidated.

1.5.2 Hypothesis: Leucine deprivation activates nutrient sensitive PKC resulting in its translocation and induces its interaction with CK2, mediating fetal hepatic IGFBP-1 phosphorylation *in vitro.*

1.5.3 Objective: The objective of this study was to determine the molecular mechanisms surrounding the key kinases involved in IGFBP-1 phosphorylation and thus, IGF-I bioavailability in leucine deprivation.

The specific aims to elucidate our objectives are as follows:

1. To investigate interactions between PKC, CK2 and IGFBP-1

2. Determine the PKC isoform involved in IGFBP-1 phosphorylation

3. To demonstrate nutrient sensitive regulation of PKC

1.6 Experimental models

1.6.1 HepG2 cells as a model for fetal hepatocytes

The fetal liver is the primary source of circulating fetal IGFBP-1 *in vivo* [166]. HepG2 cells are human liver carcinoma cells and are widely employed as a model for human fetal hepatocytes due to their biotransformation properties and the similarities amongst their transcriptome, proteome and secretome [203,204,253,254]. IGFBP-1 mRNA is induced in non-growth conducive environments in HepG2 cells, which applicably serves our purposes in studying IGFBP-1 phosphorylation [174]. We have extensively employed HepG2 cells as a model for study of IGFBP-1 phosphorylation [94,177–179,191,194]. Additionally, we have validated the use of HepG2 cells as a model for fetal hepatocytes utilizing cultured primary baboon hepatocytes [177].

1.6.2 Leucine deprivation model for nutrient restriction

Leucine is an essential amino acid with the most potent effects amongst amino acids regarding protein synthesis and degradation, energy balance regulation and leptin secretion [255]. Leucine supplementation enhances protein synthesis in several tissue and cell types [256]. Leucine deficiency specifically and not essential amino acid or BCAA deficiencies is implicated in the development of FGR. The distinct effects of leucine separate from BCAA is capable of attenuating the effects of maternal protein

undernutrition which induced growth restriction [84]. Furthermore, deficiencies in fetoplacental leucine transport results in significant reduction in feto-maternal leucine ratios and fetal circulating leucine which are consistently identified in FGR [49,72,73,82,83]. Our laboratory has extensively used leucine deprivation (L0) as a model of nutrient deprivation to induce IGFBP-1 phosphorylation *in vitro* with effects similar to maternal nutrient restriction [94,177,178,191,194].

1.6.3 Baboon maternal nutrient restriction as a model of human FGR

We utilized a well-established MNR baboon model of FGR instead of other animal models such as rodents or sheep due to differences in placental organization and IGFBP-1 phosphorylation [198,257,258]. 30% caloric restriction used in this MNR baboon model of FGR impairs placental development similarly to human maternal undernutrition [28,201]. Importantly, similar interspecies changes are also observed within the fetal hepatic and placental IGF systems [97,111,201,259]. Likewise with our utilization of leucine deprivation *in vitro*, we have previously employed this MNR baboon model of FGR to study IGFBP-1 phosphorylation in relation to CK2, mTOR and the AAR [94,177].

2 « Material and Methods

2.1 HepG2 cell culture and leucine deprivation treatments

I utilized human hepatocellular carcinoma HepG2 cells as a model for fetal hepatocytes due to their close proteomic and transcriptomic resemblance to fetal hepatocytes in respect to differentiation factors [203,204,253]. The similarities of HepG2 cells to fetal hepatocytes further extends to cultured primary baboon fetal liver cells [177,260]. HepG2 cells at 85% confluency were plated at $5x10^5$ and then allowed to adhere for 16 hours. Cells were starved for 16 hours and subsequently cultured in custom DMEM/F12 media containing either 450 µM (L450) or 0 µM (L0) of leucine for 24 hours as

previously described [178,194]. Conditioned cell media (CM) was collected and cells from L450/L0 were lysed using lysis buffer (Cell Signaling Technologies, Beverly, MA).

2.2 Immunoprecipitation

Immunoprecipitation (IP) of IGFBP-1, CK2β and PKC was performed using HepG2 cell lysate. For each IP, 100 µL of 50% Protein A Sepharose slurry (GE Health Care, Canada) was coupled with IGFBP-1 mAb 6303 (Medix Biochemica, Kauniainen, Finland), polyclonal CK2β (YenZyme, USA) or polyclonal Pan-PKC (SAB4502356, Sigma-Aldrich, USA) respectively. Antibodies were diluted in 5x HEPES buffer (50 mM HEPES, 750 mM NaCl, 15 mM EDTA) and coupled to Protein A Sepharose beads.

HepG2 cell lysate (200 µg total protein) were buffer exchanged against PBS with 0.1% Tween (PBS-T) using 10K MWCO Ultracel centrifugal filter units (Millipore, Ireland) as described previously [212]. Unbound proteins were removed (flow-through). For Western blot analysis, proteins from a small aliquot were eluted from Sepharose beads with 50 µL elution buffer (8 M urea, 5% SDS, 50 mM Tris-HCl pH 7.8) and stored –20°C. The remaining beads were processed as described below for mass spectrometry.

2.3 SDS-PAGE and Western blotting

Protein separations were conducted using SDS-PAGE with Precision Plus Protein™ All Blue protein standards (BioRad Laboratories, Canada). Proteins were transferred to nitrocellulose membranes, and blocking was performed using either 5% skim milk or 5% bovine serum albumin (BSA) in Tris-buffered saline (TBS) with 0.1% Tween-20 (TBST).

For IGFBP-1 secretion, equal volumes (30-50 µL) of direct HepG2 CM were obtained using equal number of plated cells used for normalization due to the absence of a secretory internal control. Previously validated [177,261] custom phospho-site specific IGFBP-1 antibodies for pSer101 (1:500), pSer119 (1:2000) and pSer169 (1:250) (YenZyme, USA) and a custom polyclonal total IGFBP-1 (1:10,000) (a gift from Dr. Robert Baxter, Australia) were used as primary antibodies. For PKCα, pIGF-1Rβ^{Tyr1135}

and IGF-1Rβ, equal amounts of total protein in cell lysate from HepG2 cells (30-50 µg) or from fetal liver extracts were used. Monoclonal PKCα antibody (1:1000) (NB600-201; Novus Biologicals, USA), monolonal pIGF-1R$\beta^{Tyr1135}$ (1:1000) (DA7A8; Cell Signalling Technologies, USA), polyclonal IGF-1Rβ (1:250) (sc-713; Santa-Cruz Biotechnology, USA) and loading control β-actin (sc-47778; Santa Cruz Biotechnology, USA) were used. Calnexin (1:1000) (610523; BD Biosciences; USA) and α-tubulin (1:20,000) (T5168; Sigma-Aldrich, USA) were used as controls for membrane and cytosol enriched fractions, respectively. Secondary antibodies were HRP-conjugated goat anti-rabbit IgG (1:10,000) and goat anti-mouse IgG (1:10,000) (BioRad, Canada). Precision Protein™ StepTactin-HRP conjugate (BioRad, Canada) was used to visualize the protein ladder and β-actin was used to account for any differences in protein load and transfer. Enhanced chemiluminescence (ECL) reagents were employed for detection of proteins [262]. Images were captured using the Quantity One Molecular Imager VersaDoc imaging system (BioRad, Canada) and band intensities were subjected to densitometrical analyses using Image Lab (BioRad, Canada).

2.4 Parallel Reaction Monitoring Mass Spectrometry (PRM-MS)

In-solution digestion of the IP samples was performed as described [179]. Peptide digests were desalted using C18-Zip Tip and dried in a Thermo SpeedVac. After desalting and drying, samples were loaded onto a Thermo Easy-Spray analytical column (75 µm i.d. × 500 mm) C18 column with an Easy-nLC 1000 chromatography pump. For each analysis, we reconstituted peptides in 20 µL of 0.1% trifluoroacetic acid (TFA) and loaded 4 µL onto the column. Peptides were separated on a 125 min (5–40% acetonitrile) gradient. Mass spectra were collected on a Q-Exactive hybrid quadrupole-Orbitrap mass spectrometer coupled to an Easy-nLC 1000 system (ThermoFisher, USA). The spectrometer was set in full MS/data-dependent-MS2 TopN mode: mass analyzer over m/z range of 400-1600 with a mass resolution of 70,000 (at m/z = 200), 35 NCE (normalized collision energy), 2.0 m/z isolation window and 15 second dynamic exclusion. The isolation list (not shown) with the Mass [m/z] and the sequences of the

peptides used to identify PKC and IGFBP-1 by PRM-MS were recorded. Each trace on the chromatograph represents the detection of each individual transition ion used to monitor PKC detection. Retention time indicates that transition ions result from the same parent peptide (correlating with the time that the parental peptide had eluted from the C18 column). Data were generated by PRM-MS using isolation lists that were specific to PKC and IGFBP-1.

IGFBP-1 internal peptide (NH2-ALPGEQQPLHALTR-COOH) was used to normalize phosphorylated IGFBP-1. With two possible IGFBP-1 phosphorylation sites (dual), specific transitions were used to distinguish single-site-phosphorylation from each other (specifically, y14, b6 and b9 ions for pSer169 and pSer174; y12 and b15 ions for pSer98 and pS101).

2.5 PKCα siRNA silencing

HepG2 cells were plated at 75% confluence in 6 well plates. Silencing using siRNA against PKCα (SASI_Hs01_00018816; Sigma-Aldrich, USA) in HepG2 cells was achieved using transfection [177] with 80 nM siRNA and 5 μL Dharmafect transfection reagent (Thermo Scientific, USA) in regular, serum free DMEM:F12 for 24 hours. Transfection media was replaced with L450 or L0 media 24 hours post transfection. CM and cell lysates were collected from HepG2 cells 48 hours post L450 or L0 treatment as described above. Western immunoblot analysis was used to determine the efficiency of target silencing, total IGFBP-1 secretion and IGFBP-1 phosphorylation at three sites (Ser101, 119 and 169).

2.6 Immunofluorescence (IF)

HepG2 cells were seeded at $2.2x10^5$ on 0.1% poly-L-lysine coated coverslips in 6 well plates, followed by L0 treatment. Cells were fixed with 4% paraformaldehyde for 1 hour at 4°C, permeated in 0.25% Triton X-100 for 10 minutes and blocked with Dako Background Sniper (Biocare Medical, USA) for 10 minutes.

Several combinations of primary antibodies were used in dual IF: i) mouse mAb PKCα (1:250) and rabbit polyclonal IGFBP-1 (1:2500), ii) mouse mAb PKCα and rabbit polyclonal CK2β (1:500) and mouse IGFBP-1 mAb 6303 (1:500) and rabbit polyclonal CK2β (1:500) which were incubated overnight at 4°C. Single IF staining was performed using mouse mAb PKCα (1:250). Secondary antibodies anti-mouse Alexa Fluor 488 (1:400) and anti-rabbit Alexa Fluor 568 (1:400) were applied to cells and incubated for 45 min. Phalloidin 568 (1:20) was used to stain the cytosol in single IF staining experiments with PKCα (ThermoFisher, Canada). Cells were then counterstained with DAPI (1:300) (Life Technologies, Canada). Negative controls used were rabbit (X0903) and mouse pre-immune serum (X0931) at 4 μg/mL (Agilent Technologies, Santa Clara, CA). Coverslips were mounted (Fisher Scientific, Fairlawn, NJ) with Prolong Gold Mounting Media (ThermoFisher, Canada) and dried overnight prior to imaging on an Nikon Inverted T12E Deconvolution Microscope (Nikon Instruments Inc. USA)

2.7 Proximity ligation assay (PLA)

HepG2 cells were seeded at $2.2x10^5$ on 0.1% poly-L-lysine coated coverslips in 6 well plates, followed by L0 treatment as described earlier. Cells were fixed and permeabilized as in IF. Primary antibody combinations and incubation time remained the same as in dual IF.

Fixed HepG2 cells blocked with Duolink blocking solution (Sigma Aldrich, USA) were used for PLA using PLA secondary probes (anti-rabbit plus and anti-mouse minus) diluted 1:5 in Duolink antibody diluent (Sigma-Aldrich, USA) and incubated for 1 hour at room temperature. Subsequent ligation and amplification were performed according to manufacturer's instructions (Sigma-Aldrich, USA). Samples were mounted with provided mounting media containing DAPI counterstain and image acquisition was acquired on an AxioImager Z1 Epifluorescent Microscope (Carl Zeiss Canada Ltd.). Quantification was performed through automated counting of PLA signals and cell nuclei using ImagePro Premier and normalized by the cell number. Data were analyzed in GraphPad Prism 6.

2.8 Treatment of HepG2 cells by pharmacological kinase inhibitors and activators

HepG2 cells were plated at 75% confluence and starved for 16 hours in 0% FBS (DMEM:F12) prior to treatments with inhibitors and/or activators. Following dose dependency treatments, subsequent experiments utilized PKC activator phorbol 12-myristate 13-acetate (PMA) at 100 nM; PKC inhibitor bisindolylmaleimide II (Bis II) at 7.5 μM [191] and CK2 inhibitor 4,5,6,7-tetrabromobenzotriazole (TBB) at 10 μM. Following 24 hrs of pharmacological treatment, CM and cell lysate were collected using lysis buffer (Cell Signaling Technologies, Beverly, MA) with protease and phosphatase inhibitor cocktails (P8340, P5726, P0044; Sigma-Aldrich, St. Louis, MO). Protein contents determined by Bradford assay (BioRad Laboratories, Canada) and samples were stored at –20°C.

2.9 Subcellular fractionation of HepG2 cells by differential centrifugation

HepG2 cells at 80% confluency were detached with 10 mM EDTA in PBS for 35 min. Cells were collected and centrifuged at 400 g for 4 min and resuspended 1:5 in homogenization buffer (0.25 M sucrose, 5 mM HEPES, pH 7.4, cold) with protease and phosphatase inhibitors (same as used for cell lysis). Cells were homogenized utilizing a Polytron PT3000 (Kinematica AG, Lucerne, Switzerland). Post-nuclear cell lysate was obtained by nuclear extraction by centrifugation at 2,000 g for 10 min. Post-nuclear cell lysate was centrifuged at 105,000 x g for 1 hr and the supernatant (cytosolic fraction) was collected, the pellet (membrane fraction) rinsed with homogenization buffer and then resuspended in homogenization buffer containing 0.1% Triton X-100. The supernatant and pellet fractions were then sonicated and stored at –20°C for analysis by Western blot.

2.10 Confocal image acquisition

Images were captured with a 63× Plan-Apochromat oil immersion lens on a Leica SP8 confocal microscope. The acousto-optical beamsplitters were tuned to avoid all

crosstalk between channels. Alexa 488 was excited with a blue 20 mW 488 nm HeNe laser. For Alexa 568, a green 20 mW 552 nm HeNe laser was used for excitation. DAPI signal was excited with a 50 mW 405-50 Diode.

2.11 IGF-1R autophosphorylation assay

I employed an IGF-1R autophosphorylation assay as previously described [261]. In brief, mouse embryo fibroblast P6 cells (a BALB/c3T3 cells derivative) which over-express human IGF-1R (a kind gift from Dr. R Baserga, Thomas Jefferson University, Philadelphia, PA) were seeded at $4x10^5$ in 6-well plates and allowed to adhere overnight. P6 cells were starved for 6 hours, then treated with HepG2 cell conditioned media from several treatments containing equal amounts of total IGFBP-1 incubated for 2 hours with recombinant human IGF-I (25 ng/mL) for 15 minutes at room temperature. P6 cells were lysed and equal amount of total protein (40 μg) was loaded for Western blotting to assess changes in IGF-1R autophosphorylation using pIGF-1R$\beta^{Tyr1135}$ antibody.

2.12 Cell viability assay

Standard Trypan Blue exclusion assay was utilized to ensure that pharmacological or siRNA treatments did not negatively impact cell viability. Following treatments, cells were lifted and re-suspended in 10% FBS media and diluted 1:1 with 0.4% trypan blue and counted manually with a haemocytometer.

2.13 Preparation of baboon fetal liver extracts

Baboons (*Papio cynocephalus hamadryas*, *P. cynocephalus anubis*, and *P. hamadryas anubis*) from the Southwest National Primate Research Center were housed in outdoor cages permitting social and physical activity and controlled dietary intake [263]. In this MNR model, mothers were fed 70% of the ad libitum control mothers (Purina Monkey Diet 5038). Pregnancy was confirmed at GD 30 by ultrasound and Cesarean section was performed at GD 120 and GD 165 (full term GD 185) described previously [263]. Fetuses were sourced solely from singleton pregnancies. Fetal liver tissue was frozen at −80°C. Frozen pieces (–80C) of the left lobe (~0.2 g) of fetal liver (GD 120; n=19; male=11; female=8, GD 165; n=24, male=10; female=14) were homogenized using lysis

buffer with protease and phosphatase inhibitor cocktails described in detail previously [94]. The homogenate was centrifuged, and the clear supernatant was stored at –80°C.

2.14 Immunohistochemistry (IHC) using baboon fetal liver tissue

Tissues sections (5 μm) from GD matched control and MNR liver tissue of the left lobe were mounted on the same microscope slides and baked overnight at 45°C. Slides were deparaffinized in Xylene, rehydrated through graded ethanol series, then washed in tap water followed by PBS. Endogenous peroxidases were blocked in 3% hydrogen peroxide, and tissues were incubated with Background Sniper blocking solution (Biocare Medical, LLC., Pacheco, CA). Slides were incubated overnight at 4°C with mouse PKCα mAb (1:250) (Novus Biologicals, USA) in antibody diluent (Dako, Agilent Technologies, Santa Clara, CA). Secondary antibodies (anti-mouse horseradish peroxidase polymer complex, ImmPRESS® HRP Reagent Kit, Vector Laboratories, Burlingame, CA) were incubated for 45 minutes at room temperature. Sections were treated with 3,3'-diaminobenzidine (DAB) substrate (ImmPACT® DAB Peroxidase Substrate Kit, Vector Laboratories, Burlingame, CA) for two minutes, counter-stained with Modified Mayer's Haematoxylin (ThermoFisher, USA) for 20 seconds, rinsed, immersed in tap water for 4 minutes, then dehydrated through graded alcohols, cleared with Xylene, and mounted with Permount (Fisher Scientific, Inc.) for 30 seconds. Images were captured with a Zeiss AxioImager Z1 Microscope (Carl Zeiss Canada Ltd., North York, ON Canada) using brightfield imaging with a 40x oil immersion lens.

2.15 Data presentation and statistics

Data was analyzed using GraphPad Prism 6 (GraphPad Software, USA). Quantification of controls were assigned an arbitrary value of 1 and treatments were expressed relative to this mean. All quantified experiments were performed at minimum in triplicate. Statistical significance was tested using paired t-test, one-way analysis of variance (ANOVA) or two-way ANOVA with Dunnett's Multiple Comparison Post-Test and expressed as the mean + SEM. Significance was accepted at $p<0.05$.

3 Results

3.1 IGFBP-1, CK2β, and PKCα reciprocally co-immunoprecipitate

To identify the involvement of PKC in IGFBP-1 phosphorylation under L0, I first performed simultaneous co-immunoprecipitations (co-IPs) of IGFBP-1, CK2β, and Pan-PKC (recognizes the conserved activation-loop of PKC isoforms) in HepG2 cells cultured with (L45) or without (L0) leucine. I performed western blot analysis to detect IGFBP-1, PKCα and CK2β in L450 and L0 co-IPs (**Figure 4**). Here, I demonstrate that PKCα co-IPs IGFBP-1 in L0 and that PKCα fails to co-IP IGFBP-1 in L450 (**Figure 4A)**. Similarly, PKCα also reciprocally co-IPs CK2β which occurs only in L0 conditions (**Figure 4B)**. However, IGFBP-1 and CK2β reciprocally co-IP both in L450 and L0 (**Figure 4C**). These data demonstrate that although IGFBP-1 is associated with CK2β in both L450 and L0, PKCα only co-IPs with IGFBP-1 and/or CK2β specifically in L0. These findings provide convincing evidence that PKCα is a nutritionally sensitive kinase responding to L0 conditions resulting in enhanced protein-protein interactions with both IGFBP-1 and CK2β. Furthermore, IP with rabbit pre-immune IgG used as a negative control failed to immunoprecipitate IGFBP-1, CK2β or PKCα supporting the rigor of our approach.

In order to identify and confirm the PKC isoform which co-IPs with IGFBP-1 or with CK2β in L0, PKC peptides were analyzed by PRM-MS. PRM-MS detected fifteen PKC specific peptides from the respective IGFBP-1 and CK2β IPs collected from L0 cultured HepG2 cell lysates (**Figure 5**). Three out of 15 detected PKC specific peptides were homologous peptides unique to conventional PKC isoforms while 12 of 15 were unique solely to PKCα (**Table 1**). Each detected PKC peptide spawned at least four daughter ions with co-detection of the parent immunoprecipitating protein indicating robust detection (**Figure 5B-D**). IGFBP-1 peptides were co-detected from both IGFBP-1 and CK2β IPs with specific detection of peptides containing IGFBP-1 phosphorylation sites Ser98, Ser101, Ser119 and Ser169 with the Ser119 peptide being detected with the highest intensity (**Figure 5E**). This targeted MS approach corroborates Western blot

findings (**Figure 4**); IGFBP-1 co-IPs CK2β and PKCα; CK2β co-IPs IGFBP-1; and PKCα, and Pan-PKC co-IPs IGFBP-1 and CK2β in L0. PRM-MS data provide strong evidence that the PKC isoform involved in L0 is PKCα which is the specific interacting PKCα isoform with CK2 and IGFBP-1 in L0.

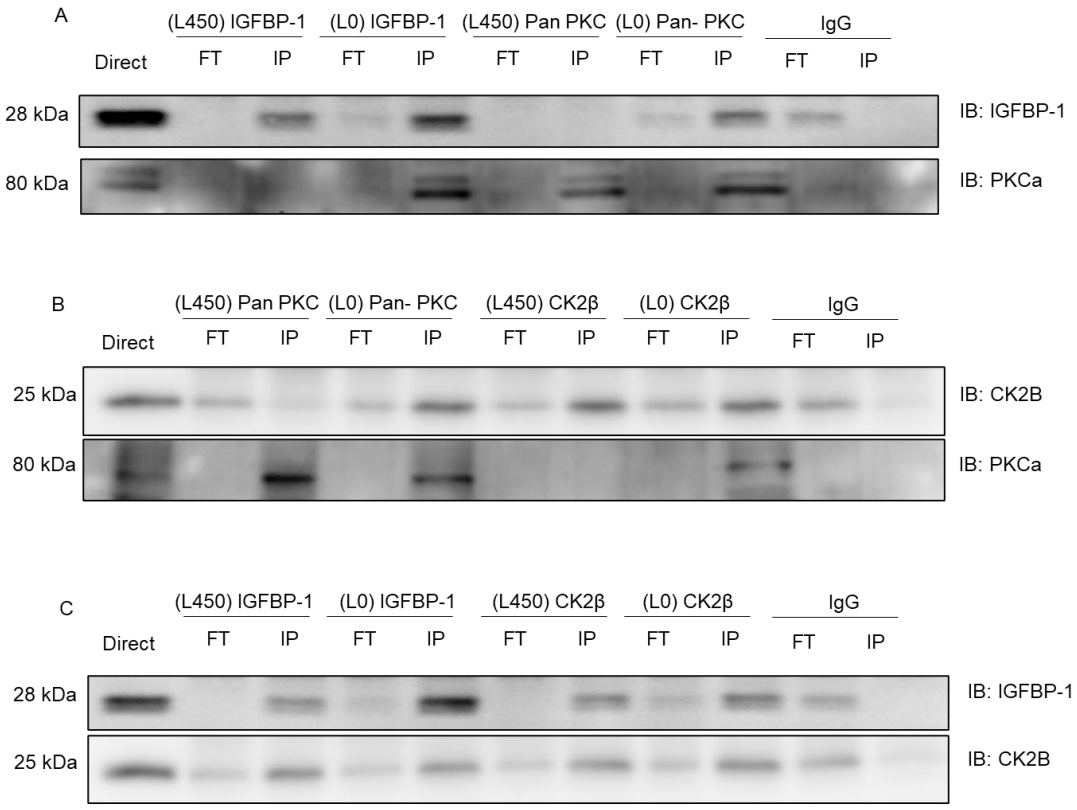

Figure 4. IGFBP-1, CK2β and PKCα reciprocally co-immunoprecipitated in L0 conditions. HepG2 cells were cultured in L450 and L0 media, lysed and immunoprecipitated (IP) using total IGFBP-1 (mAb 6303), polyclonal CK2β, polyclonal pan-PKC antibodies and rabbit pre-immune serum (IgG). (A) IP of IGFBP-1 and PKCα demonstrating reciprocal IGFBP-1+PKCα co-IP in L0. (B) IP of PKCα and CK2β demonstrating reciprocal PKCα+CK2β co-IP in L0. (C) IP of IGFBP-1 and CK2β demonstrating reciprocal IGFBP-1+CK2β co-IP in L450 and L0. The IP'd proteins were immunoblotted for total IGFBP-1 using polyclonal IGFBP-1, polyclonal CK2β, and mAb PKCα antibodies. IP using rabbit IgG failed to IP IGFBP-1, PKCα and CK2β.

A

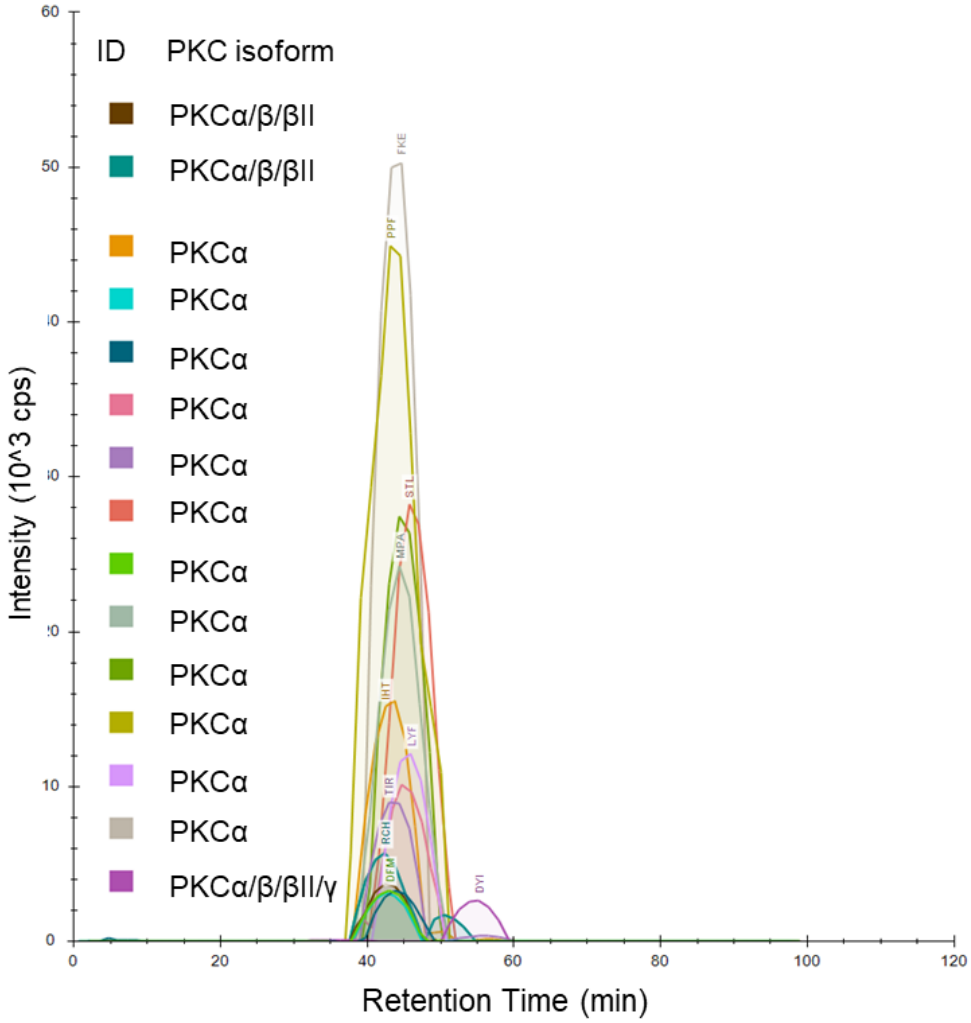
ID
PKC isoform
PKCα/β/βII
PKCα/β/βII
PKCα
PKCα
PKCα
PKCα
PKCα
PKCα
PKCα
PKCα
PKCα
PKCα
PKCα
PKCα/β/βII/γ
Intensity (10^3 cps)
Retention Time (min)
0
20
40
60
80
100
120
10
50
FKE
PPF
STL
MPA
IHT
LYF
TIR
RCH
DYI

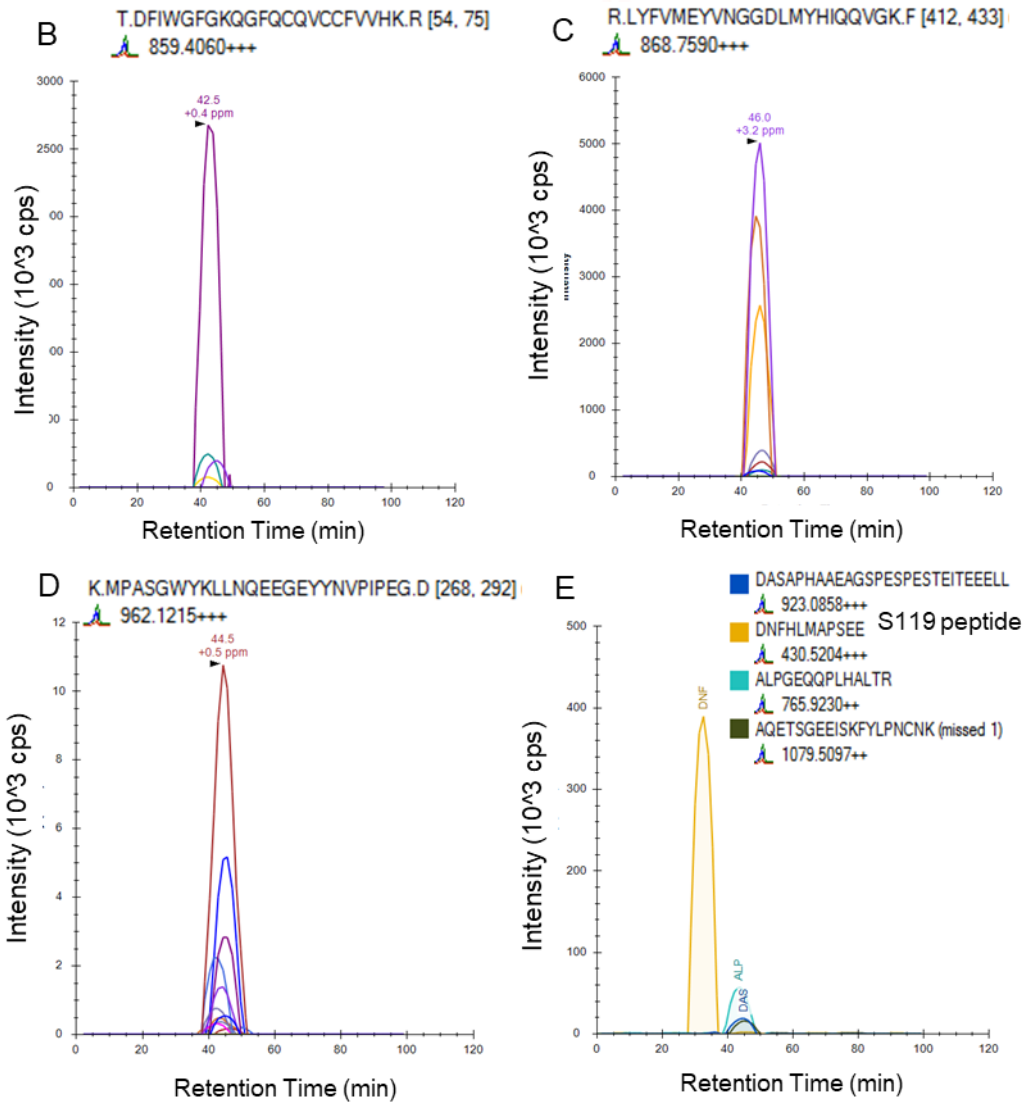

Figure 5. PKC interaction with IGFBP-1 and CK2β in L0. HepG2 cells cultured in L0 media were independently IP'd using anti-IGFBP-1 and anti-CK2β antibodies and analyzed by PRM-MS. (A) Detection of PKC peptides by PRM-MS from IGFBP-1 immunoprecipitation. Chromatogram shows total transitions for 15 PKC-specific peptides, each peaks monitor at least 4 daughter ions. (B-D) Representative spectra of each daughter ion used to detect the presence of PKC from IP samples. (E) Co-detection of IGFBP-1 protein. Chromatogram shows total transitions for 4 IGFBP-1 peptides, each peak monitors at least four daughter ions. All samples were doubly digested by trypsin and Asp-N protease and C18 cleaned prior to MS.

Table 1. Detection of PKCα peptides with shared homology among conventional PKC isoforms. IGFBP-1 and CK2β immunoprecipitation from L0 cultured HepG2 cells co-immunoprecipitated homologous cPKC and PKCα specific peptides detected by PRM-MS.

Peptide number	ID	Sequence	cPKC Homology
1		T.DFIWGFGKQGFQCQVCCFVVHK.R [54, 75]	PKCα + PKCβ + PKCβII
2		K.RCHEFVTFSCPGA.D [76, 88]	PKCα + PKCβ + PKCβII
3		K.IHTYGSPTFCDHCGSLLYGLIHQGMK.C [105, 130]	PKCα
4		C.DHCGSLLYGLIHQMKC.D [115, 131]	PKCα
5		C.DMNVHKQCVINVPSLCGM.D [135, 152]	PKCα
6		K.QCVINVPSLCGMDHTEK.R [141, 157]	PKCα
7		K.TIRSTLNPQWNESFTFK.L [213, 229]	PKCα
8		R.STLNPQWNESFTFKLK.P [216, 231]	PKCα
9		N.DFMGSLSFGVSELMKMPASGWYK.L [253, 275]	PKCα
10		K.MPASGWYKLLNQEEGEYYNVPIPEG.D [268, 292]	PKCα
11		K.LLNQEEGEYYNVPIPEG.D [276, 292]	PKCα
12		K.PPFLTQLHSCFQTVDR.L [396, 411]	PKCα
13		R.LYFVMEYVNGGDLMYHIQQVGK.F [412, 433]	PKCα
14		K.FKEPQAVFYAAEISIGLFFLHK.R [434, 455]	PKCα
15		P.DYIAPEIIAYQPYGK.S [502, 516]	PKCα + PKCβ + PKCβII + PKCγ

3.2 PKCα siRNA silencing reduces IGFBP-1 phosphorylation

To confirm the mechanistic involvement of PKCα in mediating IGFBP-1 phosphorylation in L0, I silenced the PKCα isoform in HepG2 cells cultured with and without leucine. PKCα siRNA reduced PKCα expression in both L450 and L0 conditions with high efficiency (–71% ($p = 0.0003$) and –70% ($p = <0.0001$) respectively) (Figure

A3). PKCα knockdown reduced total IGFBP-1 secretion by –51% (p = 0.015) in L450 and –36% (p = 0.0428) in L0 compared to their respective scramble siRNA controls. Further PKCα knockdown prevented L0-mediated induction of total IGFBP-1 secretion which was reduced to levels comparable to scramble siRNA transfected L450 treatment (–1%, p = 0.96) (**Figure 6A**).

PKCα knockdown affected all three IGFBP-1 phosphorylation sites (**Figure 6B-D**) both with and without leucine. In L450, PKCα knockdown reduced pSer101 by –78% (p = 0.0035), pSer119 by –67% (p = 0.0106) and pSer169 by –75% (p=0.0193). In L0, PKCα knockdown also reduced pSer101 by –56% (p = 0.0014), pSer119 by –39% (p = 0.005) and pSer169 by –39% (p = 0.0086).

Furthermore, PKCα knockdown reduced L0 mediated induction of IGFBP-1 at pSer101 (–37%, p = 0.0309) and IGFBP-1 pSer119 (–21%, p = 0.0447) compared to L450 transfected with scrambled siRNA (**Figure 6B, C**). Overall, these data suggest that the PKCα is involved in mediating both the increased total IGFBP-1 secretion and the IGFBP-1 hyperphosphorylation in response to L0.

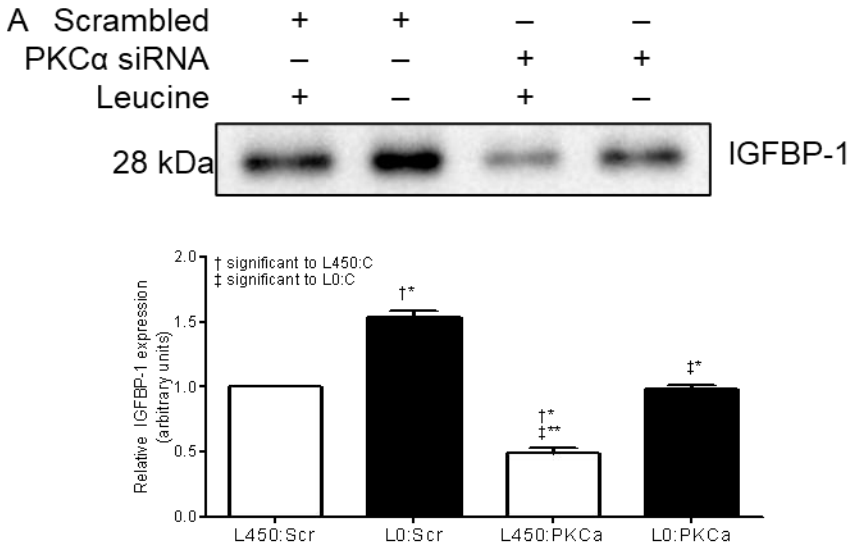

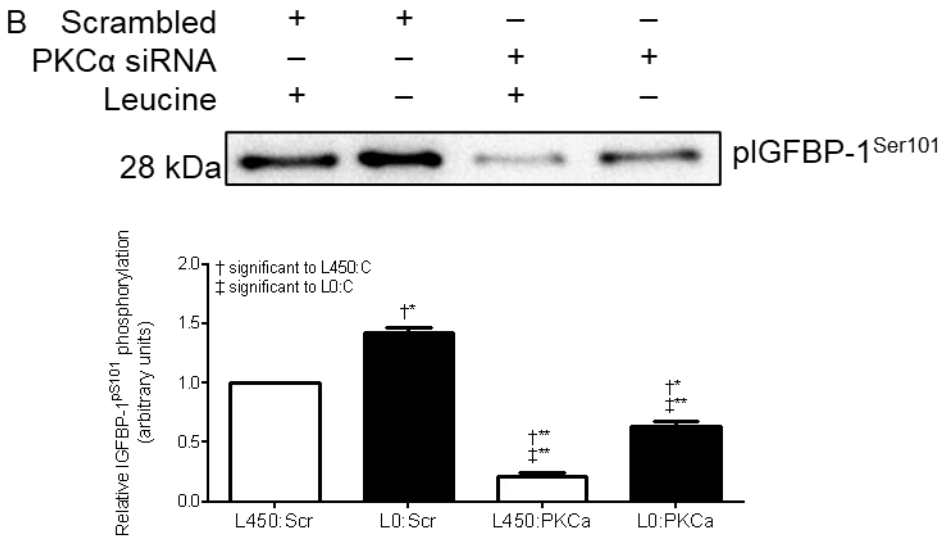
B Scrambled + + – –
PKCα siRNA – – + +
Leucine + – + –
28 kDa
pIGFBP-1Ser101
Relative IGFBP-1pS101 phosphorylation (arbitrary units)
† significant to L450:C
‡ significant to L0:C
2.0
1.5
1.0
0.5
0.0
L450:Scr
L0:Scr
L450:PKCa
L0:PKCa

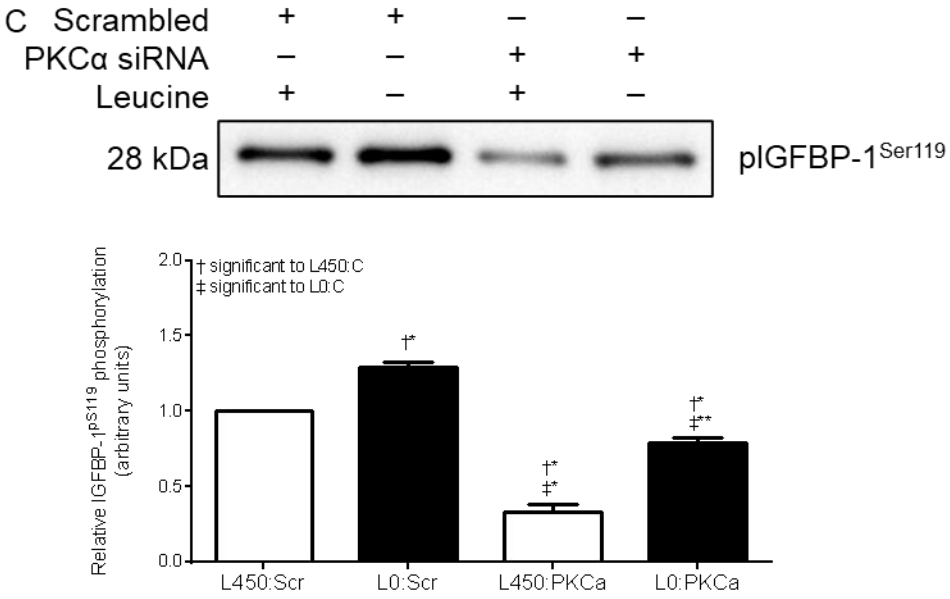
C Scrambled + + – –
PKCα siRNA – – + +
Leucine + – + –
28 kDa
pIGFBP-1Ser119
Relative IGFBP-1pS119 phosphorylation (arbitrary units)
† significant to L450:C
‡ significant to L0:C
2.0
1.5
1.0
0.5
0.0
L450:Scr
L0:Scr
L450:PKCa
L0:PKCa

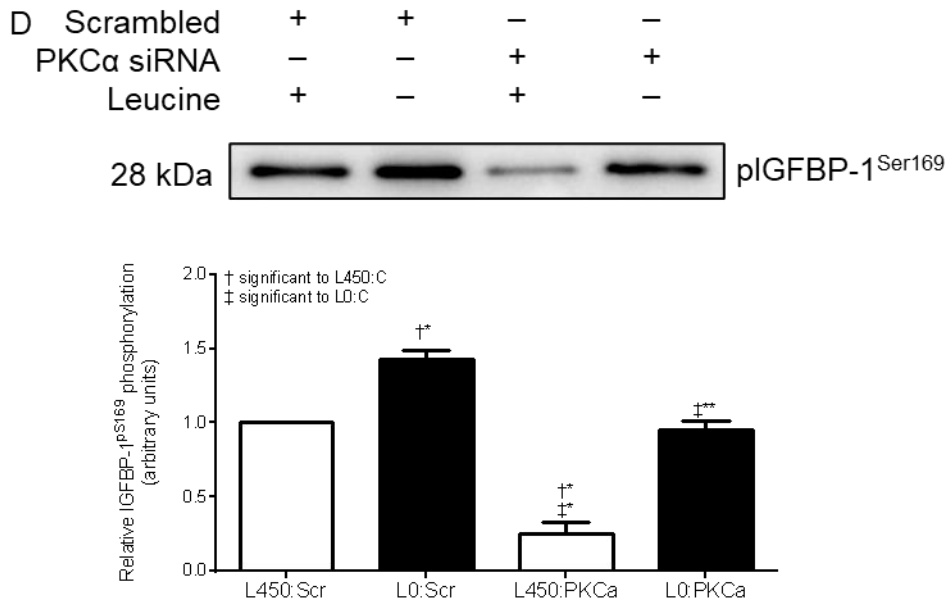

Figure 6. The effect of PKC*α* silencing on IGFBP-1 secretion and phosphorylation. HepG2 cells were treated with scrambled or PKCα siRNA for 24 hours and subsequently cultured in L450 or L0 media for 48 hours (n=3 each). Representative western blots of conditioned HepG2 CM indicating (A) total IGFBP-1 and IGFBP-1 phosphorylation at (B) Ser101, (C) Ser119 and (D) Ser169. Values are displayed as mean + SEM. **p*< 0.05, ***p*= 0.001-0.05, ****p* < 0.0001 versus control; One-way analysis of variance; Dunnet's Multiple Comparison Test; n=3.

3.3 Immunofluorescence staining and proximity ligation assay indicate PKCα + IGFBP-1 and PKCα + CK2β interactions are induced by leucine deprivation

I performed dual immunofluorescence (IF) to investigate cellular staining as an additional alternative approach to investigate potential interactions between PKCα+IGFBP-1 (**Figure 7**). Dual IF of PKCα+IGFBP-1 (**Figure 7A**) demonstrates mostly cytosolic PKCα (**Figure 7A; i, v**) and IGFBP-1 (**Figure 7A; ii, vi**) staining with more pronounced perinuclear IGFBP-1 staining in L0. Merged channel images (**Figure 7A; iii, vii**) of PKCα+IGFBP-1 demonstrate greater yellow fluorescence, indicating an increased overlap between PKCα and IGFBP-1 fluorescence signals suggesting increased co-localization between PKCα and IGFBP-1 as compared to L450 conditions.

I then employed the highly sensitive and specific *in situ* proximity ligation assay (PLA) complementary to dual IF for PKCα+IGFBP-1 (**Figure 7B**). Within HepG2 cells cultured in L450, limited PLA signals were observed (**Figure 7B; a**). PLA signals between PKCα+IGFBP-1 were induced by L0 (**Figure 7B; b**). L0 significantly increased PKCα+IGFBP-1 proximity reactions by +193% ($p < 0.0001$) (**Figure 7B; d**).

I then investigated a potential PKCα+CK2β interaction in L0 utilizing similar dual IF staining which demonstrated strong co-localization of PKCα+CK2β in L450 and L0 (**Figure 8A**). Furthermore, PLA demonstrated an abundance of proximity signals between PKCα+CK2β in L450 (**Figure 8B; a**) and L0 (**Figure 8B; b**). Automated quantification of PLA signals demonstrated a modest increase in PLA signals derived from PKCα and CK2β proximity signals in L0 compared to L450 (+24%, $p = 0.0293$) (**Figure 8B; d**). Considering the failure to detect co-IP of PKCα and CK2β in L450 (**Figure 4B**), the abundance of proximity reactions between PKCα+CK2β in L450 (**Figure 8B; a**) may be due to the ubiquitous nature of both proteins [213,264]. However, successful co-IP of PKCα and CK2β and the increase of PKCα+CK2β PLA signals in L0 indicate that a limitation in leucine availability induces a PKCα+CK2β interaction. Overall, PLA indicates close proximity and potentially increased interactions of both PKCα+IGFBP-1 and PKCα+CK2β in HepG2 cells cultured under L0.

Furthermore, we previously found that IGFBP-1+CK2β interactions were induced in hypoxia in HepG2 cells [212]. Here, I examined IGFBP-1+CK2β interactions in L0 (**Figure 9**) in HepG2 cells. Co-localization between IGFBP-1 and CK2β were similarly induced by L0 (**Figure 9A**). Complementary PLA demonstrated an +60% increase ($p = 0.0131$) in IGFBP-1+CK2β proximity reactions (**Figure 9B; d**).

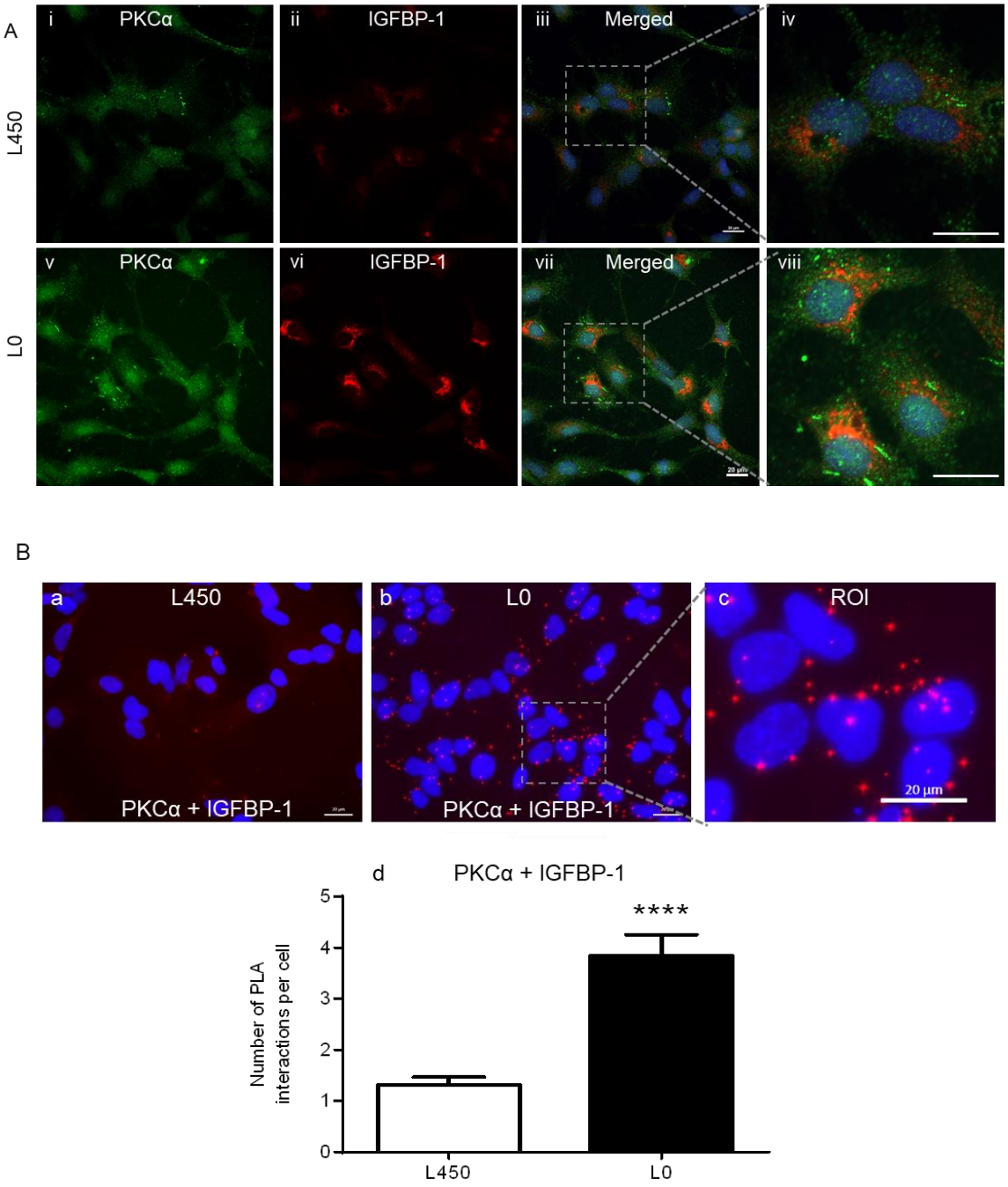

Figure 7. L0 mediates PKCα interaction with IGFBP-1. HepG2 cells were cultured in L450 or L0 media and (A) immunostained to visualize (i, v) PKCα (green) with (ii, vi) IGFBP-1 (red). (iii, vii) Merged images demonstrate co-localization of PKCα and IGFBP-1. (iv, viii) Region of interest within merged channel images. (B) Proximity ligation assay (PLA) for PKCα and IGFBP-1 in (a) L450 and (b) L0 conditions. (c) Region of interest of proximity interactions between PKCα and IGFBP-1 in L0

conditions. (d) Number of PLA signals (red dots) per cell for PKCα and IGFBP-1 proximity reactions in HepG2 cells cultured in L450 and L0 media. Values are displayed as mean + SEM. *p< 0.05, **p= 0.001-0.05, ***p < 0.0001 versus control; paired t-test; Dunnet's Multiple Comparison Test; n=3. Scale bars: 20 μm.

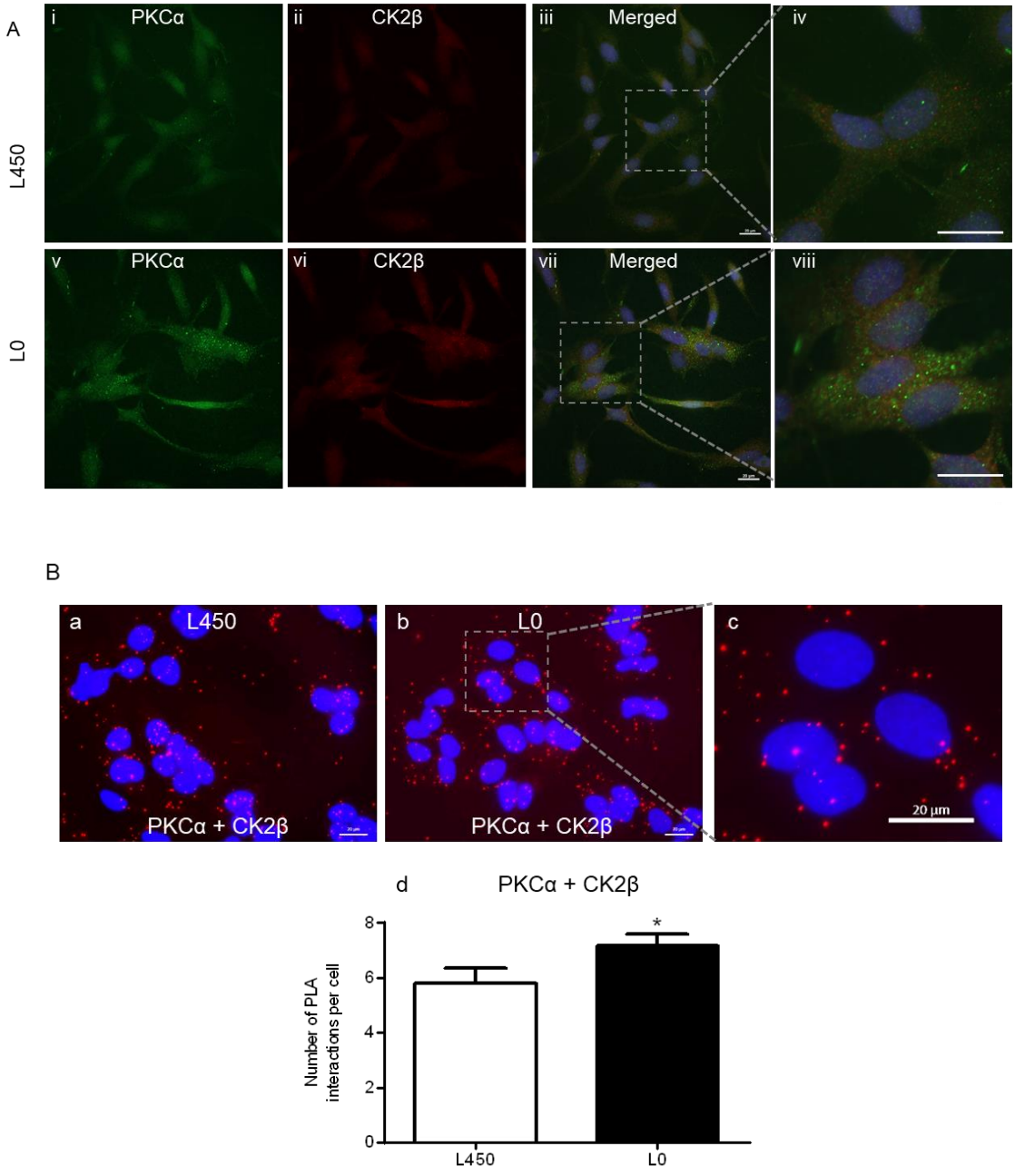

Figure 8. L0 mediates PKCα interaction with CK2β. HepG2 cells were cultured in L450 or L0 media and (A) immunostained to visualize (i, v) PKCα (green) with (ii, vi) CK2β (red). (iii, vii) Merged images demonstrate co-localization of PKCα and CK2β. (iv, viii) Region of interest within merged channel images. (B) Proximity ligation assay (PLA) for PKCα and CK2β in (a) L450 and (b) L0 conditions. (c) Region of interest of proximity interactions between PKCα and CK2β in L0 conditions. (d) Number of PLA

signals (red dots) per cell for PKCα and CK2β proximity reactions in HepG2 cells cultured in L450 and L0 media. Values are displayed as mean + SEM. *p< 0.05, **p= 0.001-0.05, ***p < 0.0001 versus control; paired t-test; Dunnet's Multiple Comparison Test; n=3. Scale bars: 20 μm.

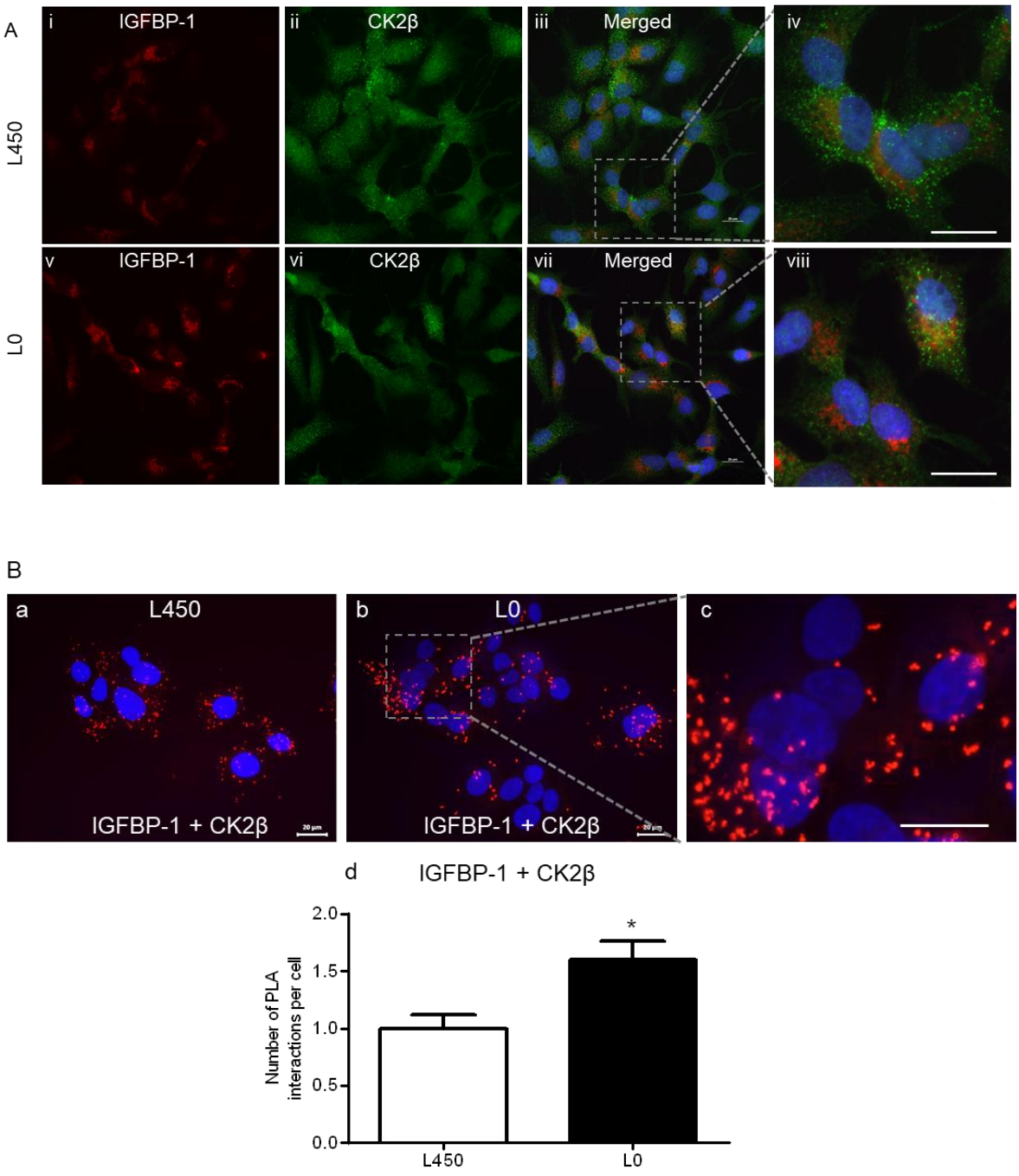

Figure 9. L0 mediates IGFBP-1 interaction with CK2β. HepG2 cells were cultured in L450 or L0 media and (A) immunostained to visualize (i, v) IGFBP-1 (red) with (ii, vi) CK2β (green). (iii, vii) Merged images demonstrate co-localization of PKCα and CK2β. (iv, viii) Region of interest within merged channel images. (B) Proximity ligation assay (PLA) for PKCα and CK2β in (a) L450 and (b) L0 conditions. (c) Region of interest of

proximity interactions between PKCα and CK2β in L0 conditions. (d) Number of PLA signals (red dots) per cell for PKCα and CK2β proximity reactions in HepG2 cells cultured in L450 and L0 media. Values are displayed as mean + SEM. *p< 0.05, **p= 0.001-0.05, ***p < 0.0001 versus control; paired t-test; Dunnet's Multiple Comparison Test; n=3. Scale bars: 20 μm.

3.4 Pharmacological inhibition and activation of PKC demonstrates that PKC mediates IGFBP-1 phosphorylation

Next, I investigated whether PKC inhibition with Bis II and activation with PMA in HepG2 cells cultured with and without leucine alter phosphorylation of IGFBP-1 (**Figure 10**). While total IGFBP-1 secretion in cell media (CM) was increased in response to L0 (+162%, p=0.014), PKC inhibition by Bis II reduced L0 mediated increases in IGFBP-1 secretion (–57%, p=0.02). Bis II also reduced total IGFBP-1 secretion in L450 (–86%, p=0.0004). On the other hand, induction of PKC by PMA enhanced total IGFBP-1 secretion both in L0 (+912%, p=0.0013) and in L450 (+649%, p=0.016) (**Figure 10A**).

The effects of Bis II and PMA were also tested on phosphorylation of IGFBP-1. Phosphorylation at all three IGFBP-1 sites were significantly induced in response to -L0 (pSer101 +376%, p=0.009; pSer119 +110%, p=0.033; pSer169 +404%, p=0.008). Bis II treatment largely prevented IGFBP-1 phosphorylation induced by L0 (pSer101 –78%, p=0.009; pSer119 –66%, p=0.017; pSer169 –89%, p=0.0073) (**Figure 10B-D**), resulting in no significant difference between IGFBP-1 phosphorylation in L450 and L0 with Bis II. PKC inhibition by Bis II in L450 reduced IGFBP-1 phosphorylation (pSer101 –80%, p=0.008; pSer119 –77%, p=0.01; pSer169 –78%, p=0.002).

PMA induced IGFBP-1 phosphorylation in L0 at pSer101 and pSer169 (pS101 +443%, p=0.03; and pSer169 +311%) but to a lesser extent than observed in L450 (pSer101 +1013%, p=0.02; pSer119 +121%, p=0.016; pSer169 +1644%, p=0.0131) (**Figure 10B, D**). However, PKC induction by PMA in L0 did not induce IGFBP-1 phosphorylation at pSer119 (+11%, p=0.58) (**Figure 10C**). Overall, these data led us to conclude that PKC inhibition leads to reduced IGFBP-1 and secretion and phosphorylation while PKC activation increases both IGFBP-1 secretion and phosphorylation, providing strong evidence for a key role of PKCα in IGFBP-1 phosphorylation and secretion in HepG2 cells Furthermore, PKC inhibition prevented L0-induced IGFBP-1 phosphorylation and secretion and L0 prevented PMA induced IGFBP-1 phosphorylation specifically at pS119 (+11%, p=0.58) indicating that PKC mediates L0 induced IGFBP-1 phosphorylation particularly at Ser119 which is consistent

with our previous findings [194]. Heat map analysis derived from PRM-MS data was then utilized to gain a visual overview and demonstrate that PKC contributes to IGFBP-1 phosphorylation at specific dual sites. HepG2 cells treated with Bis II, PMA and 4,5,6,7-tetrabromobenzotriazole (TBB), an ATP site selective inhibitor of CK2 singly and in combination clearly demonstrated the respective expected changes in phosphorylation sites in response to kinase inhibition and activation (**Figure 11**). Dual phosphorylation site analysis of IGFBP-1 at Ser169+Ser174 (**Figure 11A**) and at Ser98+Ser101 (**Figure 11B**) within targeted doubly phosphorylated peptides identified in relation to their relative retention time of an IGFBP-1 internal peptide demonstrated similar findings to our Western blot data (**Figure 10)**. In brief, PKC inhibition and activation with Bis II and PMA universally reduced and induced IGFBP-1 phosphorylation atSer169+174 and Ser98+101, respectively Treatment with Bis II+PMA expectedly minimized the induction of IGFBP-1 phosphorylation by PMA treatment. CK2 inhibition with TBB additionally reduced IGFBP-1 phosphorylation. TBB in conjunction with PMA further mediated the effects of PMA alone on induction of IGFBP-1 phosphorylation, suggesting that PKC and CK2 act in concert in mediating IGFBP-1 phosphorylation.

A

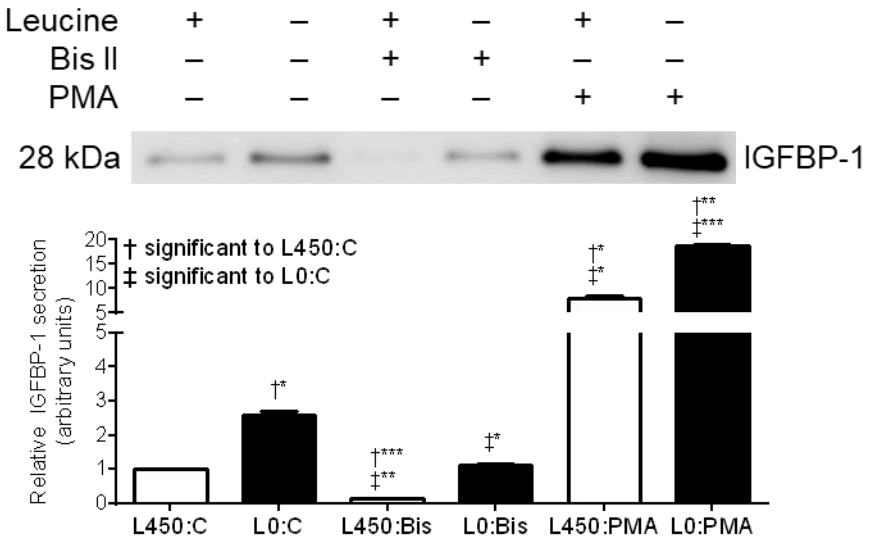
Leucine + – + – + –
Bis II – – + + – –
PMA – – – – + +
28 kDa
IGFBP-1
† significant to L450:C
‡ significant to L0:C
Relative IGFBP-1 secretion (arbitrary units)
L450:C
L0:C
L450:Bis
L0:Bis
L450:PMA
L0:PMA

B

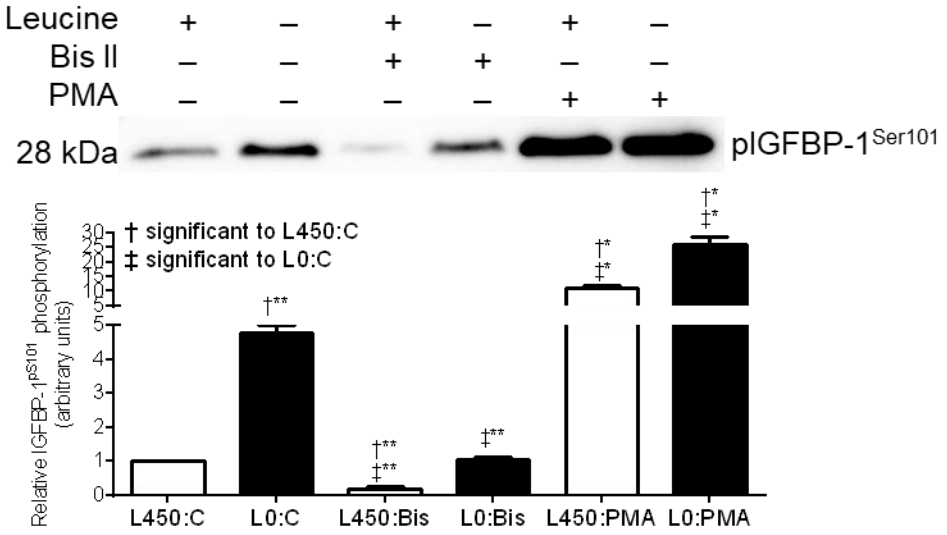
Leucine + – + – + –
Bis II – – + + – –
PMA – – – – + +
28 kDa
pIGFBP-1Ser101
† significant to L450:C
‡ significant to L0:C
Relative IGFBP-1pS101 phosphorylation (arbitrary units)
L450:C
L0:C
L450:Bis
L0:Bis
L450:PMA
L0:PMA

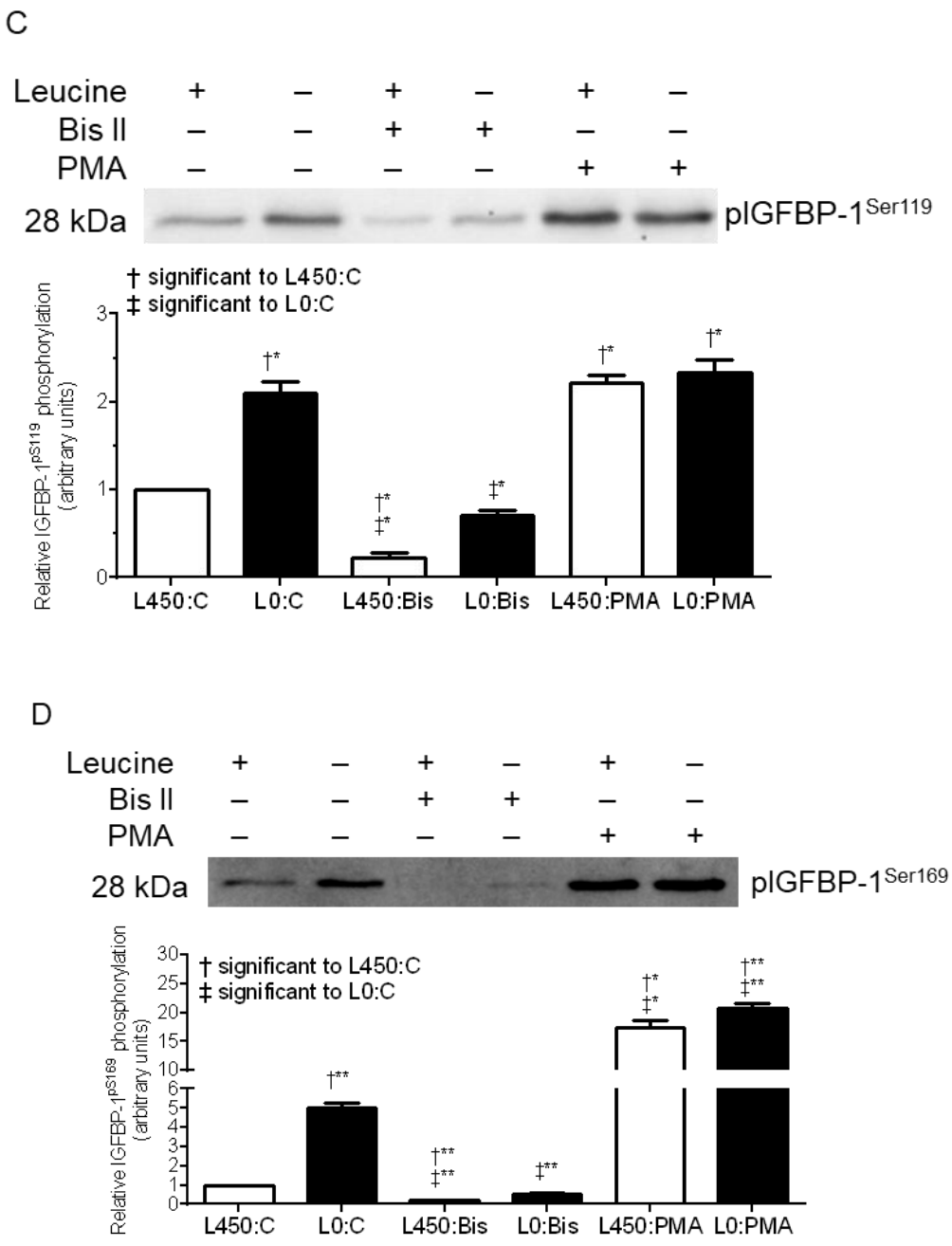

Figure 10. PKC mediates IGFBP-1 phosphorylation. HepG2 cells were treated with Bis II (7.5 μM) and PMA (100 nM) and cultured with (L450) and without (L0) leucine. Representative western blots of HepG2 CM indicating (A) total IGFBP-1 and IGFBP-1 phosphorylation at (B) Ser101, (C) Ser119 and (D) Ser169. Values are displayed as mean

+ SEM. *p< 0.05, **p= 0.001-0.05, ***p < 0.0001 versus control; One-way analysis of variance; Dunnet's Multiple Comparison Test; n=3.

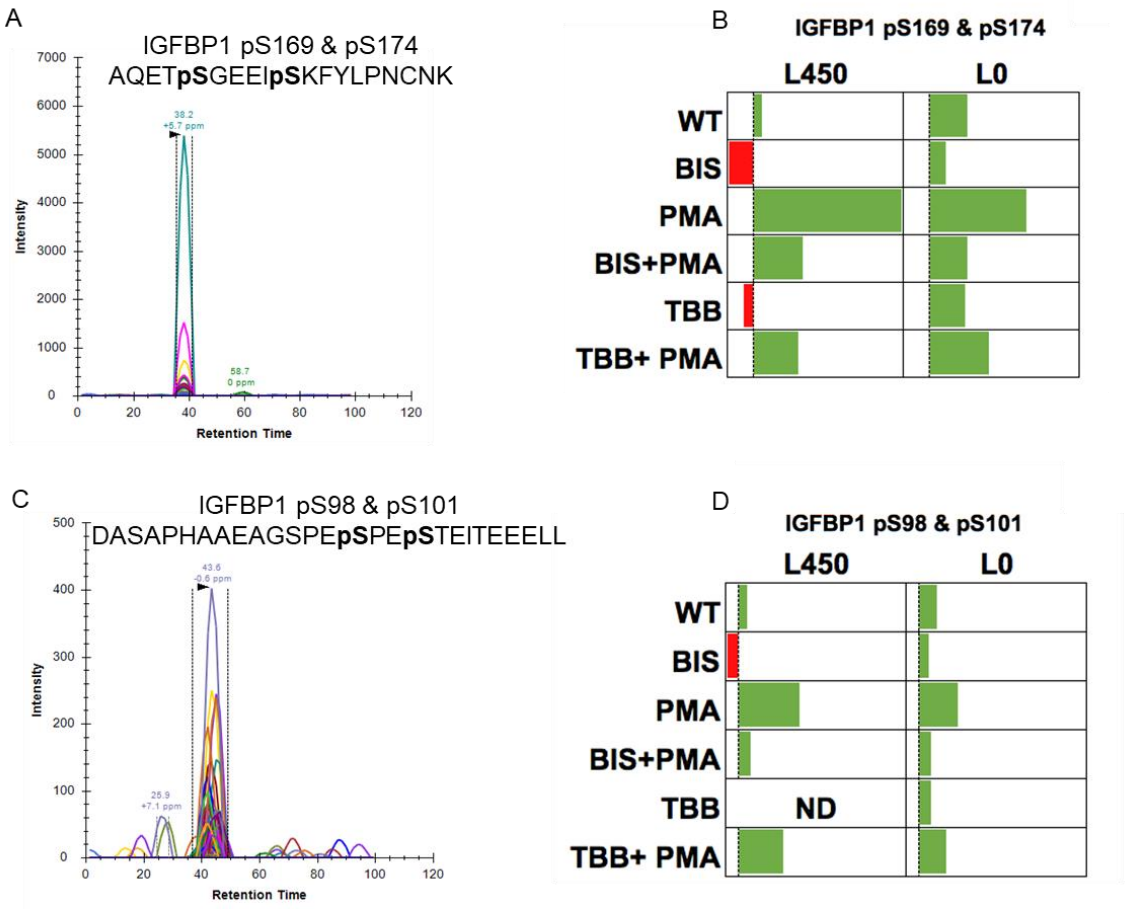

Figure 11. Relative IGFBP-1 phosphorylation detected by PRM-MS. Chromatogram depiction of transitions used for the discovery and detection of dual phosphorylation at (A) IGFBP-1 at Ser169/Ser174 and (B) IGFBP-1 at Ser98/Ser101 sites. Colored traces represent the detection and specificity of each transition ion. (C) Horizontal bar graphs show relative phosphorylation levels of IGFBP-1 combined phosphorylation at Ser169 + Ser174 and Ser98 + Ser101 dually phosphorylated peptide, as determined from total peak intensities of transition ions from PRM MS. Bars show relative positive (green) and negative (red) fold-change.

3.5 Leucine deprivation induces PKCα translocation concurrent with IGFBP-1 secretion in a time dependent manner

As established earlier in this study, PKCα mediates both IGFBP-1 phosphorylation and secretion (**Figures 6, 10 and 11**). I then aimed to identify whether PKCα is specifically activated by L0. HepG2 cells were exposed to L0 (**Figure 12A)** or PKC inducer PMA (**Figure 12B**) in a time dependent manner (0 hrs, 6 hrs, 12 hrs) and were differentially fractionated for enrichment of cytosolic (supernatant) and membrane (pellet) fractions (**Figure 12A-B).** Western blot demonstrated time dependent PKCα translocation to a membrane compartment (pellet) when cells were cultured under L0 (**Figure 12A**). At 0 hrs and 6 hrs, the expression of PKCα was relatively more prominent in the supernatant fraction as compared to pellet fraction. PKCα membrane translocation was induced at 12 hrs where an observed increase in PKCα in the pellet fraction and a decrease in PKCα in the supernatant fraction (**Figure 12A**). Importantly, IGFBP-1 expression was highest at 12 hours of L0 exposure, concomitant with translocation of PKCα. Treatment of cells in parallel with PMA (**Figure 12B**) induced PKCα membrane translocation at 6 hrs which persisted at 12 hrs (**Figure 12B**), showing a similar time course of PKCα translocation.

To obtain additional evidence for PKCα time-dependent translocation as a novel mechanism in nutrient sensitive regulation of IGFBP-1, HepG2 cells exposed to L0 or PMA over the same time course were used to perform IF staining for PKCα (green) (**Figure 13**). PKCα translocation to membrane compartments are shown by white arrows and occurred at 12 hrs of L0 exposure. PMA which mimicked L0 effects as detected by western blot analysis (**Figure 12B**), induced a comparable degree of PKCα membrane translocation. These data corroborate western blot findings of observable PKCα translocation at 12 hrs of L0 exposure and 6 hrs of PMA exposure.

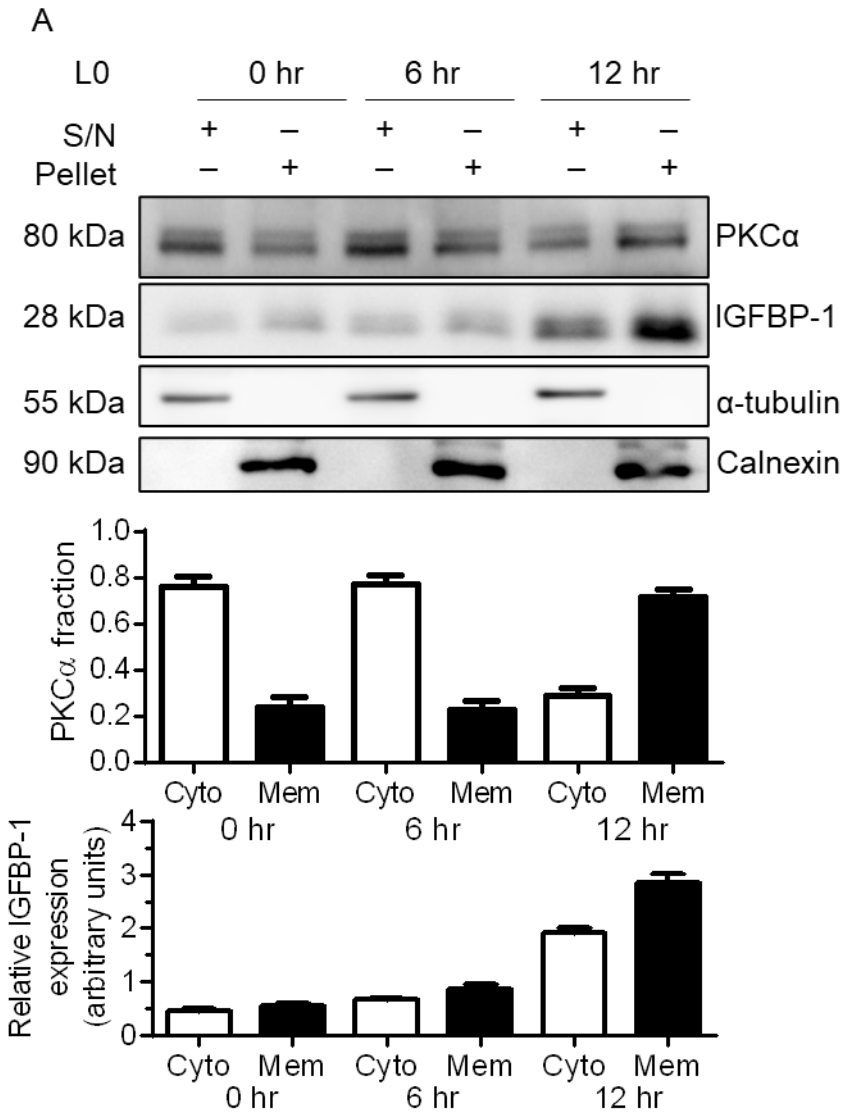
A
L0
0 hr
6 hr
12 hr
S/N
Pellet
80 kDa
PKCα
28 kDa
IGFBP-1
55 kDa
α-tubulin
90 kDa
Calnexin
PKCα fraction
Cyto
Mem
0 hr
6 hr
12 hr
Relative IGFBP-1 expression (arbitrary units)

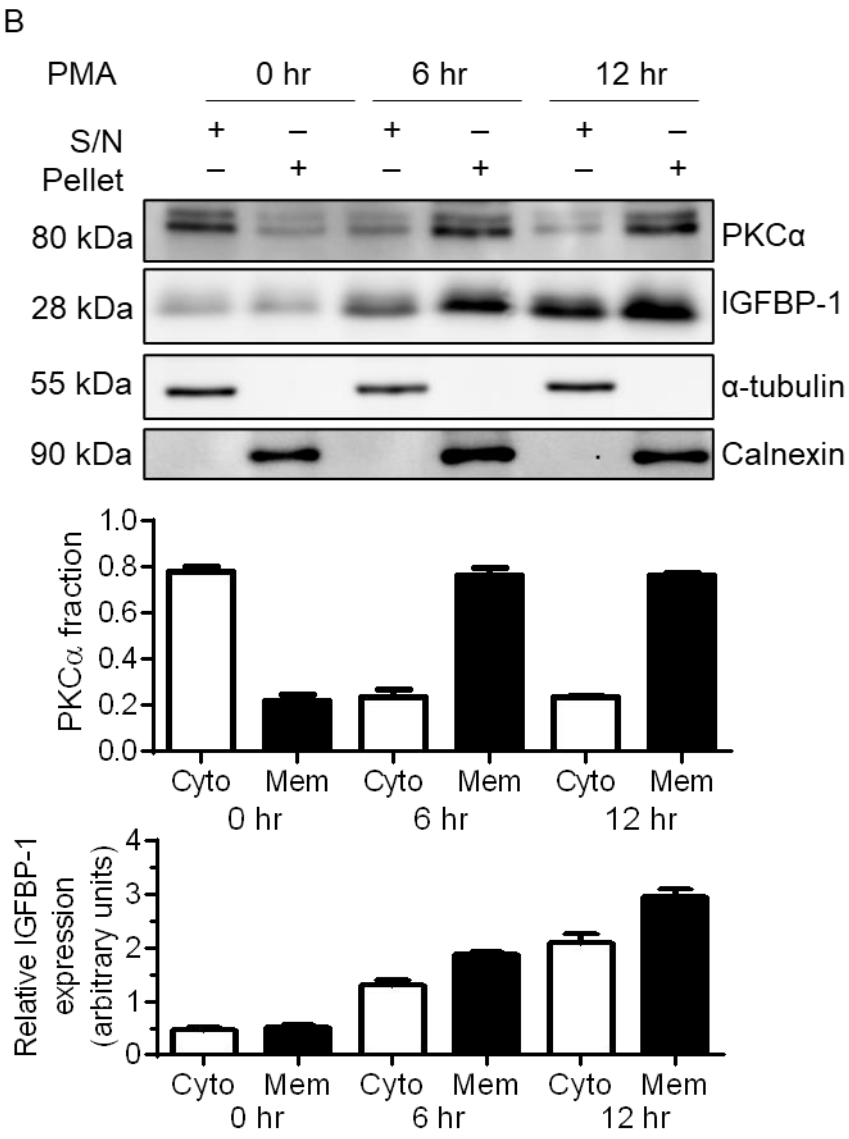

Figure 12. Induction of IGFBP-1 expression is correlated with PKCα translocation. HepG2 cells were deprived of leucine (L0) or treated with PMA in a time dependent manner and subcellularly fractionated by differential centrifugation to yield enriched cytosolic (S/N) and enriched membrane (pellet) fractions. (A) Western immunoblot of fractionated time course treated L0-cultured HepG2 cells for PKCα and IGFBP-1. (B) Western immunoblot of fractionated time course PMA treated HepG2 cells for PKCα and IGFBP-1.

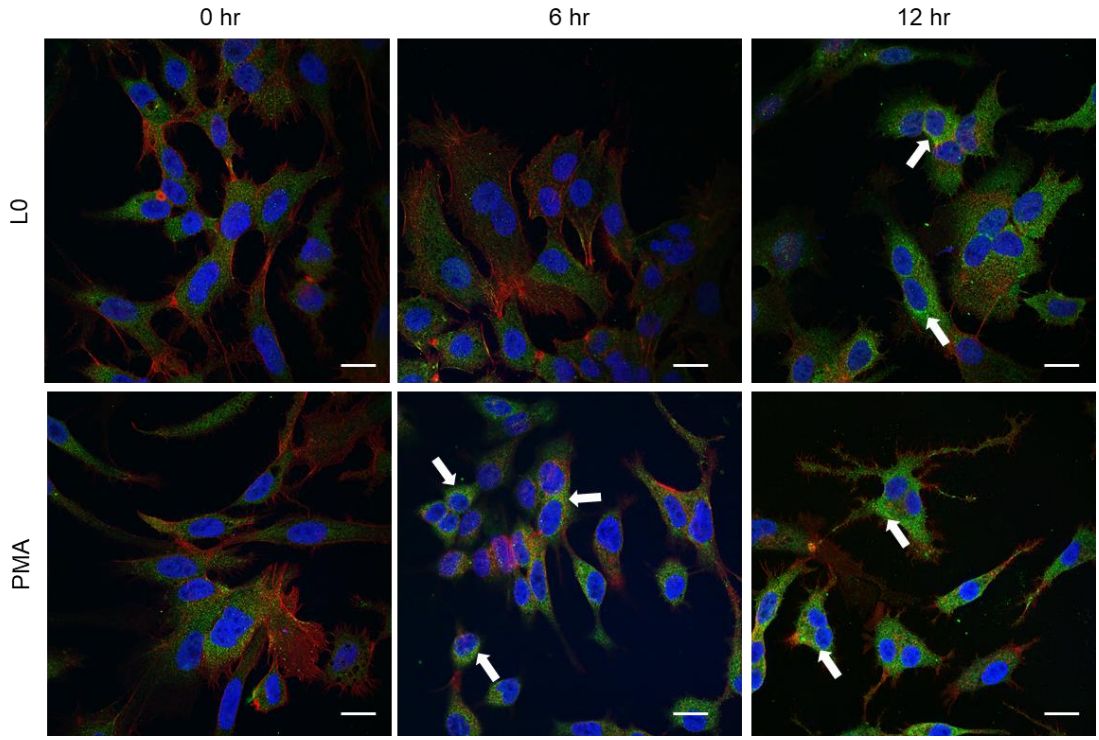

Figure 13. Translocation of PKCα under leucine deprivation and pharmacological activation is time dependent. Dual immunofluorescence of PKCα (green) and F-actin stain phalloidin (red) with nuclear DAPI staining (blue) demonstrate translocation of PKCα with L0 and PMA treatments. Arrows represent areas of high density PKCα staining not present in the controls. Cell morphology changes with PMA treatment but not with L0 treatment. Scale bars: 20 µm.

3.6 IGF-1 bioactivity is altered by PKCα contributions to IGFBP-1 phosphorylation

Cord blood plasma levels of IGF-I and IGFBP-1 are approximately 100 µg/L at term, thus IGFBP-1 cannot bind all circulating IGF-I molecules [265]. However, additional IGFBPs act as IGF-I carrier proteins and both potentiate and inhibit IGF-I mediated actions [151]. Therefore, utilizing an IGF-1R autophosphorylation assay in P6 cells, I combined IGF-I (25 ng) with excess IGFBP-1 (40 µg) (thereby making IGF-I limiting) and demonstrated that changes in IGFBP-1 phosphorylation by PMA treatment (Figure 14A) and PKCα silencing (Figure 14B) affected the bioactivity of IGF-I. IGF-I binding to the IGF-1R results in the autophosphorylation of IGF-1Rβ (Tyr1135) which is an indicator of cell growth and proliferation [131]. IGF-I alone (+IGF-I, positive control) induced pIGF-1R^{Tyr1135} by –1050% ($p < 0.0001$) opposed to the absence of IGF-I (–IGF-I, negative control). Treatment with L450 and L0 media reduced pIGF-1R^{Tyr1135} by –55% ($p = 0.0014$) and –73% ($p < 0.0001$) against +IGF-I alone, respectively. A further –80% decrease ($p < 0.0001$) in IGF-1R autophosphorylation was observed with L450+PMA whilst L0+PMA produced a –88% decrease ($p < 0.0001$). Compared to L450, L0 reduced pIGF-1R^{Tyr1135} by –39% ($p = 0.0492$) while PMA reduced pIGF-1R^{Tyr1135} by –56% ($p = 0.0032$). L0+PMA still produced a significant decrease in IGF-1R activation compared to L0 (–55%, $p = 0.0155$). Scramble siRNA in L450 (–57%, $p = 0.0004$) and L0 (–75%, $p < 0.0001$) markedly reduced +IGF-I stimulated IGF-1Rβ^{Tyr1135} phosphorylation but had little effect on IGF-1R autophosphorylation compared to L450 and L0 treatment alone. PKCα knockdown in L450 and L0 resulted in –44% ($p = 0.0187$) and –49% ($p = 0.0001$) decreases in IGF-1R^{Tyr1135} phosphorylation, respectively. Compared to scramble, PKCα knockdown in L450 induced a +30% ($p = 0.2347$) increase in IGF-1R activation in L450 and a +99% ($p < 0.0001$) increase in IGF-1R activation in L0.

A

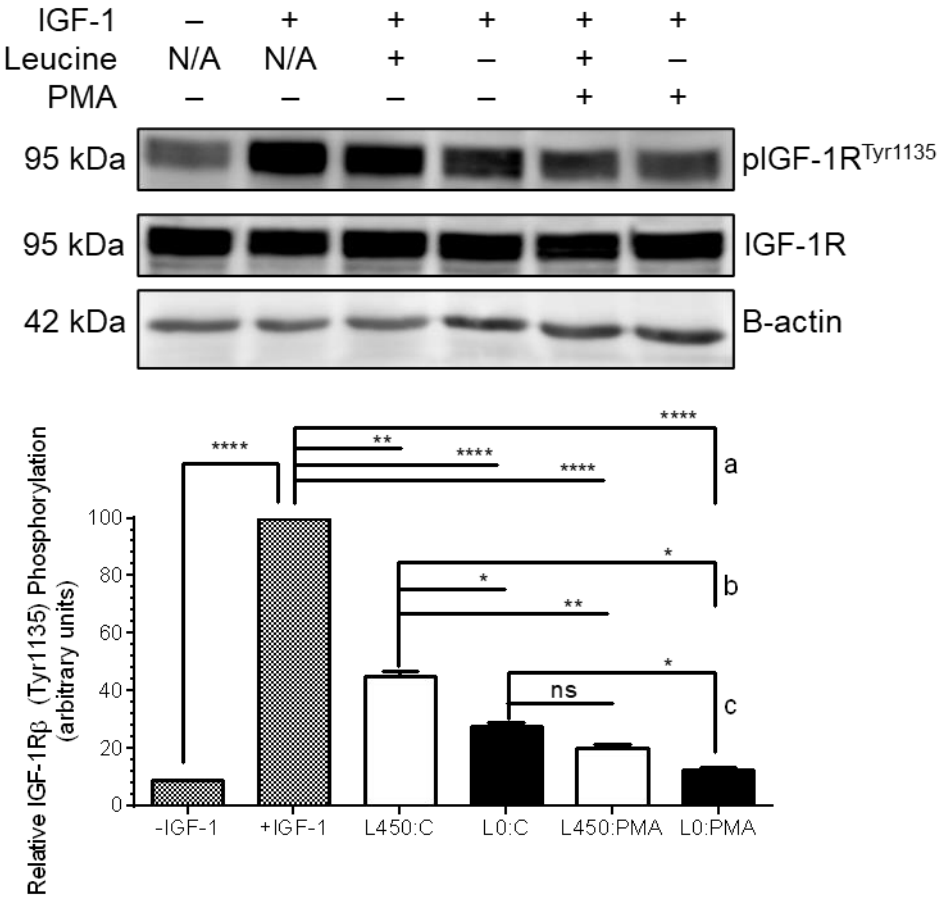
IGF-1 – + + + + +
Leucine N/A N/A + – + –
PMA – – – – + +
95 kDa
pIGF-1R Tyr1135
95 kDa
IGF-1R
42 kDa
B-actin
Relative IGF-1Rβ (Tyr1135) Phosphorylation (arbitrary units)
0
20
40
60
80
100
****
**
****
****
****
a
*
*
**
b
*
ns
c
-IGF-1
+IGF-1
L450:C
L0:C
L450:PMA
L0:PMA

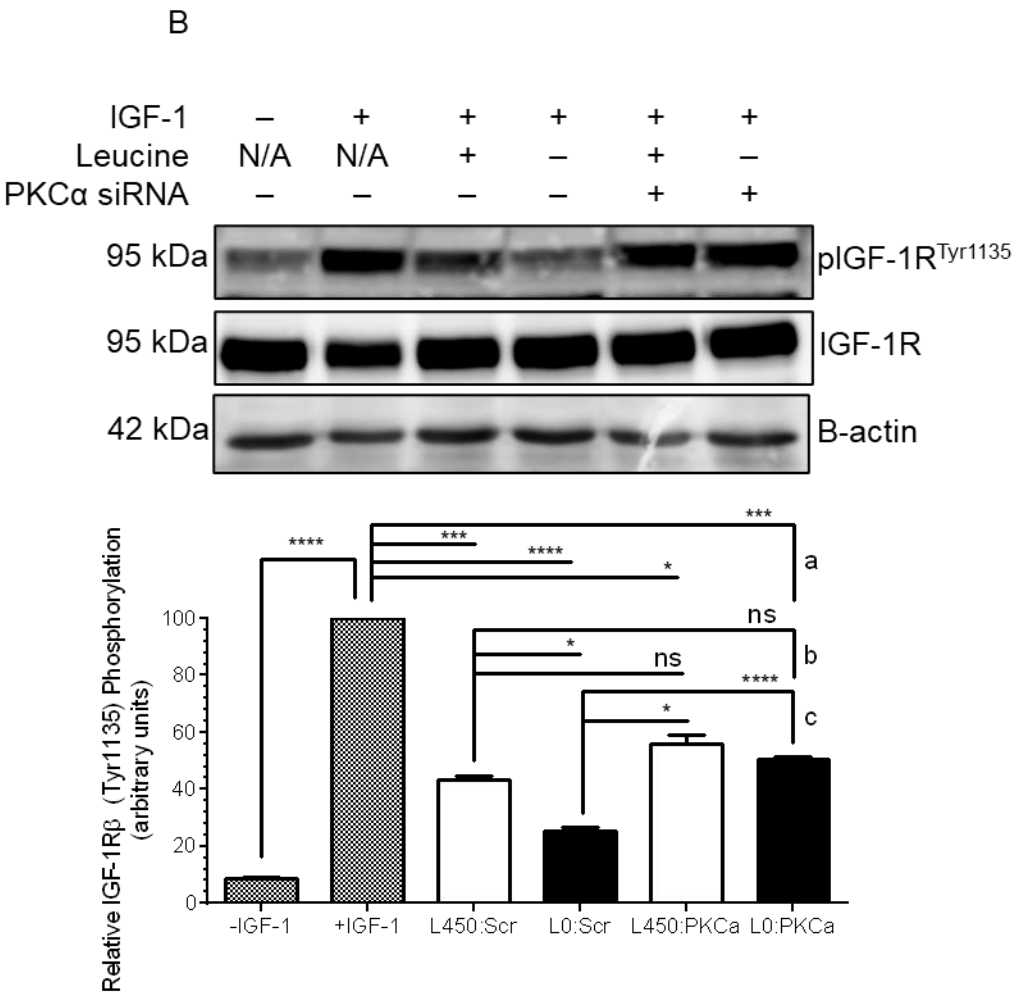

Figure 14. PKCα mediates IGFBP-1 phosphorylation and functionally affects IGF-1Rβ autophosphorylation. Representative Western blots demonstrating the effect of equal amounts of total IGFBP-1 secreted by HepG2 cells bound with IGF-I and incubated with P6 cells to induce IGF-1Rβ autophosphorylation. (A) Equal amounts of total IGFBP-1 from L450, L0, L450+PMA and L0+PMA treatments. Increased abundance of hyperphosphorylated IGFBP-1 species due to L0, PMA or combined L0+PMA treatments significantly decreased IGF-1R activation compared with control (L450). (B) Equal amounts of total IGFBP-1 from L450, L0, L450+PKCα siRNA and L0+PKCα siRNA treatments. Decreased abundance of hyperphosphorylated IGFBP-1 species due to PKCα silencing in L450 and L0 significantly increased IGF-1R activation compared with control (L450). Equal amounts of P6 cell lysate (40 μg) were used on Western blot to detect IGF-1Rβ (Tyr1135) autophosphorylation. Values are displayed as mean + SEM.

*p< 0.05, **p= 0.001-0.05, ***p < 0.0001 versus control; One-way analysis of variance; Dunnet's Multiple Comparison Test; n=3. Significance vs +IGF-I positive control (a). Significance vs basal control (L450:C; L450:Scr) (b). Significance vs leucine deprivation (L0:C, L0:Scr) (c).

3.7 PKCα expression is induced by MNR in baboon fetal liver tissue

Next, I examined the expression of PKCα *in vivo* utilizing the left lobe of baboon fetal liver from a well-established model of MNR associated with moderate FGR [199,200,202]. PKCα expression was determined by Western blot analysis of control and MNR baboon fetal liver tissue which indicated greater expression of PKCα in MNR (+51%, p = 0.0326) at GD 120 (**Figure 15A**) and also at GD 165 (+27%, p = 0.0093) compared to control (**Figure 15B**). These findings were consistent with qualitative IHC data with the same tissue samples. Baboon fetal liver tissue sections also from left lobe showed more prominent immunostaining for PKCα within the parenchyma around the central vein at GD 120 and GD 165 (**Figure 15C-F)** both in MNR and control. MNR induced darker staining within the hepatocytes of the parenchyma and around the central vein at GD 120 (**Figure 15D**) which remained equally increased at GD 165 (**Figure 15F**). These findings demonstrate that PKCα expression is upregulated in MNR at GD 120, preceding the development of FGR which is observable at GD 165. PKCα expression in fetal liver remained elevated at GD 165 (term GD 185). Furthermore, these data are important in suggesting that fetal liver PKCα is sensitive to nutrient restriction *in vivo* due to baboon MNR supporting our *in vitro* data in HepG2 cells showing PKCα activity is nutrient responsive.

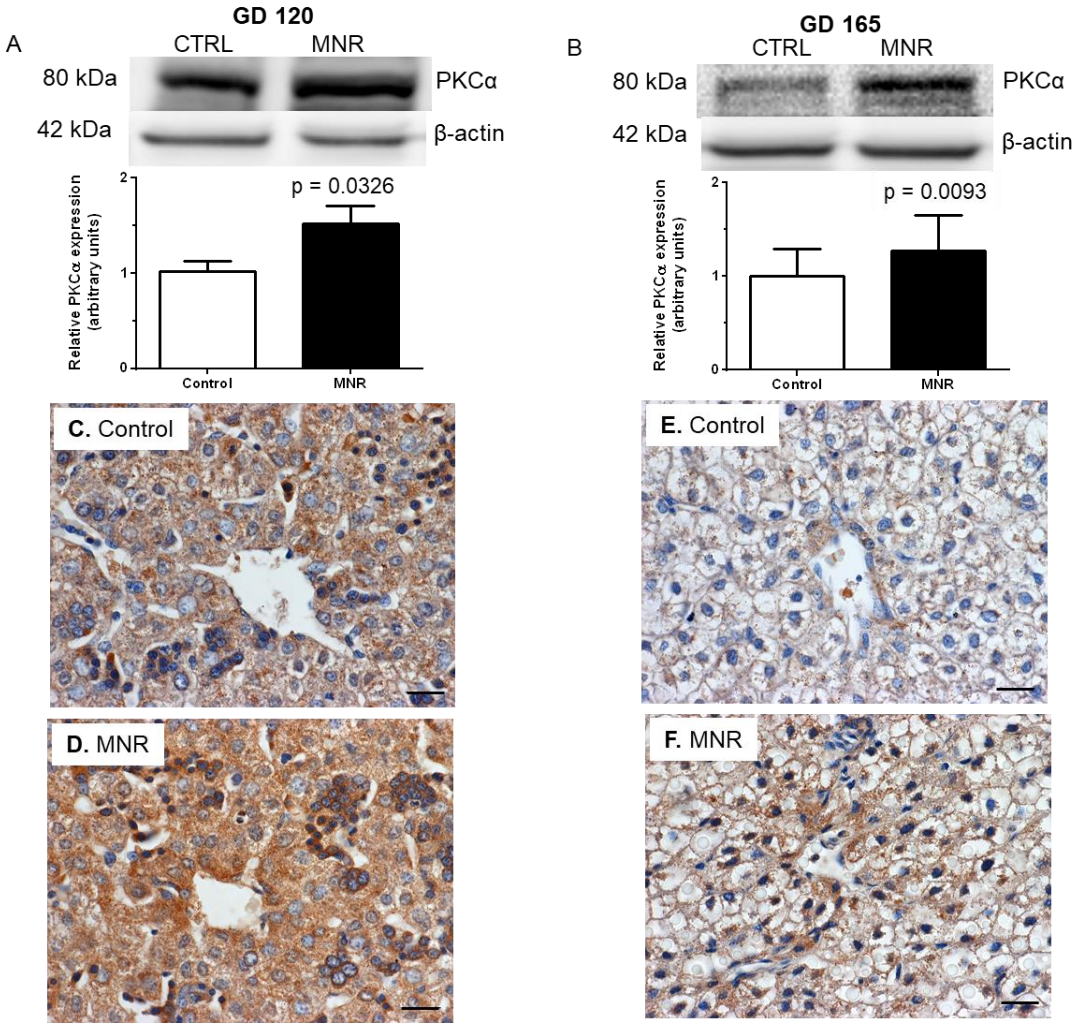

Figure 15. PKCα expression is increased in MNR baboon fetal liver tissue at GD 120 and GD 165. Representative western blot and quantitation for PKCα expression in baboon fetal liver tissue at (A) GD 120 and (B) GD 165. Immunohistochemistry (IHC) for PKCα in sectioned baboon fetal liver tissue at GD 120 (C, D) and GD 165 (E, F). Control and MNR liver tissue sections were fixed on the same slide and immunostained against PKCα and the nucleus counterstained with hematoxylin. All IHC images are 40x. Scale bars are 20 µm. Values are displayed as mean + SEM. One-way analysis of variance; Dunnet's Multiple Comparison Test; n=19 (GD 120), n=24 (GD 165).

4 Discussion

4.1 Key findings

Using HepG2 cells as a model for fetal hepatocytes [203,204,253,254], I report compelling evidence of a novel mechanism of PKCα mediated phosphorylation of IGFBP-1 in response to leucine deprivation. I demonstrate L0-dependent interactions between PKCα, IGFBP-1, and CK2β all of which are induced by L0 and results in IGFBP-1 phosphorylation at sites which mediate IGF-I binding (Ser101 Ser119 and Ser169) [190]. Moreover, I report a novel PKCα translocation stimulus to a membrane compartment dependent on L0, which was mimicked by pharmacological PKC activation and concomitantly induces IGFBP-1 expression. Using a well-established baboon model [94,97,177,201,202,259], I demonstrate for the first time, increased greater PKCα expression in baboon fetal liver in MNR at GD 120 prior to the development of FGR *in vivo*. Our data supports a nutrient sensitive response via PKCα mediates increased fetal hepatic IGFBP-1 expression and phosphorylation in FGR.

4.2 The models of nutrient deprivation

4.2.1 Utilizing leucine deprivation *in vitro*

Provision of the BCAAs mimics the effects of complete amino acids in protein synthesis stimulation however, perfusion of a complete amino acid mixture except the BCAAs has no effect on protein synthesis [266]. Overall, leucine appears to be the most potent BCAA in stimulating protein synthesis [267,268] as well as energy balance regulation [255]. In the liver, leucine does not stimulate global rates of protein synthesis however, promotes the phosphorylation of the downstream effectors of the nutrient sensor mTOR indicating that leucine still enhances signaling in the liver through mTOR [269,270]. The fetal liver is highly involved in regulation of fetal growth and controls the circulation of maternal blood and nutrients [36–38,43,54,55]. During fetal growth, leucine deficiencies specifically are implicated in the development of FGR [30,58,62,65,67,72,73,84,175]. Reduction in placental transfer of leucine to fetal supply is characteristic of FGR [62,67]. Downregulation of amino acid transporter activity responsible for transplacental leucine transport in the

placenta has been further demonstrated [30,58]. The distinct effect of leucine separate from BCAAs have been demonstrated to attenuate maternal nutrient restriction induced growth restriction [84]. The use of leucine deprivation as a cell culture model has been extensively used in our lab to induce IGFBP-1 phosphorylation, mimicking the effects of nutrient restriction induced FGR [94,178,191,194].

4.2.2 Utilizing MNR baboon model of FGR

I further used a well-established MNR baboon model of FGR [97,199–202] to investigate the expression of PKCα in FGR in relation to IGFBP-1 phosphorylation. Previous work using the same baboon model demonstrated specific FGR effects due to 30% caloric restriction, impairing placental development similar to human maternal undernutrition [28,201]. Fetal hepatic and placental IGF systems were similarly impacted in this model compared to human FGR [97,111,201,259]. The fetal liver of this MNR baboon model of FGR previously demonstrated hyperphosphorylation of IGFBP-1, upregulation of the AAR pathway, inhibition of mTOR and increased CK2 activity/expression similarly to our leucine deprivation model in HepG2 cells [94,178,191].

4.3 Significance of nutrient deprivation induced IGFBP-1 hyperphosphorylation in FGR and IGF-I bioavailability

Perturbation of the IGF-axis by IGFBP-1 has been previously proposed as an important mechanism linking limited nutrient availability to FGR [182,271]. Increased IGFBP-1 binding affinity to IGF-I occurs via IGFBP-1 phosphorylation at multiple but discrete serine residues [181,190] which reduces IGF-I bioavailability and has been associated with FGR [189,206,207].

IGFBP-1 phosphorylation has been demonstrated to be induced by mTOR inhibition in hypoxia [179] and the AAR pathway in leucine deprivation [178]. Systematic mTOR inhibition targeting both mTORC1 and mTORC2 induced IGFBP-1 secretion and phosphorylation [179]. The involvement of mTOR in FGR and IGFBP-1 phosphorylation has been well correlated in previous studies [94,177,180,272]. However, Malkani et al., (2015) demonstrated that mTOR regulates only the secretion of IGFBP-1 in leucine deprivation and instead, the AAR pathway regulates IGFBP-1 phosphorylation. FGR is characterized

by decreased amino acid availability which induces the AAR pathway [39,85,274]. Activation of the AAR pathway results in a kinase cascade originating with autophosphorylation of general control nonderepressible 2 (GCN2) in the presence of uncharged tRNA molecules which then phosphorylates eukaryotic initiation factor 2 alpha (eiF2α) subsequently inhibiting global protein synthesis and promoting the translation of activating transcription factor 4 (ATF4) [275–277]. The AAR pathway is additionally intimately intertwined with the mitogen activated protein kinase kinase (MEK)/extracellular signal regulated-kinase (ERK) pathway [278]. Our group evaluated the effectors of the AAR pathway via knockdown and/or inhibition of GCN2, MEK and ERK and determined that inhibition of any of these effectors results in decreased IGFBP-1 phosphorylation, attenuating leucine deprivation induced phosphorylation of IGFBP-1 [178]. Nutrient deprivation directly induces IGFBP-1 mRNA with evidence of mTOR directly mediating IGFBP-1 gene expression [279,280]. Furthermore, we have previously demonstrated that CK2 activity is correlated with IGFBP-1 phosphorylation in leucine deprivation *in vitro* [178,191] and MNR *in vivo* [94,177] and that PKC activity may play a supporting role [191].

4.4 Determining PKC interactions with IGFBP-1 and CK2 in leucine deprivation

Previously, we demonstrated increased IGFBP-1 expression and IGFBP-1 phosphorylation, downregulated mTOR activity, upregulation of the AAR pathway and increased CK2 activity and expression in FGR *in vivo* [94,177]. Furthermore, we have previously demonstrated induced mTOR+CK2β interactions in HepG2 cells in response to hypoxia with accordant increases in IGFBP-1 phosphorylation [212]. However, mTOR does not mediate IGFBP-1 phosphorylation in leucine deprivation, thus, we proposed that PKC may act as a nutrient responsive kinase in mediating IGFBP-1 phosphorylation [178]. In this study, we demonstrated leucine deprivation dependent co-IP of PKCα with IGFBP-1 and PKCα with CK2β. Utilizing PRM-MS, I identified the PKCα as the leucine deprivation dependent PKC isoform interacting with both IGFBP-1 and CK2β. I additionally report leucine deprivation induced interactions of PKCα with IGFBP-1, PKCα with CK2β and IGFBP-1 with CK2β via dual immunofluorescence and proximity

ligation assay with accordant leucine deprivation induced increases in IGFBP-1 phosphorylation. I propose that PKCα instead of mTOR, mediates IGFBP-1 phosphorylation in leucine deprivation via its interactions with IGFBP-1 and CK2β (Figure 16). Previous experimental data implicated a role for PKC in leucine deprivation mediated IGFBP-1 phosphorylation through modulating CK2 activity [191]. Consistent with literature reports, three PKC isoforms, PKCα, PKCβ and PKCζ are reported to regulate CK2 activity in HCT116 and HEK293 cells by directly phosphorylating CK2α at Ser194 and Ser277 [281]. The substrates of intracellular kinases PKC and CK2 are ordinarily cellularly contained.[213,233,282]. However, IGFBP-1 is a secretory protein – likely separated from the same intracellular compartment as PKC and CK2 – and its direct contact with either PKC or CK2 *in vivo* has not been investigated. Extracellular ecto-CK2 may phosphorylate secreted biomineralization proteins, although this seemingly occurs after secretion of the protein; therefore, the current mechanisms as to how CK2 regulates the phosphorylation of IGFBP-1 are unknown [283]. The discovery of Fam20C as the primary secretory protein kinase and its ability to phosphorylate IGFBP-1, albeit at sites distinct from this study, suggests a valuable avenue for pursuing a potential *bona fide* IGFBP-1 kinase [218,284]. Increased Fam20C activity may be necessary to produce hyperphosphorylated IGFBP-1 species; however, regulation of Fam20C activity is not well understood. Increased expression of Fam20A may potentiate the catalytic activity of Fam20C which may be related to increased CK2 activity [213,285].

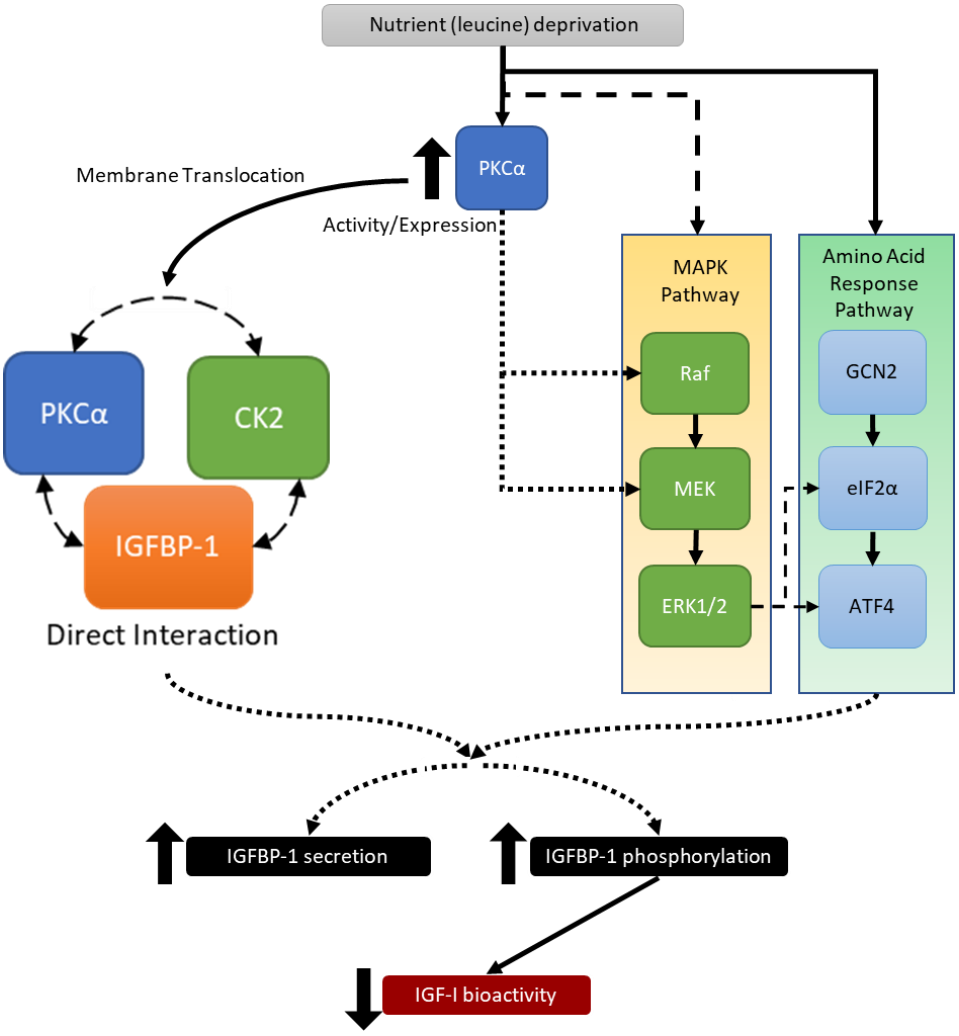

Figure 16. Proposed model of the mechanistic contributions of PKCα in mediating IGFBP-1 secretion and phosphorylation in leucine deprivation. Deprivation of the essential amino acid, leucine, activates PKCα which interacts with CK2 and IGFBP-1 and leads to increased IGFBP-1 secretion and phosphorylation. Leucine deprivation additionally activates the two intimately linked MAPK and AAR pathways which have been previously demonstrated to mediate IGFBP-1 secretion and phosphorylation, in a coordinate manner. PKCα may activate the MAPK pathway and, thus, the AAR pathway. Solid arrows: known mechanism, large dashed arrows: putative direct mechanism, small dashed arrows: putative, indirect mechanism.

4.5 Identification of the PKCα isoform and its role in IGFBP-1 secretion and phosphorylation

Studies on PKC in FGR are limited with little implications of the mechanisms involved and are not applicable to FGR or particularly related to IGFBP-1 phosphorylation [239,240]. PKC regulation of IGFBP-1 expression and secretion has been established previously in HepG2 cells [221] and in human endometrial carcinoma cells [220], but a role for PKC in IGFBP-1 phosphorylation has yet to be demonstrated prior to this study. More than ten PKC isozymes have been identified in humans [286] thus, [239] examined placental PKC isoform profiles in the context of placental insufficiency and demonstrated reduced expression of "anti-apoptotic" cPKC isoforms -α, -βI and -βII while induced expression of "pro-apoptotic" nPKC isoforms -δ and -ε [239]. Specific fetal liver PKC isoform(s) however, have not been investigated. In this study, I aimed to identify the PKC isoform which regulates fetal growth by modulating IGFBP-1 phosphorylation.

Through PRM-MS of co-immunoprecipitation samples followed by gene silencing, I identified PKCα as the PKC isoform which interacts with IGFBP-1 and CK2β and demonstrated that PKCα mediates IGFBP-1 expression and phosphorylation at acidic serine residues in response to leucine deprivation in HepG2 cells. Using conventional inhibitor and activator approaches, I identified respective changes in IGFBP-1 at single sites and close proximity dually phosphorylated IGFBP-1 peptides demonstrating that PKC is positively correlated with IGFBP-1 hyperphosphorylation and that CK2 and PKC act in concert. Using multiple approaches (co-IP, PRM-MS, IF and PLA), I provide convincing data to demonstrate induced interactions between PKCα+IGFBP-1 and PKCα+CK2β are consistent with increased IGFBP-1 phosphorylation and expression in response to L0. I further characterized functional effects of PKCα mediated IGFBP-1 phosphorylation utilizing an IGF-1R autophosphorylation assay in P6 cells, demonstrating that the IGFBP-1 phosphoisoforms generated through PKCα activation and PKCα knockdown reduced and induced the bioactivity of IGF-I, respectively.

4.6 Nutrient responsive activation of PKCα via translocation

Decreased nutrient availability, believed to be central to the development of FGR, differentially affects the multiple isoforms of PKC with distinct functions in a wide variety of biological systems [240–242,244,245]. Low protein diets inhibit PKC activity, abrogating insulin secretion in pancreatic islets [244]. Amino acid deprivation in the MCF-7 breast cancer cell line induces PKCη expression [245]. Leucine stimulates PKC activity in skeletal muscle independent of mTOR and insulin, suggesting a direct nutrient sensitive PKC response [241]. Additionally, leucine also stimulated PKC activity associated with increased mTOR and ERK activity in chicken hepatocytes [242]. Functionally, PKC is activated via phosphorylation and second messengers which mediate mechanisms such as protein-protein interactions, subcellular targeting and PKC translocation to membrane compartments [235]. Activation of conventional PKC isoforms (cPKCs) has been reported by conserved autophosphorylation of PKC at Thr250 [287]. Prior to this study, whether any specific PKC isoform(s) played a role in fetal hepatic IGFBP-1 phosphorylation was undetermined.

Activation of PKC isozymes are associated with its translocation from the cytosol to a membrane compartment [231,288,289].). In our study, I used membrane fraction enrichment and IF to demonstrate time dependent PKCα membrane translocation, indicative of PKCα activation in response to L0 which was mimicked by PMA [289,290]. Concomitantly, IGFBP-1 expression was induced on the same time course as PKCα translocation, linking PKCα activation to increased IGFBP-1 expression in L0. Overall, our findings demonstrate that L0 activates and induces PKCα translocation which is associated with increased IGFBP-1 expression and induces an interaction of PKCα with IGFBP-1 associated with an increase in IGFBP-1 phosphorylation. Furthermore, I report significant increases in PKCα expression prior and during the gestational dates which physical manifestations of pathological growth restriction occur in an established MNR baboon model of FGR [199–202]. Our previous work utilizing the same baboon model demonstrated increased IGFBP-1 expression and IGFBP-1 phosphorylation, downregulated mTORC1/ C2 activity, upregulation of the AAR pathway and increased CK2 activity/expression in FGR *in vivo* [94,177]. mTOR is largely involved in FGR [180] and

has been shown to mediate CK2 activity [177] while CK2 has been demonstrated to phosphorylate IGFBP-1 *in vitro* [214,215]. We have previously demonstrated induced mTOR+CK2β interactions in HepG2 cells in response to hypoxia with accordant increases in IGFBP-1 phosphorylation [212]. In accordance to our *in vitro* and *in vivo* data demonstrating nutrient responsive PKCα activity and expression, I propose that PKCα instead of mTOR, mediates IGFBP-1 phosphorylation via its interactions with IGFBP-1 and CK2β in leucine deprivation and MNR.

4.7 The involvement of PKC in nutrient responsive signaling

The models we previously used all implicate the involvement of mTOR and the AAR as nutrient responsive signaling pathways controlling the phosphorylation of IGFBP-1 both *in vitro* and *in vivo* [94,177–179]. mTOR signaling is highly responsive to concentration changes in leucine and essential amino acids in general [255,291,292]. Our group has characterized the involvement of mTOR inhibition in FGR via increased IGFBP-1 phosphorylation [177,180]. Our data demonstrating that PKC is nutrient responsive to leucine availability has further application to FGR pathology via mTOR. PKC functions both upstream and downstream of mTOR in several different tissue types via integration of nutrient related stimuli. Upstream activation of mTOR in response to hypertrophic stress, e.g. high leucine or insulin is dependent upon coordinated activation of both PKCε and PKCδ [293,294]. Activation of mTOR via PKC is dependent upon translocation of PKC to perinuclear endosomes adjacent to mTOR localized to perinuclear lysosomes in response to high amino acid stimuli [295]. Within FGR pathology, low nutrient stress resulting in mTOR inhibition may be involved to coordinate PKC through a separate mechanism to induce IGFBP-1 phosphorylation in place of coordinated activation of mTOR via PKC in high nutrient conditions.

Amino acid deprivation activates the AAR, a separate nutrient sensitive mechanism distinct from mTOR signaling [296,297]. The AAR pathway mediating IGFBP-1 phosphorylation is dependent upon GCN2, eiF2α and MEK/ERK and AAR upregulation is highly correlated with FGR onset [94,178,180,298]. Although the MEK/ERK pathway is not

consolidated as part of the AAR pathway, MEK/ERK is required for the translational responses of AAR in amino acid deprivation [278]. PKC is largely integrated in the MEK/ERK pathway in several cell types. PKCα, specifically, seemingly mediates MEK/ERK activation at several effectors. Activation of MEK/ERK by rapidly accelerated fibrosarcoma (Raf) kinase is the classical pathway of transmitting extracellular signals to mediate cell cycle progression and apoptosis [299]. Amino acid deprivation activates the Raf/MEK/ERK pathway via protein phosphatase 2A (PP2A) by activating dephosphorylation of Raf at Ser259 [300,301]. PKCα can similarly activate the Raf/MEK/ERK pathway in a manner independent of Raf phosphorylation at Ser259 [302], possibly through direct phosphorylation of Raf [303] or through de-activating phosphorylation of Raf kinase inhibitory protein (RKIP) [304]. Downstream of Raf, PKCα has additionally been demonstrated to mediate growth inhibition in HepG2 cells via MEK [305,306]. In this way, PKCα may be additionally involved in activating the AAR pathway in leucine deprivation conditions, thus contributing to IGFBP-1 phosphorylation and FGR onset through a signaling mechanism (Figure 16).

4.8 Future directions

4.8.1 Determining direct phosphorylation of IGFBP-1 by PKC at novel consensus sites

IGFBP-1 contains two possible phosphorylation sites (Thr50, Ser58) which conform to the basic requirements of the PKC consensus sequence [191]. Due to the evidence of leucine deprivation induced direct interaction between PKCα and IGFBP-1, these novel sites may be phosphorylated under leucine deprivation directly by PKCα. Phosphorylation at these discrete sites has not been investigated and their functional effects have not been characterized. Future studies utilizing targeted mass spectrometry to identify whether changes in phosphorylation at these sites with PKCα inhibition or knockdown occur is a valuable avenue to pursue. Furthermore, Thr50Ala and Ser58Ala mutagenesis may additionally help characterize these sites effects on IGFBP-1 binding affinity towards IGF-I or perhaps demonstrate new phosphorylation dependent effects independent of IGF-I function.

4.8.2 PKC regulation of CK2 and its role in IGFBP-1 phosphorylation

There is limited evidence of PKC and its interaction with CK2 within current literature. Lee et al., (2016) demonstrated that conventional PKC isoforms -α and -β as well as the atypical isoform -ζ directly phosphorylate CK2α at Ser194 and Ser277, stimulating CK2α activity [307]. Increased CK2 expression/activity is consistently found in FGR models and is associated with increased IGFBP-1 phosphorylation [177,191]. We have previously demonstrated increased CK2α activation loop autophosphorylation at Tyr182 in FGR [94]. In this study, my data demonstrated an interaction of PKCα with CK2β, but not the catalytic CK2α subunit although knockdown of any CK2 subunit results in decreased IGFBP-1 phosphorylation, implicating that the whole CK2 holoenzyme regulates IGFBP-1 phosphorylation [177]. Therefore, investigating the phosphorylation status of CK2α at Tyr182, Ser194 and Ser277 within leucine deprivation and PMA treatments may prove valuable in the future to demonstrate PKC mediated regulation of CK2 activity which results in increased IGFBP-1 phosphorylation.

4.8.3 Investigating the role of PKC signaling via ERK activation mediating IGFBP-1 phosphorylation

Nutrient responsive signal integration upstream and downstream of mTOR by PKC [293–295] and the involvement of PKC in the AAR pathway via ERK activation [300,301,303,304,308] provides further justification for investigating possible roles for PKC in mediating IGFBP-1 phosphorylation in FGR models. Although mTOR does not mediate IGFBP-1 phosphorylation in leucine deprivation [178], IGFBP-1 is mediated by mTOR in hypoxia [179]. Furthermore, because PKCα specifically has been demonstrated to be activated by leucine deprivation and regulates ERK activation at several different upstream effectors, PKCα may play a signaling role in mediating IGFBP-1 phosphorylation indirectly through mediating the AAR pathway. Investigating potential roles for the PKC isoforms in mediating mTOR, AAR or other nutrient sensitive signaling pathways has thus far not been investigated and may provide additional context as to how PKC mediates the phosphorylation of IGFBP-1.

4.9 Limitations

The functionality IGFBP-1 phosphorylation and its inhibitory properties pertaining to IGF-I dependent IGF-1R mediated growth is often scrutinized due to the commonly observed lack of change in phosphorylated IGFBP-1 to total secreted IGFBP-1 ratio where increased IGFBP-1 phosphorylation is observed concomitantly with IGFBP-1 secretion resulting in an unchanged pIGFBP-1/IGFBP-1 ratio which is most aptly outlined in Seferovic *et al.,* (2009) [194]. However, unlike other proteins which evidence of change in functionality is dependent on phosphorylated to total protein ratios, the functionality of IGFBP-1 phosphorylation is reflected by increased binding affinity for IGF-I and increased IGFBP-1 phosphorylation irrespective of total IGFBP-1 secretion. This largely results in the increase of high affinity IGFBP-1 within a total pool of IGFBP-1 which outcompetes lower affinity IGFBP-1 species at binding IGF-I. This line of reasoning is strongly supported by the following experimental data where proportional changes in pIGFBP-1/IGFBP-1 are not observed. First, surface plasmon resonance-based BiaCore analysis indicated the hyperphosphorylated IGFBP-1 isoforms found in leucine deprivation treated cells demonstrated a ~30-fold increase in binding affinity for IGF-I [194]. Second, highly phosphorylated species of IGFBP-1 produced irrespective of pIGFBP-1/IGFBP-1 ratio is evident in our previous work using 2-D gel electrophoresis [177]. Collectively, our previous findings suggest that the predominant increase in IGF-I affinity of IGFBP-1 is due to an increase in the abundance of specific phospho-IGFBP-1 isoforms (site and degree of phosphorylation) rather than increases in total IGFBP-1 or even total pIGFBP-1. Within this study, PKCα mediated changes in IGFBP-1 phosphorylation and functionality are reflected in the IGF-1R autophosphorylation assay (Figure 14) which uses equal amounts of total IGFBP-1 to inhibit IGF-I function therefore demonstrating the functional effects of IGFBP-1 phosphorylation (site and degree) is independent of pIGFBP-1/total IGFBP-1 ratio.

Furthermore, confounding variables within PLA may reflect bias in our data sets due to L0 increasing intracellular IGFBP-1 expression (Figures 7 and 9). Increased IGFBP-1 concentration may result in the induction of PLA signals between PKCα+IGFBP-1 and CK2β+IGFBP-1 as a result of increased total IGFBP-1 and not due

to L0 induced interactions between two proteins. However, lack of reciprocal co-immunoprecipitation between PKCα+IGFBP-1 in L450 (Figure 3) suggests that decreased leucine availability is necessary for an intracellular PKCα+IGFBP-1 interaction. Conversely, CK2β+IGFBP-1 reciprocally co-immunoprecipitate in both L450 and L0 (Figure 3) therefore, L0 mediated induced interactions CK2β+IGFBP-1 demonstrated by PLA may indeed be result of increased intracellular IGFBP-1 content. The expression of PKCα or CK2β is unchanged in L0 (Figure A4), thus we do not consider the effect of total protein concentration as a possible confounding variable for L0 induced PKCα+CK2β interactions (Figure 8).

The cellular compartment where IGFBP-1 phosphorylation is not well understood. Although cell fractionation into cytosolic and membrane compartments was performed in this study to investigate the translocation of PKCα in L0 , IGFBP-1 phosphorylation was not probed for within these fractions. Further study utilizing more robust fractionation techniques may elucidate the cell compartment or organelles where IGFBP-1 is phosphorylated.

4.10 Overall conclusions

The aims of this study were to establish mechanistic roles for PKC in mediating IGFBP-1 phosphorylation which is correlated to FGR. Using two models contextually related to fetal hepatic IGFBP-1 phosphorylation: leucine deprived HepG2 cells and the fetal liver of MNR baboons, I investigated the effects of amino acid deprivation on PKC and the resultant effects on IGFBP-1 phosphorylation. I found that within leucine deprivation, PKCα is the specific isoform which interacts with both IGFBP-1 and CK2β and that these interactions were both dependent on and induced by leucine deprivation. Furthermore, I demonstrate that PKCα is the specific isoform which mediates IGFBP-1 phosphorylation and acts in concert with CK2. PKCα knockdown mediated IGFBP-1 phosphorylation, resulting in phosphoisoforms which induced IGF-1R autophosphorylation indicative of decreased binding affinity for IGF-I. For the first time, PKCα is demonstrated as a nutrient sensitive kinase that translocates to a membrane compartment in leucine deprivation. Increased expression of PKCα within FGR baboon

fetal liver prior the physical manifestations of FGR further implicates PKCα as a key kinase regulating FGR pathophysiology. Altogether, our data presented in this study demonstrates new mechanisms in which IGFBP-1 phosphorylation occurs and adds to the numerous effectors discovered to be altered in FGR such as mTOR inhibition, AAR upregulation and CK2 upregulation. Subsequently, the implication of upregulated PKCα activity and/or expression provides new research avenues into FGR pathophysiology related to PKC signaling as well as direct PKC phosphorylation. Through elucidating mechanisms underlying the pathophysiology of FGR, improvements in therapeutic treatments which are currently lacking may result in improved prognosis in antenatal, neonatal and adult life.

References

1. Easter, S. R. *et al.* Fetal growth restriction: Case definition & guidelines for data collection, analysis, and presentation of immunization safety data. *Vaccine* **35**, 6546–6554 (2017).
2. Ananth, C. V. & Vintzileos, A. M. Distinguishing pathological from constitutional small for gestational age births in population-based studies. *Early Hum. Dev.* **85**, 653–658 (2009).
3. Pallotto, E. K. & Kilbride, H. W. Perinatal outcome and later implications of intrauterine growth restriction. *Clin. Obstet. Gynecol.* **49**, 257–269 (2006).
4. Barker, D. J. P. Adult consequences of fetal growth restriction. *Clin. Obstet. Gynecol.* **49**, 270–283 (2006).
5. Snijders, R. J., Sherrod, C., Gosden, C. M. & Nicolaides, K. H. Fetal growth retardation: associated malformations and chromosomal abnormalities. *Am. J. Obstet. Gynecol.* **168**, 547–555 (1993).
6. Offenbacher, S. *et al.* Maternal periodontitis and prematurity. Part I: Obstetric outcome of prematurity and growth restriction. *Ann. Periodontol.* **6**, 164–174 (2001).
7. Shulman, C. E. *et al.* Malaria in pregnancy: adverse effects on haemoglobin levels and birthweight in primigravidae and multigravidae. *Trop. Med. Int. Health TM IH* **6**, 770–778 (2001).
8. National Institutes of Health Consensus Development Panel. Antenatal corticosteroids revisited: repeat courses - National Institutes of Health Consensus

Development Conference Statement, August 17-18, 2000. *Obstet. Gynecol.* **98**, 144–150 (2001).

9. Maisonet, M., Correa, A., Misra, D. & Jaakkola, J. J. K. A review of the literature on the effects of ambient air pollution on fetal growth. *Environ. Res.* **95**, 106–115 (2004).
10. Perera, F. P. *et al.* Relationships among polycyclic aromatic hydrocarbon-DNA adducts, proximity to the World Trade Center, and effects on fetal growth. *Environ. Health Perspect.* **113**, 1062–1067 (2005).
11. Gluckman, P. D. & Hanson, M. A. Maternal constraint of fetal growth and its consequences. *Semin. Fetal. Neonatal Med.* **9**, 419–425 (2004).
12. Murphy, V. E., Smith, R., Giles, W. B. & Clifton, V. L. Endocrine regulation of human fetal growth: the role of the mother, placenta, and fetus. *Endocr. Rev.* **27**, 141–169 (2006).
13. Chew, L. C. & Verma, R. P. Fetal Growth Restriction. in *StatPearls* (StatPearls Publishing, 2021).
14. Nardozza, L. M. M. *et al.* Fetal growth restriction: current knowledge. *Arch. Gynecol. Obstet.* **295**, 1061–1077 (2017).
15. Kinzler, W. L. & Vintzileos, A. M. Fetal growth restriction: a modern approach. *Curr. Opin. Obstet. Gynecol.* **20**, 125–131 (2008).
16. Cogswell, M. E. & Yip, R. The influence of fetal and maternal factors on the distribution of birthweight. *Semin. Perinatol.* **19**, 222–240 (1995).
17. Kliman, H. J. Uteroplacental Blood Flow. *Am. J. Pathol.* **157**, 1759–1768 (2000).

18. Ueland, K. Maternal cardiovascular dynamics. VII. Intrapartum blood volume changes. *Am. J. Obstet. Gynecol.* **126**, 671–677 (1976).

19. Rockwell, L. C., Vargas, E. & Moore, L. G. Human physiological adaptation to pregnancy: inter- and intraspecific perspectives. *Am. J. Hum. Biol. Off. J. Hum. Biol. Counc.* **15**, 330–341 (2003).

20. Bauer, M. K. *et al.* Fetal growth and placental function. *Mol. Cell. Endocrinol.* **140**, 115–120 (1998).

21. Pardi, G., Marconi, A. M. & Cetin, I. Placental-fetal interrelationship in IUGR fetuses--a review. *Placenta* **23 Suppl A**, S136-141 (2002).

22. Sibley, C. P. *et al.* Regulation of placental transfer: the Na(+)/H(+) exchanger--a review. *Placenta* **23 Suppl A**, S39-46 (2002).

23. Heasman, L., Clarke, L., Firth, K., Stephenson, T. & Symonds, M. E. Influence of restricted maternal nutrition in early to mid gestation on placental and fetal development at term in sheep. *Pediatr. Res.* **44**, 546–551 (1998).

24. Lumey, L. Compensatory placental growth after restricted maternal nutrition in early pregnancy. *Placenta* (1998).

25. Belkacemi, L., Chen, C. H., Ross, M. G. & Desai, M. Increased Placental Apoptosis in Maternal Food Restricted Gestations: Role of the Fas Pathway. *Placenta* **30**, 739–751 (2009).

26. Aherne, W. & Dunnill, M. S. Morphometry of the human placenta. *Br. Med. Bull.* **22**, 5–8 (1966).

27. Reynolds, L. P. & Redmer, D. A. Utero-placental vascular development and placental function. *J. Anim. Sci.* **73**, 1839–1851 (1995).

28. Belkacemi, L., Nelson, D. M., Desai, M. & Ross, M. G. Maternal Undernutrition Influences Placental-Fetal Development. *Biol. Reprod.* **83**, 325–331 (2010).

29. Jansson, N. *et al.* Down-regulation of placental transport of amino acids precedes the development of intrauterine growth restriction in rats fed a low protein diet. *J. Physiol.* **576**, 935–946 (2006).

30. Pantham, P. *et al.* Down-Regulation of Placental Transport of Amino Acids Precedes the Development of Intrauterine Growth Restriction in Maternal Nutrient Restricted Baboons. *Biol. Reprod.* **95**, (2016).

31. Picciano, M. F. Pregnancy and lactation: physiological adjustments, nutritional requirements and the role of dietary supplements. *J. Nutr.* **133**, 1997S-2002S (2003).

32. Godfrey, K., Robinson, S., Barker, D. J., Osmond, C. & Cox, V. Maternal nutrition in early and late pregnancy in relation to placental and fetal growth. *BMJ* **312**, 410–414 (1996).

33. Kramer, M. S. & Kakuma, R. Energy and protein intake in pregnancy. *Cochrane Database Syst. Rev.* CD000032 (2003) doi:10.1002/14651858.CD000032.

34. Moore, V. M., Davies, M. J., Willson, K. J., Worsley, A. & Robinson, J. S. Dietary composition of pregnant women is related to size of the baby at birth. *J. Nutr.* **134**, 1820–1826 (2004).

35. Wu, G., Bazer, F. W., Cudd, T. A., Meininger, C. J. & Spencer, T. E. Maternal Nutrition and Fetal Development. *J. Nutr.* **134**, 2169–2172 (2004).

36. Gao, F. *et al.* Effects of maternal undernutrition during late pregnancy on the development and function of ovine fetal liver. *Anim. Reprod. Sci.* **147**, 99–105 (2014).

37. Radford, B. N. & Han, V. K. M. Offspring from maternal nutrient restriction in mice show variations in adult glucose metabolism similar to human fetal growth restriction. *J. Dev. Orig. Health Dis.* **10**, 469–478 (2019).

38. Hellmuth, C. *et al.* Influence of moderate maternal nutrition restriction on the fetal baboon metabolome at 0.5 and 0.9 gestation. *Nutr. Metab. Cardiovasc. Dis.* **26**, 786–796 (2016).

39. Kloesz, J. L., Serdikoff, C. M., MaClennan, N. K., Adibi, S. A. & Lane, R. H. Uteroplacental Insufficiency Alters Liver and Skeletal Muscle Branched-Chain Amino Acid Metabolism in Intrauterine Growth-Restricted Fetal Rats. *Pediatr. Res.* **50**, 604–610 (2001).

40. Sarli, P.-M. *et al.* Liver Proteome Profile of Growth Restricted and Appropriately Grown Newborn Wistar Rats Associated With Maternal Undernutrition. *Front. Endocrinol.* **12**, 684220 (2021).

41. Seferovic, M. D., Chen, S., Pinto, D. M. & Gupta, M. B. Altered liver secretion of vascular regulatory proteins in hypoxic pregnancies stimulate angiogenesis in vitro. *J. Proteome Res.* **10**, 1495–1504 (2011).

42. Zhou, X. *et al.* Evidence for liver energy metabolism programming in offspring subjected to intrauterine undernutrition during midgestation. *Nutr. Metab.* **16**, 20 (2019).

43. Kiserud, T. The ductus venosus. *Semin. Perinatol.* **25**, 11–20 (2001).

44. Burton, G. J. & Jauniaux, E. Pathophysiology of placental-derived fetal growth restriction. *Am. J. Obstet. Gynecol.* **218**, S745–S761 (2018).

45. Karl, P. I. Insulin-like growth factor-1 stimulates amino acid uptake by the cultured human placental trophoblast. *J. Cell. Physiol.* **165**, 83–88 (1995).

46. Roberts, C. T., Owens, J. A. & Sferruzzi-Perri, A. N. Distinct actions of insulin-like growth factors (IGFs) on placental development and fetal growth: lessons from mice and guinea pigs. *Placenta* **29 Suppl A**, S42-47 (2008).

47. Newbern, D. & Freemark, M. Placental hormones and the control of maternal metabolism and fetal growth. *Curr. Opin. Endocrinol. Diabetes Obes.* **18**, 409–416 (2011).

48. Díaz, P., Powell, T. L. & Jansson, T. The role of placental nutrient sensing in maternal-fetal resource allocation. *Biol. Reprod.* **91**, 82 (2014).

49. Kavitha, J. V. *et al.* Down-regulation of placental mTOR, insulin/IGF-I signaling, and nutrient transporters in response to maternal nutrient restriction in the baboon. *FASEB J.* **28**, 1294–1305 (2014).

50. Sferruzzi-Perri, A. N. *et al.* Placental-specific Igf2 deficiency alters developmental adaptations to undernutrition in mice. *Endocrinology* **152**, 3202–3212 (2011).

51. Rosario, F. J. *et al.* Maternal protein restriction in the rat inhibits placental insulin, mTOR, and STAT3 signaling and down-regulates placental amino acid transporters. *Endocrinology* **152**, 1119–1129 (2011).

52. Jansson, T., Aye, I. L. M. H. & Goberdhan, D. C. I. The emerging role of mTORC1 signaling in placental nutrient-sensing. *Placenta* **33 Suppl 2**, e23-29 (2012).

53. Gaccioli, F., Lager, S., Powell, T. & Jansson, T. Placental Transport in Response to Altered Maternal Nutrition. *J. Dev. Orig. Health Dis.* **4**, 101–115 (2013).

54. al-Ghazali, W., Chita, S. K., Chapman, M. G. & Allan, L. D. Evidence of redistribution of cardiac output in asymmetrical growth retardation. *Br. J. Obstet. Gynaecol.* **96**, 697–704 (1989).

55. Rizzo, G. & Arduini, D. Fetal cardiac function in intrauterine growth retardation. *Am. J. Obstet. Gynecol.* **165**, 876–882 (1991).

56. Ebbing, C., Rasmussen, S., Godfrey, K. M., Hanson, M. A. & Kiserud, T. Redistribution pattern of fetal liver circulation in intrauterine growth restriction. *Acta Obstet. Gynecol. Scand.* **88**, 1118–1123 (2009).

57. Malhotra, A. *et al.* Neonatal Morbidities of Fetal Growth Restriction: Pathophysiology and Impact. *Front. Endocrinol.* **10**, 55 (2019).

58. Pantham, P. *et al.* Reduced placental amino acid transport in response to maternal nutrient restriction in the baboon. *Am. J. Physiol. - Regul. Integr. Comp. Physiol.* **309**, R740–R746 (2015).

59. Philipps, A. F., Holzman, I. R., Teng, C. & Battaglia, F. C. Tissue concentrations of free amino acids in term human placentas. *Am. J. Obstet. Gynecol.* **131**, 881–887 (1978).

60. Montgomery, D. & Young, M. The uptake of naturally occurring amino acids by the plasma membrane of the human placenta. *Placenta* **3**, 13–20 (1982).

61. Soltesz, G., Harris, D., Mackenzie, I. Z. & Aynsley-Green, A. The metabolic and endocrine milieu of the human fetus and mother at 18-21 weeks of gestation. I. Plasma amino acid concentrations. *Pediatr. Res.* **19**, 91–93 (1985).

62. Cetin, I. *et al.* Umbilical amino acid concentrations in appropriate and small for gestational age infants: a biochemical difference present in utero. *Am. J. Obstet. Gynecol.* **158**, 120–126 (1988).

63. Regnault, T. R. H., de Vrijer, B. & Battaglia, F. C. Transport and metabolism of amino acids in placenta. *Endocrine* **19**, 23–41 (2002).

64. Regnault, T. R. H., Friedman, J. E., Wilkening, R. B., Anthony, R. V. & Hay, W. W. Fetoplacental transport and utilization of amino acids in IUGR--a review. *Placenta* **26 Suppl A**, S52-62 (2005).

65. Marconi, A. M. *et al.* Steady state maternal-fetal leucine enrichments in normal and intrauterine growth-restricted pregnancies. *Pediatr. Res.* **46**, 114–119 (1999).

66. Economides, D. L., Nicolaides, K. H., Gahl, W. A., Bernardini, I. & Evans, M. I. Plasma amino acids in appropriate- and small-for-gestational-age fetuses. *Am. J. Obstet. Gynecol.* **161**, 1219–1227 (1989).

67. Cetin, I. *et al.* Umbilical amino acid concentrations in normal and growth-retarded fetuses sampled in utero by cordocentesis. *Am. J. Obstet. Gynecol.* **162**, 253–261 (1990).

68. Cetin, I. *et al.* Maternal concentrations and fetal-maternal concentration differences of plasma amino acids in normal and intrauterine growth-restricted pregnancies. *Am. J. Obstet. Gynecol.* **174**, 1575–1583 (1996).

69. Jansson, T. Amino acid transporters in the human placenta. *Pediatr. Res.* **49**, 141–147 (2001).

70. Lewis, R. M. *et al.* Review: Modelling placental amino acid transfer--from transporters to placental function. *Placenta* **34 Suppl**, S46-51 (2013).

71. Avagliano, L., Garò, C. & Marconi, A. M. Placental Amino Acids Transport in Intrauterine Growth Restriction. *Journal of Pregnancy* https://www.hindawi.com/journals/jp/2012/972562/ (2012) doi:https://doi.org/10.1155/2012/972562.

72. Ross, J. C., Fennessey, P. V., Wilkening, R. B., Battaglia, F. C. & Meschia, G. Placental transport and fetal utilization of leucine in a model of fetal growth retardation. *Am. J. Physiol.* **270**, E491-503 (1996).

73. Jansson, T., Scholtbach, V. & Powell, T. L. Placental transport of leucine and lysine is reduced in intrauterine growth restriction. *Pediatr. Res.* **44**, 532–537 (1998).

74. Paolini, C. L. *et al.* Placental transport of leucine, phenylalanine, glycine, and proline in intrauterine growth-restricted pregnancies. *J. Clin. Endocrinol. Metab.* **86**, 5427–5432 (2001).

75. Glazier, J. D. *et al.* Association between the activity of the system A amino acid transporter in the microvillous plasma membrane of the human placenta and severity of fetal compromise in intrauterine growth restriction. *Pediatr. Res.* **42**, 514–519 (1997).

76. Harrington, B., Glazier, J., D'Souza, S. & Sibley, C. System A amino acid transporter activity in human placental microvillous membrane vesicles in relation to various anthropometric measurements in appropriate and small for gestational age babies. *Pediatr. Res.* **45**, 810–814 (1999).

77. Jansson, T., Ylvén, K., Wennergren, M. & Powell, T. L. Glucose transport and system A activity in syncytiotrophoblast microvillous and basal plasma membranes in intrauterine growth restriction. *Placenta* **23**, 392–399 (2002).

78. Verrey, F. System L: heteromeric exchangers of large, neutral amino acids involved in directional transport. *Pflugers Arch.* **445**, 529–533 (2003).

79. Mahendran, D. *et al.* Amino acid (system A) transporter activity in microvillous membrane vesicles from the placentas of appropriate and small for gestational age babies. *Pediatr. Res.* **34**, 661–665 (1993).

80. Jansson, T., Ekstrand, Y., Björn, C., Wennergren, M. & Powell, T. L. Alterations in the activity of placental amino acid transporters in pregnancies complicated by diabetes. *Diabetes* **51**, 2214–2219 (2002).

81. Jansson, N. *et al.* Activation of placental mTOR signaling and amino acid transporters in obese women giving birth to large babies. *J. Clin. Endocrinol. Metab.* **98**, 105–113 (2013).

82. Norberg, S., Powell, T. L. & Jansson, T. Intrauterine growth restriction is associated with a reduced activity of placental taurine transporters. *Pediatr. Res.* **44**, 233–238 (1998).

83. Bajoria, R., Sooranna, S. R., Ward, S. & Hancock, M. Placenta as a link between amino acids, insulin-IGF axis, and low birth weight: evidence from twin studies. *J. Clin. Endocrinol. Metab.* **87**, 308–315 (2002).

84. Teodoro, G. F. R. *et al.* Leucine Is Essential for Attenuating Fetal Growth Restriction Caused by a Protein-Restricted Diet in Rats. *J. Nutr.* **142**, 924–930 (2012).

85. Baschat, A. A. Fetal responses to placental insufficiency: an update. *BJOG Int. J. Obstet. Gynaecol.* **111**, 1031–1041 (2004).

86. Gagnon, R. Placental insufficiency and its consequences. *Eur. J. Obstet. Gynecol. Reprod. Biol.* **110 Suppl 1**, S99-107 (2003).

87. Zhang, S. *et al.* Placental Adaptations in Growth Restriction. *Nutrients* **7**, 360–389 (2015).

88. Wesolowski, S. R. & Hay, W. W. Role of placental insufficiency and intrauterine growth restriction on the activation of fetal hepatic glucose production. *Mol. Cell. Endocrinol.* **435**, 61–68 (2016).

89. Thorpe-Beeston, J. G. *et al.* Relations between the fetal circulation and pituitary-thyroid function. *Br. J. Obstet. Gynaecol.* **98**, 1163–1167 (1991).

90. Thorpe-Beeston, J. G., Nicolaides, K. H. & McGregor, A. M. Fetal thyroid function. *Thyroid Off. J. Am. Thyroid Assoc.* **2**, 207–217 (1992).

91. Goland, R. S. *et al.* Elevated levels of umbilical cord plasma corticotropin-releasing hormone in growth-retarded fetuses. *J. Clin. Endocrinol. Metab.* **77**, 1174–1179 (1993).

92. Giles, W. B., McLean, M., Davies, J. J. & Smith, R. Abnormal umbilical artery Doppler waveforms and cord blood corticotropin-releasing hormone. *Obstet. Gynecol.* **87**, 107–111 (1996).

93. Thorn, S. R. *et al.* Intrauterine Growth Restriction Increases Fetal Hepatic Gluconeogenic Capacity and Reduces Messenger Ribonucleic Acid Translation Initiation and Nutrient Sensing in Fetal Liver and Skeletal Muscle. *Endocrinology* **150**, 3021–3030 (2009).

94. Kakadia, J. H. *et al.* Hyperphosphorylation of fetal liver IGFBP-1 precedes slowing of fetal growth in nutrient-restricted baboons and may be a mechanism underlying IUGR. *Am. J. Physiol. Endocrinol. Metab.* **319**, E614–E628 (2020).

95. Hyatt, M. A. *et al.* Maternal nutrient restriction in early pregnancy programs hepatic mRNA expression of growth-related genes and liver size in adult male sheep. *J. Endocrinol.* **192**, 87–97 (2007).

96. Fant, M. E. & Weisoly, D. Insulin and insulin-like growth factors in human development: implications for the perinatal period. *Semin. Perinatol.* **25**, 426–435 (2001).

97. Li, C. *et al.* Effects of maternal global nutrient restriction on fetal baboon hepatic insulin-like growth factor system genes and gene products. *Endocrinology* **150**, 4634–4642 (2009).

98. Gluckman, P. D. & Harding, J. E. The physiology and pathophysiology of intrauterine growth retardation. *Horm. Res.* **48 Suppl 1**, 11–16 (1997).

99. Humbel, R. E. Insulin-like growth factors I and II. *Eur. J. Biochem.* **190**, 445–462 (1990).

100. Herington, A. C. Insulin-like growth factors: biochemistry and physiology. *Baillieres Clin. Endocrinol. Metab.* **5**, 531–551 (1991).

101. Baker, J., Liu, J. P., Robertson, E. J. & Efstratiadis, A. Role of insulin-like growth factors in embryonic and postnatal growth. *Cell* **75**, 73–82 (1993).

102. DeChiara, T. M., Efstratiadis, A. & Robertsen, E. J. A growth-deficiency phenotype in heterozygous mice carrying an insulin-like growth factor II gene disrupted by targeting. *Nature* **345**, 78–80 (1990).

103. Randhawa, R. & Cohen, P. The role of the insulin-like growth factor system in prenatal growth. *Mol. Genet. Metab.* **86**, 84–90 (2005).

104. Gicquel, C. & Le Bouc, Y. Hormonal regulation of fetal growth. *Horm. Res.* **65 Suppl 3**, 28–33 (2006).

105. Agrogiannis, G. D., Sifakis, S., Patsouris, E. S. & Konstantinidou, A. E. Insulin-like growth factors in embryonic and fetal growth and skeletal development (Review). *Mol. Med. Rep.* **10**, 579–584 (2014).

106. Gluckman, P., Johnsonbarrett, J., Butler, J., Edgar, B. & Gunn, T. Studies of Insulin-Like Growth Factor-I and Factor-Ii by Specific Radioligand Assays in Umbilical-Cord Blood. *Clin. Endocrinol. (Oxf.)* **19**, 405–413 (1983).

107. Lassarre, C. *et al.* Serum insulin-like growth factors and insulin-like growth factor binding proteins in the human fetus. Relationships with growth in normal subjects and in subjects with intrauterine growth retardation. *Pediatr. Res.* **29**, 219–225 (1991).

108. Bang, P. *et al.* Ontogeny of Insulin-Like Growth Factor-Binding Protein-1, −2, and −3: Quantitative Measurements by Radioimmunoassay in Human Fetal Serum. *Pediatr. Res.* **36**, 528–535 (1994).

109. Langford, K., Nicolaides, K. & Miell, J. P. Maternal and fetal insulin-like growth factors and their binding proteins in the second and third trimesters of human pregnancy. *Hum. Reprod. Oxf. Engl.* **13**, 1389–1393 (1998).

110. Gluckman, P. D. *et al.* Congenital idiopathic growth hormone deficiency associated with prenatal and early postnatal growth failure. The International Board of the Kabi Pharmacia International Growth Study. *J. Pediatr.* **121**, 920–923 (1992).

111. Fowden, A. L. The insulin-like growth factors and feto-placental growth. *Placenta* **24**, 803–812 (2003).

112. Lund, P. K. *et al.* Somatomedin-C/insulin-like growth factor-I and insulin-like growth factor-II mRNAs in rat fetal and adult tissues. *J. Biol. Chem.* **261**, 14539–14544 (1986).

113. Han, V. K., Lund, P. K., Lee, D. C. & D'Ercole, A. J. Expression of somatomedin/insulin-like growth factor messenger ribonucleic acids in the human fetus: identification, characterization, and tissue distribution. *J. Clin. Endocrinol. Metab.* **66**, 422–429 (1988).

114. Verhaeghe, J. *et al.* C-peptide, insulin-like growth factors I and II, and insulin-like growth factor binding protein-1 in umbilical cord serum: correlations with birth weight. *Am. J. Obstet. Gynecol.* **169**, 89–97 (1993).

115. Giudice, L. C. *et al.* Insulin-like growth factors and their binding proteins in the term and preterm human fetus and neonate with normal and extremes of intrauterine growth. *J. Clin. Endocrinol. Metab.* **80**, 1548–1555 (1995).

116. Lee, J. E., Pintar, J. & Efstratiadis, A. Pattern of the insulin-like growth factor II gene expression during early mouse embryogenesis. *Dev. Camb. Engl.* **110**, 151–159 (1990).

117. Louvi, A., Accili, D. & Efstratiadis, A. Growth-promoting interaction of IGF-II with the insulin receptor during mouse embryonic development. *Dev. Biol.* **189**, 33–48 (1997).

118. Allan, G. J., Flint, D. J. & Patel, K. Insulin-like growth factor axis during embryonic development. *Reprod. Camb. Engl.* **122**, 31–39 (2001).

119. Le Roith, D., Bondy, C., Yakar, S., Liu, J. L. & Butler, A. The somatomedin hypothesis: 2001. *Endocr. Rev.* **22**, 53–74 (2001).

120. DeChiara, T. M., Robertson, E. J. & Efstratiadis, A. Parental imprinting of the mouse insulin-like growth factor II gene. *Cell* **64**, 849–859 (1991).

121. Holt, R. I. G. Fetal programming of the growth hormone-insulin-like growth factor axis. *Trends Endocrinol. Metab. TEM* **13**, 392–397 (2002).

122. Sferruzzi-Perri, A. N., Owens, J. A., Pringle, K. G. & Roberts, C. T. The neglected role of insulin-like growth factors in the maternal circulation regulating fetal growth. *J. Physiol.* **589**, 7–20 (2011).

123. Peter, M. A., Winterhalter, K. H., Böni-Schnetzler, M., Froesch, E. R. & Zapf, J. Regulation of insulin-like growth factor-I (IGF-I) and IGF-binding proteins by growth hormone in rat white adipose tissue. *Endocrinology* **133**, 2624–2631 (1993).

124. Coleman, M. E., Russell, L. & Etherton, T. D. Porcine somatotropin (pST) increases IGF-I mRNA abundance in liver and subcutaneous adipose tissue but not in skeletal muscle of growing pigs. *J. Anim. Sci.* **72**, 918–924 (1994).

125. Sterle, J. A. *et al.* Insulin-like growth factor (IGF)-I, IGF-II, IGF-binding protein-2 and pregnancy-associated glycoprotein mRNA in pigs with somatotropin-enhanced fetal growth. *J. Endocrinol.* **159**, 441–450 (1998).

126. Olausson, H. & Sohlström, A. Effects of food restriction and pregnancy on the expression of insulin-like growth factors-I and -II in tIssues from guinea pigs. *J. Endocrinol.* **179**, 437–445 (2003).

127. Han, V. K. & Carter, A. M. Spatial and temporal patterns of expression of messenger RNA for insulin-like growth factors and their binding proteins in the placenta of man and laboratory animals. *Placenta* **21**, 289–305 (2000).

128. Gargosky, S. E. *et al.* Circulating levels of insulin-like growth factors increase and molecular forms of their serum binding proteins change with human pregnancy. *Biochem. Biophys. Res. Commun.* **170**, 1157–1163 (1990).

129. Davenport, M. L. *et al.* Regulation of serum insulin-like growth factor-I (IGF-I) and IGF binding proteins during rat pregnancy. *Endocrinology* **127**, 1278–1286 (1990).

130. Grimberg, A. & Cohen, P. Role of Insulin-Like Growth Factors and Their Binding Proteins in Growth Control and Carcinogenesis. *J. Cell. Physiol.* **183**, 1–9 (2000).

131. Girnita, L., Worrall, C., Takahashi, S.-I., Seregard, S. & Girnita, A. Something old, something new and something borrowed: emerging paradigm of insulin-like growth factor type 1 receptor (IGF-1R) signaling regulation. *Cell. Mol. Life Sci. CMLS* **71**, 2403–2427 (2014).

132. Patti, M. E. & Kahn, C. R. The insulin receptor--a critical link in glucose homeostasis and insulin action. *J. Basic Clin. Physiol. Pharmacol.* **9**, 89–109 (1998).

133. Ludwig, T. *et al.* Mouse mutants lacking the type 2 IGF receptor (IGF2R) are rescued from perinatal lethality in Igf2 and Igf1r null backgrounds. *Dev. Biol.* **177**, 517–535 (1996).

134. Lou, M. *et al.* The first three domains of the insulin receptor differ structurally from the insulin-like growth factor 1 receptor in the regions governing ligand specificity. *Proc. Natl. Acad. Sci. U. S. A.* **103**, 12429–12434 (2006).

135. Ullrich, A. *et al.* Insulin-like growth factor I receptor primary structure: comparison with insulin receptor suggests structural determinants that define functional specificity. *EMBO J.* **5**, 2503–2512 (1986).

136. Sepp-Lorenzino, L. Structure and function of the insulin-like growth factor I receptor. *Breast Cancer Res. Treat.* **47**, 235–253 (1998).

137. Adams, T. E., Epa, V. C., Garrett, T. P. & Ward, C. W. Structure and function of the type 1 insulin-like growth factor receptor. *Cell. Mol. Life Sci. CMLS* **57**, 1050–1093 (2000).

138. Zhang, B. & Roth, R. A. Binding properties of chimeric insulin receptors containing the cysteine-rich domain of either the insulin-like growth factor I receptor or the insulin receptor related receptor. *Biochemistry* **30**, 5113–5117 (1991).

139. Garrett, T. P. *et al.* Crystal structure of the first three domains of the type-1 insulin-like growth factor receptor. *Nature* **394**, 395–399 (1998).

140. Gustafson, T. A. & Rutter, W. J. The cysteine-rich domains of the insulin and insulin-like growth factor I receptors are primary determinants of hormone binding specificity. Evidence from receptor chimeras. *J. Biol. Chem.* **265**, 18663–18667 (1990).

141. Ward, C. W. *et al. The Structure of the Type 1 Insulin-Like Growth Factor Receptor*. *Madame Curie Bioscience Database [Internet]* (Landes Bioscience, 2013).

142. Kavran, J. M. *et al.* How IGF-1 activates its receptor. *eLife* **3**, (2014).

143. Backer, J. M., Kahn, C. R., Cahill, D. A., Ullrich, A. & White, M. F. Receptor-mediated internalization of insulin requires a 12-amino acid sequence in the

juxtamembrane region of the insulin receptor beta-subunit. *J. Biol. Chem.* **265**, 16450–16454 (1990).

144. Hsu, D., Knudson, P. E., Zapf, A., Rolband, G. C. & Olefsky, J. M. NPXY motif in the insulin-like growth factor-I receptor is required for efficient ligand-mediated receptor internalization and biological signaling. *Endocrinology* **134**, 744–750 (1994).
145. Favelyukis, S., Till, J. H., Hubbard, S. R. & Miller, W. T. Structure and autoregulation of the insulin-like growth factor 1 receptor kinase. *Nat. Struct. Biol.* **8**, 1058–1063 (2001).
146. Kim, H.-S., Rosenfeld, R. G. & Oh, Y. Biological roles of insulin-like growth factor binding proteins (IGFBPs). *Exp. Mol. Med.* **29**, 85–96 (1997).
147. Forbes, B. E., McCarthy, P. & Norton, R. S. Insulin-Like Growth Factor Binding Proteins: A Structural Perspective. *Front. Endocrinol.* **3**, (2012).
148. Shimasaki, S. & Ling, N. Identification and molecular characterization of insulin-like growth factor binding proteins (IGFBP-1, -2, -3, -4, -5 and -6). *Prog. Growth Factor Res.* **3**, 243–266 (1991).
149. Rajaram, S., Baylink, D. J. & Mohan, S. Insulin-like growth factor-binding proteins in serum and other biological fluids: regulation and functions. *Endocr. Rev.* **18**, 801–831 (1997).
150. Guler, H. P., Zapf, J., Schmid, C. & Froesch, E. R. Insulin-like growth factors I and II in healthy man. Estimations of half-lives and production rates. *Acta Endocrinol. (Copenh.)* **121**, 753–758 (1989).

151. Baxter, R. C. Insulin-like growth factor binding proteins in the human circulation: a review. *Horm. Res.* **42**, 140–144 (1994).

152. Clemmons, D. R. Role of IGF-binding proteins in regulating IGF responses to changes in metabolism. *J. Mol. Endocrinol.* **61**, T139–T169 (2018).

153. Jones, J. I., Gockerman, A., Busby, W. H., Wright, G. & Clemmons, D. R. Insulin-like growth factor binding protein 1 stimulates cell migration and binds to the alpha 5 beta 1 integrin by means of its Arg-Gly-Asp sequence. *Proc. Natl. Acad. Sci. U. S. A.* **90**, 10553–10557 (1993).

154. Jogie-Brahim, S., Feldman, D. & Oh, Y. Unraveling Insulin-Like Growth Factor Binding Protein-3 Actions in Human Disease. *Endocr. Rev.* **30**, 417–437 (2009).

155. Andress, D. L. & Birnbaum, R. S. Human osteoblast-derived insulin-like growth factor (IGF) binding protein-5 stimulates osteoblast mitogenesis and potentiates IGF action. *J. Biol. Chem.* **267**, 22467–22472 (1992).

156. Forbes, B. E. *et al.* Localization of an Insulin-like Growth Factor (IGF) Binding Site of Bovine IGF Binding Protein-2 Using Disulfide Mapping and Deletion Mutation Analysis of the C-terminal Domain*. *J. Biol. Chem.* **273**, 4647–4652 (1998).

157. Carrick, F. E. *et al.* Interaction of insulin-like growth factor (IGF)-I and -II with IGF binding protein-2: mapping the binding surfaces by nuclear magnetic resonance. *J. Mol. Endocrinol.* **34**, 685–698 (2005).

158. Żesławski, W. *et al.* The interaction of insulin-like growth factor-I with the N-terminal domain of IGFBP-5. *EMBO J.* **20**, 3638–3644 (2001).

159. Sitar, T., Popowicz, G. M., Siwanowicz, I., Huber, R. & Holak, T. A. Structural basis for the inhibition of insulin-like growth factors by insulin-like growth factor-binding proteins. *Proc. Natl. Acad. Sci.* **103**, 13028–13033 (2006).

160. Imai, Y. *et al.* Substitutions for Hydrophobic Amino Acids in the N-terminal Domains of IGFBP-3 and -5 Markedly Reduce IGF-I Binding and Alter Their Biologic Actions*. *J. Biol. Chem.* **275**, 18188–18194 (2000).

161. Yan, X., Forbes, B. E., McNeil, K. A., Baxter, R. C. & Firth, S. M. Role of N- and C-terminal Residues of Insulin-like Growth Factor (IGF)-binding Protein-3 in Regulating IGF Complex Formation and Receptor Activation*. *J. Biol. Chem.* **279**, 53232–53240 (2004).

162. Fu, P., Thompson, J. A. & Bach, L. A. Promotion of Cancer Cell Migration: AN INSULIN-LIKE GROWTH FACTOR (IGF)-INDEPENDENT ACTION OF IGF-BINDING PROTEIN-6*. *J. Biol. Chem.* **282**, 22298–22306 (2007).

163. Clemmons, D. R. Use of Mutagenesis to Probe IGF-Binding Protein Structure/Function Relationships. *Endocr. Rev.* **22**, 800–817 (2001).

164. Payet, L. D., Wang, X.-H., Baxter, R. C. & Firth, S. M. Amino- and Carboxyl-Terminal Fragments of Insulin-Like Growth Factor (IGF) Binding Protein-3 Cooperate to Bind IGFs with High Affinity and Inhibit IGF Receptor Interactions. *Endocrinology* **144**, 2797–2806 (2003).

165. Coverley, J. A. & Baxter, R. C. Phosphorylation of insulin-like growth factor binding proteins. *Mol. Cell. Endocrinol.* **128**, 1–5 (1997).

166. Han, V. K. *et al.* IGF-binding protein mRNAs in the human fetus: tissue and cellular distribution of developmental expression. *Horm. Res.* **45**, 160–166 (1996).

167. Burch, W. M., Correa, J., Shively, J. E. & Powell, D. R. The 25-kilodalton insulin-like growth factor (IGF)-binding protein inhibits both basal and IGF-I-mediated growth of chick embryo pelvic cartilage in vitro. *J. Clin. Endocrinol. Metab.* **70**, 173–180 (1990).

168. Ritvos, O. *et al.* Insulin-like growth factor (IGF) binding protein from human decidua inhibits the binding and biological action of IGF-I in cultured choriocarcinoma cells. *Endocrinology* **122**, 2150–2157 (1988).

169. Cox, G. N. *et al.* Recombinant human insulin-like growth factor (IGF)-binding protein-1 inhibits somatic growth stimulated by IGF-I and growth hormone in hypophysectomized rats. *Endocrinology* **135**, 1913–1920 (1994).

170. Chard, T. Insulin-like growth factors and their binding proteins in normal and abnormal human fetal growth. *Growth Regul.* **4**, 91–100 (1994).

171. Osgerby, J. C., Gadd, T. S. & Wathes, D. C. Expression of insulin-like growth factor binding protein-1 (IGFBP-1) mRNA in the ovine uterus throughout the oestrous cycle and early pregnancy. *J. Endocrinol.* **162**, 279–287 (1999).

172. Monaghan, J. M. *et al.* Longitudinal changes of insulin-like growth factors and their binding proteins throughout normal pregnancy. *Ann. Clin. Biochem.* **41**, 220–226 (2004).

173. Ketelslegers, J. M., Maiter, D., Maes, M., Underwood, L. E. & Thissen, J. P. Nutritional regulation of the growth hormone and insulin-like growth factor-binding proteins. *Horm. Res.* **45**, 252–257 (1996).

174. Tazuke, S. I. *et al.* Hypoxia stimulates insulin-like growth factor binding protein 1 (IGFBP-1) gene expression in HepG2 cells: A possible model for IGFBP-1 expression in fetal hypoxia. *Proc. Natl. Acad. Sci. U. S. A.* **95**, 10188–10193 (1998).

175. Straus, D. S., Ooi, G. T., Orlowski, C. C. & Rechler, M. M. Expression of the genes for insulin-like growth factor-I (IGF-I), IGF-II, and IGF-binding proteins-1 and -2 in fetal rat under conditions of intrauterine growth retardation caused by maternal fasting. *Endocrinology* **128**, 518–525 (1991).

176. Price, W. A., Rong, L., Stiles, A. D. & D'ercole, A. J. Changes in IGF-I and -II, IGF Binding Protein, and IGF Receptor Transcript Abundance after Uterine Artery Ligation. *Pediatr. Res.* **32**, 291–295 (1992).

177. Abu Shehab, M. *et al.* Liver mTOR Controls IGF-I Bioavailability by Regulation of Protein Kinase CK2 and IGFBP-1 Phosphorylation in Fetal Growth Restriction. *Endocrinology* **155**, 1327–1339 (2014).

178. Malkani, N., Jansson, T. & Gupta, M. B. IGFBP-1 hyperphosphorylation in response to leucine deprivation is mediated by the AAR pathway. *Mol. Cell. Endocrinol.* **412**, 182–195 (2015).

179. Damerill, I. *et al.* Hypoxia Increases IGFBP-1 Phosphorylation Mediated by mTOR Inhibition. *Mol. Endocrinol.* **30**, 201–216 (2016).

180. Gupta, M. B. & Jansson, T. Novel roles of mechanistic target of rapamycin signaling in regulating fetal growth†. *Biol. Reprod.* **100**, 872–884 (2019).

181. Jones, J. I. *et al.* Identification of the sites of phosphorylation in insulin-like growth factor binding protein-1. Regulation of its affinity by phosphorylation of serine 101. *J. Biol. Chem.* **268**, 1125–1131 (1993).

182. Westwood, M. Role of insulin-like growth factor binding protein 1 in human pregnancy. *Rev. Reprod.* **4**, 160–167 (1999).

183. Firth, S. M. & Baxter, R. C. Cellular actions of the insulin-like growth factor binding proteins. *Endocr. Rev.* **23**, 824–854 (2002).

184. Yu, J., Iwashita, M., Kudo, Y. & Takeda, Y. Phosphorylated insulin-like growth factor (IGF)-binding protein-1 (IGFBP-1) inhibits while non-phosphorylated IGFBP-1 stimulates IGF-I-induced amino acid uptake by cultured trophoblast cells. *Growth Horm. IGF Res. Off. J. Growth Horm. Res. Soc. Int. IGF Res. Soc.* **8**, 65–70 (1998).

185. Busby, W. H., Klapper, D. G. & Clemmons, D. R. Purification of a 31,000-dalton insulin-like growth factor binding protein from human amniotic fluid. Isolation of two forms with different biologic actions. *J. Biol. Chem.* **263**, 14203–14210 (1988).

186. Koistinen, R., Angervo, M., Leinonen, P., Hakala, T. & Seppälä, M. Phosphorylation of insulin-like growth factor-binding protein-1 increases in human amniotic fluid and decidua from early to late pregnancy. *Clin. Chim. Acta Int. J. Clin. Chem.* **215**, 189–199 (1993).

187. Dolcini, L. *et al.* Identification of the amniotic fluid insulin-like growth factor binding protein-1 phosphorylation sites and propensity to proteolysis of the isoforms. *FEBS J.* **276**, 6033–6046 (2009).

188. Jones, J. I., D'Ercole, A. J., Camacho-Hubner, C. & Clemmons, D. R. Phosphorylation of insulin-like growth factor (IGF)-binding protein 1 in cell culture and in vivo: effects on affinity for IGF-I. *Proc. Natl. Acad. Sci. U. S. A.* **88**, 7481–7485 (1991).

189. Abu Shehab, M., Khosravi, J., Han, V. K. M., Shilton, B. H. & Gupta, M. B. Site-specific IGFBP-1 hyper-phosphorylation in fetal growth restriction: clinical and functional relevance. *J. Proteome Res.* **9**, 1873–1881 (2010).

190. Abu Shehab, M., Iosef, C., Wildgruber, R., Sardana, G. & Gupta, M. B. Phosphorylation of IGFBP-1 at discrete sites elicits variable effects on IGF-I receptor autophosphorylation. *Endocrinology* **154**, 1130–1143 (2013).

191. Malkani, N. *et al.* Increased IGFBP-1 phosphorylation in response to leucine deprivation is mediated by CK2 and PKC. *Mol. Cell. Endocrinol.* **425**, 48–60 (2016).

192. Westwood, M., Gibson, J. M. & White, A. Purification and characterization of the insulin-like growth factor-binding protein-1 phosphoform found in normal plasma. *Endocrinology* **138**, 1130–1136 (1997).

193. Gupta, M. B. The role and regulation of IGFBP-1 phosphorylation in fetal growth restriction. *J. Cell Commun. Signal.* **9**, 111–123 (2015).

194. Seferovic, M. D. *et al.* Hypoxia and Leucine Deprivation Induce Human Insulin-Like Growth Factor Binding Protein-1 Hyperphosphorylation and Increase Its Biological Activity. *Endocrinology* **150**, 220–231 (2009).

195. Martina, N. A. *et al.* Gestational age-dependent expression of insulin-like growth factor-binding protein-1 (IGFBP-1) phosphoisoforms in human extraembryonic cavities, maternal serum, and decidua suggests decidua as the primary source of IGFBP-1 in these fluids during early pregnancy. *J. Clin. Endocrinol. Metab.* **82**, 1894–1898 (1997).

196. Gibson, J. M., Aplin, J. D., White, A. & Westwood, M. Regulation of IGF bioavailability in pregnancy. *Mol. Hum. Reprod.* **7**, 79–87 (2001).

197. Watson, C. S. *et al.* Elevated circulating insulin-like growth factor binding protein-1 is sufficient to cause fetal growth restriction. *Endocrinology* **147**, 1175–1186 (2006).

198. Sakai, K., D'Ercole, A. J., Murphy, L. J. & Clemmons, D. R. Physiological differences in insulin-like growth factor binding protein-1 (IGFBP-1) phosphorylation in IGFBP-1 transgenic mice. *Diabetes* **50**, 32–38 (2001).

199. Cox, L. A. *et al.* Effect of 30 per cent maternal nutrient restriction from 0.16 to 0.5 gestation on fetal baboon kidney gene expression. *J. Physiol.* **572**, 67–85 (2006).

200. Nijland, M. J. *et al.* Epigenetic modification of fetal baboon hepatic phosphoenolpyruvate carboxykinase following exposure to moderately reduced nutrient availability. *J. Physiol.* **588**, 1349–1359 (2010).

201. Schlabritz-Loutsevitch, N. E. *et al.* Metabolic adjustments to moderate maternal nutrient restriction. *Br. J. Nutr.* **98**, 276–284 (2007).

202. Antonow-Schlorke, I. *et al.* Vulnerability of the fetal primate brain to moderate reduction in maternal global nutrient availability. *Proc. Natl. Acad. Sci. U. S. A.* **108**, 3011–3016 (2011).

203. Kelly, J. H. & Darlington, G. J. Modulation of the liver specific phenotype in the human hepatoblastoma line Hep G2. *Vitro Cell. Dev. Biol. J. Tissue Cult. Assoc.* **25**, 217–222 (1989).

204. Rowe, C. *et al.* Proteome-wide analyses of human hepatocytes during differentiation and dedifferentiation. *Hepatol. Baltim. Md* **58**, 799–809 (2013).

205. Westwood, M., Gibson, J. M., Davies, A. J., Young, R. J. & White, A. The phosphorylation pattern of insulin-like growth factor-binding protein-1 in normal plasma is different from that in amniotic fluid and changes during pregnancy. *J. Clin. Endocrinol. Metab.* **79**, 1735–1741 (1994).

206. Iwashita, M., Sakai, K., Kudo, Y. & Takeda, Y. Phosphoisoforms of insulin-like growth factor binding protein-1 in appropriate-for-gestational-age and small-for-gestational-age fetuses. *Growth Horm. IGF Res. Off. J. Growth Horm. Res. Soc. Int. IGF Res. Soc.* **8**, 487–493 (1998).

207. Gibson, J. M. *et al.* Phosphorylated insulin-like growth factor binding protein 1 is increased in pregnant diabetic subjects. *Diabetes* **48**, 321–326 (1999).

208. Fowler, D. J., Nicolaides, K. H. & Miell, J. P. Insulin-like growth factor binding protein-1 (IGFBP-1): a multifunctional role in the human female reproductive tract. *Hum. Reprod. Update* **6**, 495–504 (2000).

209. Bhatia, S. *et al.* A longitudinal analysis of maternal serum insulin-like growth factor I (IGF-I) and total and nonphosphorylated IGF-binding protein-1 in human pregnancies complicated by intrauterine growth restriction. *J. Clin. Endocrinol. Metab.* **87**, 1864–1870 (2002).

210. Abu Shehab, M., Inoue, S., Han, V. K. M. & Gupta, M. B. Site specific phosphorylation of insulin-like growth factor binding protein-1 (IGFBP-1) for evaluating clinical relevancy in fetal growth restriction. *J. Proteome Res.* **8**, 5325–5335 (2009).

211. Nissum, M. *et al.* Functional and Complementary Phosphorylation State Attributes of Human Insulin-like Growth Factor-Binding Protein-1 (IGFBP-1) Isoforms

Resolved by Free Flow Electrophoresis. *Mol. Cell. Proteomics MCP* **8**, 1424–1435 (2009).

212. Singal, S. S. *et al.* Co-Localization of Insulin-Like Growth Factor Binding Protein-1, Casein Kinase-2β, and Mechanistic Target of Rapamycin in Human Hepatocellular Carcinoma Cells as Demonstrated by Dual Immunofluorescence and in Situ Proximity Ligation Assay. *Am. J. Pathol.* **188**, 111–124 (2018).
213. Litchfield, D. W. Protein kinase CK2: structure, regulation and role in cellular decisions of life and death. *Biochem. J.* **369**, 1–15 (2003).
214. Frost, R. A. & Tseng, L. Insulin-like growth factor-binding protein-1 is phosphorylated by cultured human endometrial stromal cells and multiple protein kinases in vitro. *J. Biol. Chem.* **266**, 18082–18088 (1991).
215. Ankrapp, D. P., Jones, J. I. & Clemmons, D. R. Characterization of insulin-like growth factor binding protein-1 kinases from human hepatoma cells. *J. Cell. Biochem.* **60**, 387–399 (1996).
216. Bingham, E. W. & Farrell, H. M. Casein Kinase from the Golgi Apparatus of Lactating Mammary Gland. *J. Biol. Chem.* **249**, 3647–3651 (1974).
217. Venerando, A., Ruzzene, M. & Pinna, L. A. Casein kinase: the triple meaning of a misnomer. *Biochem. J.* **460**, 141–156 (2014).
218. Tagliabracci, V. S. *et al.* A Single Kinase Generates the Majority of the Secreted Phosphoproteome. *Cell* **161**, 1619–1632 (2015).
219. Tang, M., Mazella, J., Zhu, H. H. & Tseng, L. Ligand activated relaxin receptor increases the transcription of IGFBP-1 and prolactin in human decidual and endometrial stromal cells. *Mol. Hum. Reprod.* **11**, 237–243 (2005).

220. Gong, Y. *et al.* Phorbol esters differentially regulate the expression of insulin-like growth factor-binding proteins in endometrial carcinoma cells. *Endocrinology* **131**, 2747–2754 (1992).

221. Lee, P. D., Abdel-Maguid, L. S. & Snuggs, M. B. Role of protein kinase-C in regulation of insulin-like growth factor-binding protein-1 production by HepG2 cells. *J. Clin. Endocrinol. Metab.* **75**, 459–464 (1992).

222. Meggio, F., Marin, O. & Pinna, L. A. Substrate specificity of protein kinase CK2. *Cell. Mol. Biol. Res.* **40**, 401–409 (1994).

223. St-Denis, N. *et al.* Systematic investigation of hierarchical phosphorylation by protein kinase CK2. *J. Proteomics* **118**, 49–62 (2015).

224. Meggio, F. & Pinna, L. A. One-thousand-and-one substrates of protein kinase CK2? *FASEB J. Off. Publ. Fed. Am. Soc. Exp. Biol.* **17**, 349–368 (2003).

225. Inoue, M., Kishimoto, A., Takai, Y. & Nishizuka, Y. Guanosine 3':5'-monophosphate-dependent protein kinase from silkworm, properties of a catalytic fragment obtained by limited proteolysis. *J. Biol. Chem.* **251**, 4476–4478 (1976).

226. Walsh, D. A., Perkins, J. P. & Krebs, E. G. An adenosine 3',5'-monophosphate-dependant protein kinase from rabbit skeletal muscle. *J. Biol. Chem.* **243**, 3763–3765 (1968).

227. Inoue, M., Kishimoto, A., Takai, Y. & Nishizuka, Y. Studies on a cyclic nucleotide-independent protein kinase and its proenzyme in mammalian tissues. II. Proenzyme and its activation by calcium-dependent protease from rat brain. *J. Biol. Chem.* **252**, 7610–7616 (1977).

228. Takai, Y., Kishimoto, A., Inoue, M. & Nishizuka, Y. Studies on a cyclic nucleotide-independent protein kinase and its proenzyme in mammalian tissues. I. Purification and characterization of an active enzyme from bovine cerebellum. *J. Biol. Chem.* **252**, 7603–7609 (1977).

229. Takai, Y. *et al.* Calcium-dependent activation of a multifunctional protein kinase by membrane phospholipids. *J. Biol. Chem.* **254**, 3692–3695 (1979).

230. Castagna, M. *et al.* Direct activation of calcium-activated, phospholipid-dependent protein kinase by tumor-promoting phorbol esters. *J. Biol. Chem.* **257**, 7847–7851 (1982).

231. Dempsey, E. C. *et al.* Protein kinase C isozymes and the regulation of diverse cell responses. *Am. J. Physiol. Lung Cell. Mol. Physiol.* **279**, L429-438 (2000).

232. Newton, A. C. Protein kinase C: structure, function, and regulation. *J. Biol. Chem.* **270**, 28495–28498 (1995).

233. Newton, A. C. Protein Kinase C: Perfectly Balanced. *Crit. Rev. Biochem. Mol. Biol.* **53**, 208–230 (2018).

234. Newton, A. C. Protein kinase C: poised to signal. *Am. J. Physiol. Endocrinol. Metab.* **298**, E395-402 (2010).

235. Steinberg, S. F. Structural Basis of Protein Kinase C Isoform Function. *Physiol. Rev.* **88**, 1341–1378 (2008).

236. Zidovetzki, R. & Lester, D. S. The mechanism of activation of protein kinase C: a biophysical perspective. *Biochim. Biophys. Acta* **1134**, 261–272 (1992).

237. Lester, D. S., Doll, L., Brumfeld, V. & Miller, I. R. Lipid dependence of surface conformations of protein kinase C. *Biochim. Biophys. Acta* **1039**, 33–41 (1990).

238. Webb, B. L. J., Hirst, S. J. & Giembycz, M. A. Protein kinase C isoenzymes: a review of their structure, regulation and role in regulating airways smooth muscle tone and mitogenesis. *Br. J. Pharmacol.* **130**, 1433–1452 (2000).

239. Sugden, M. C. & Langdown, M. L. Possible involvement of PKC isoforms in signalling placental apoptosis in intrauterine growth retardation. *Mol. Cell. Endocrinol.* **185**, 119–126 (2001).

240. Langdown, M. L., Holness, M. J. & Sugden, M. C. Early growth retardation induced by excessive exposure to glucocorticoids in utero selectively increases cardiac GLUT1 protein expression and Akt/protein kinase B activity in adulthood. *J. Endocrinol.* **169**, 11–22 (2001).

241. Vary, T. C., Goodman, S., Kilpatrick, L. E. & Lynch, C. J. Nutrient regulation of PKCepsilon is mediated by leucine, not insulin, in skeletal muscle. *Am. J. Physiol. Endocrinol. Metab.* **289**, E684-694 (2005).

242. Lee, M. Y., Jo, S. D., Lee, J. H. & Han, H. J. L-leucine increases [3H]-thymidine incorporation in chicken hepatocytes: involvement of the PKC, PI3K/Akt, ERK1/2, and mTOR signaling pathways. *J. Cell. Biochem.* **105**, 1410–1419 (2008).

243. Ignácio-Souza, L. M. *et al.* Protein restriction in early life is associated with changes in insulin sensitivity and pancreatic β-cell function during pregnancy. *Br. J. Nutr.* **109**, 236–247 (2013).

244. Lippo, B. R. da S. *et al.* Low-protein diet disrupts the crosstalk between the PKA and PKC signaling pathways in isolated pancreatic islets. *J. Nutr. Biochem.* **26**, 556–562 (2015).

245. Raveh-Amit, H. *et al.* Translational Control of Protein Kinase Cη by Two Upstream Open Reading Frames. *Mol. Cell. Biol.* **29**, 6140–6148 (2009).

246. Gan, X. *et al.* PRR5L degradation promotes mTORC2-mediated PKC-δ phosphorylation and cell migration downstream of Gα 12. *Nat. Cell Biol.* **14**, 686–696 (2012).

247. Thomanetz, V. *et al.* Ablation of the mTORC2 component rictor in brain or Purkinje cells affects size and neuron morphology. *J. Cell Biol.* **201**, 293–308 (2013).

248. Li, X. & Gao, T. mTORC2 phosphorylates protein kinase Cζ to regulate its stability and activity. *EMBO Rep.* **15**, 191–198 (2014).

249. Casanello, P. *et al.* Reduced l-Arginine Transport and Nitric Oxide Synthesis in Human Umbilical Vein Endothelial Cells from Intrauterine Growth Restriction Pregnancies is Not Further Altered by Hypoxia. *Placenta* **30**, 625–633 (2009).

250. Mehta, N. K. & Mehta, K. D. Protein kinase C-beta: An emerging connection between nutrient excess and obesity. *Biochim. Biophys. Acta-Mol. Cell Biol. Lipids* **1841**, 1491–1497 (2014).

251. Xie, Y. *et al.* The mTORC2/PKC pathway sustains compensatory insulin secretion of pancreatic beta cells in response to metabolic stress. *Biochim. Biophys. Acta-Gen. Subj.* **1861**, 2039–2047 (2017).

252. Torelli Hijo, A. H. *et al.* High fat diet modulates the protein content of nutrient transporters in the small intestine of mice: possible involvement of PKA and PKC activity. *Heliyon* **5**, e02611 (2019).

253. Wilkening, S., Stahl, F. & Bader, A. Comparison of primary human hepatocytes and hepatoma cell line Hepg2 with regard to their biotransformation properties. *Drug Metab. Dispos. Biol. Fate Chem.* **31**, 1035–1042 (2003).

254. Hart, S. N. *et al.* A Comparison of Whole Genome Gene Expression Profiles of HepaRG Cells and HepG2 Cells to Primary Human Hepatocytes and Human Liver Tissues. *Drug Metab. Dispos.* **38**, 988–994 (2010).

255. Li, F., Yin, Y., Tan, B., Kong, X. & Wu, G. Leucine nutrition in animals and humans: mTOR signaling and beyond. *Amino Acids* **41**, 1185–1193 (2011).

256. Lynch, C. J., Hutson, S. M., Patson, B. J., Vaval, A. & Vary, T. C. Tissue-specific effects of chronic dietary leucine and norleucine supplementation on protein synthesis in rats. *Am. J. Physiol. Endocrinol. Metab.* **283**, E824-835 (2002).

257. Armitage, J. A., Khan, I. Y., Taylor, P. D., Nathanielsz, P. W. & Poston, L. Developmental programming of the metabolic syndrome by maternal nutritional imbalance: how strong is the evidence from experimental models in mammals? *J. Physiol.* **561**, 355–377 (2004).

258. Soares, M. J., Varberg, K. M. & Iqbal, K. Hemochorial placentation: development, function, and adaptations. *Biol. Reprod.* **99**, 196–211 (2018).

259. Li, C. *et al.* The IGF axis in baboon pregnancy: placental and systemic responses to feeding 70% global ad libitum diet. *Placenta* **28**, 1200–1210 (2007).

260. Li, C. *et al.* Effects of Maternal Nutrient Restriction, IUGR, and Glucocorticoid Exposure on Phosphoenolpyruvate Carboxykinase-1 Expression in Fetal Baboon Hepatocytes In Vitro. *J. Med. Primatol.* **42**, 211–219 (2013).

261. Abu Shehab, M., Iosef, C., Wildgruber, R., Sardana, G. & Gupta, M. B. Phosphorylation of IGFBP-1 at discrete sites elicits variable effects on IGF-I receptor autophosphorylation. *Endocrinology* **154**, 1130–1143 (2013).

262. Mruk, D. D. & Cheng, C. Y. Enhanced chemiluminescence (ECL) for routine immunoblotting. *Spermatogenesis* **1**, 121–122 (2011).

263. Schlabritz-Loutsevitch, N. E. *et al.* Development of a system for individual feeding of baboons maintained in an outdoor group social environment. *J. Med. Primatol.* **33**, 117–126 (2004).

264. Webb, B. L. J., Hirst, S. J. & Giembycz, M. A. Protein kinase C isoenzymes: a review of their structure, regulation and role in regulating airways smooth muscle tone and mitogenesis. *Br. J. Pharmacol.* **130**, 1433–1452 (2000).

265. Ong, K. *et al.* Size at birth and cord blood levels of insulin, insulin-like growth factor I (IGF-I), IGF-II, IGF-binding protein-1 (IGFBP-1), IGFBP-3, and the soluble IGF-II/mannose-6-phosphate receptor in term human infants. The ALSPAC Study Team. Avon Longitudinal Study of Pregnancy and Childhood. *J. Clin. Endocrinol. Metab.* **85**, 4266–4269 (2000).

266. Kimball, S. R. & Jefferson, L. S. Signaling pathways and molecular mechanisms through which branched-chain amino acids mediate translational control of protein synthesis. *J. Nutr.* **136**, 227S–31S (2006).

267. Fulks, R. M., Li, J. B. & Goldberg, A. L. Effects of insulin, glucose, and amino acids on protein turnover in rat diaphragm. *J. Biol. Chem.* **250**, 290–298 (1975).

268. Buse, M. G. & Reid, S. S. Leucine. A possible regulator of protein turnover in muscle. *J. Clin. Invest.* **56**, 1250–1261 (1975).

269. Lynch, C. J. *et al.* Leucine is a direct-acting nutrient signal that regulates protein synthesis in adipose tissue. *Am. J. Physiol. Endocrinol. Metab.* **283**, E503-513 (2002).

270. Reiter, A. K., Anthony, T. G., Anthony, J. C., Jefferson, L. S. & Kimball, S. R. The mTOR signaling pathway mediates control of ribosomal protein mRNA translation in rat liver. *Int. J. Biochem. Cell Biol.* **36**, 2169–2179 (2004).

271. Martín-Estal, I., de la Garza, R. G. & Castilla-Cortázar, I. Intrauterine Growth Retardation (IUGR) as a Novel Condition of Insulin-Like Growth Factor-1 (IGF-1) Deficiency. *Rev. Physiol. Biochem. Pharmacol.* **170**, 1–35 (2016).

272. Shehab, M. A. *et al.* Exposure of decidualized HIESC to low oxygen tension and leucine deprivation results in increased IGFBP-1 phosphorylation and reduced IGF-I bioactivity. *Mol. Cell. Endocrinol.* **452**, 1–14 (2017).

273. Malkani, N., Jansson, T. & Gupta, M. B. IGFBP-1 hyperphosphorylation in response to leucine deprivation is mediated by the AAR pathway. *Mol. Cell. Endocrinol.* **412**, 182–195 (2015).

274. Regnault, T. R. H. *et al.* Umbilical uptakes and transplacental concentration ratios of amino acids in severe fetal growth restriction. *Pediatr. Res.* **73**, 602–611 (2013).

275. Hinnebusch, A. G. Translational regulation of yeast GCN4. A window on factors that control initiator-trna binding to the ribosome. *J. Biol. Chem.* **272**, 21661–21664 (1997).

276. Dong, J., Qiu, H., Garcia-Barrio, M., Anderson, J. & Hinnebusch, A. G. Uncharged tRNA activates GCN2 by displacing the protein kinase moiety from a bipartite tRNA-binding domain. *Mol. Cell* **6**, 269–279 (2000).

277. Deng, J. *et al.* Activation of GCN2 in UV-irradiated cells inhibits translation. *Curr. Biol. CB* **12**, 1279–1286 (2002).

278. Thiaville, M. M. *et al.* MEK Signaling Is Required for Phosphorylation of eIF2α following Amino Acid Limitation of HepG2 Human Hepatoma Cells. *J. Biol. Chem.* **283**, 10848–10857 (2008).

279. Straus, D. S., Burke, E. J. & Marten, N. W. Induction of insulin-like growth factor binding protein-1 gene expression in liver of protein-restricted rats and in rat hepatoma cells limited for a single amino acid. *Endocrinology* **132**, 1090–1100 (1993).

280. Mounier, C., Dumas, V. & Posner, B. I. Regulation of Hepatic Insulin-Like Growth Factor-Binding Protein-1 Gene Expression by Insulin: Central Role for Mammalian Target of Rapamycin Independent of Forkhead Box O Proteins. *Endocrinology* **147**, 2383–2391 (2006).

281. Lee, Y.-H., Park, J.-W. & Bae, Y.-S. Regulation of protein kinase CK2 catalytic activity by protein kinase C and phospholipase D2. *Biochimie* **121**, 131–139 (2016).

282. Jaken, S. Protein kinase C isozymes and substrates. *Curr. Opin. Cell Biol.* **8**, 168–173 (1996).

283. Montenarh, M. & Götz, C. Ecto-protein kinase CK2, the neglected form of CK2. *Biomed. Rep.* **8**, 307–313 (2018).

284. Ishikawa, H. O., Xu, A., Ogura, E., Manning, G. & Irvine, K. D. The Raine Syndrome Protein FAM20C Is a Golgi Kinase That Phosphorylates Bio-Mineralization Proteins. *PLoS ONE* **7**, e42988 (2012).

285. Zhang, H. *et al.* Structure and evolution of the Fam20 kinases. *Nat. Commun.* **9**, 1218 (2018).

286. Liu, W. S. & Heckman, C. A. The sevenfold way of PKC regulation. *Cell. Signal.* **10**, 529–542 (1998).

287. Ng, T. *et al.* Imaging protein kinase Calpha activation in cells. *Science* **283**, 2085–2089 (1999).

288. Luria, A., Tennenbaum, T., Sun, Q. Y., Rubinstein, S. & Breitbart, H. Differential localization of conventional protein kinase C isoforms during mouse oocyte development. *Biol. Reprod.* **62**, 1564–1570 (2000).

289. Hui, X., Kaestner, L. & Lipp, P. Differential targeting of cPKC and nPKC decodes and regulates Ca2+ and lipid signalling. *Biochem. Soc. Trans.* **42**, 1538–1542 (2014).

290. Freeley, M., Kelleher, D. & Long, A. Regulation of Protein Kinase C function by phosphorylation on conserved and non-conserved sites. *Cell. Signal.* **23**, 753–762 (2011).

291. Dodd, K. M. & Tee, A. R. Leucine and mTORC1: a complex relationship. *Am. J. Physiol.-Endocrinol. Metab.* **302**, E1329–E1342 (2012).

292. Mazor, K. M. *et al.* Effects of single amino acid deficiency on mRNA translation are markedly different for methionine versus leucine. *Sci. Rep.* **8**, 8076 (2018).

293. Fan, Q.-W. *et al.* EGFR Signals to mTOR Through PKC and Independently of Akt in Glioma. *Sci. Signal.* **2**, ra4 (2009).

294. Moschella, P. C., Rao, V. U., McDermott, P. J. & Kuppuswamy, D. Regulation of mTOR and S6K1 activation by the nPKC isoforms, PKC epsilon and PKC epsilon in adult cardiac muscle cells. *J. Mol. Cell. Cardiol.* **43**, 754–766 (2007).

295. Liu, M. *et al.* Co-ordinated activation of classical and novel PKC isoforms is required for PMA-induced mTORC1 activation. *PLoS ONE* **12**, (2017).

296. Kilberg, M. S., Shan, J. & Su, N. ATF4-dependent transcription mediates signaling of amino acid limitation. *Trends Endocrinol. Metab. TEM* **20**, 436–443 (2009).

297. Kilberg, M. S., Pan, Y.-X., Chen, H. & Leung-Pineda, V. Nutritional control of gene expression: how mammalian cells respond to amino acid limitation. *Annu. Rev. Nutr.* **25**, 59–85 (2005).

298. Abu Shehab, M. *et al.* Inhibition of decidual IGF-1 signaling in response to hypoxia and leucine deprivation is mediated by mTOR and AAR pathways and increased IGFBP-1 phosphorylation. *Mol. Cell. Endocrinol.* **512**, 110865 (2020).

299. Schaeffer, H. J. & Weber, M. J. Mitogen-Activated Protein Kinases: Specific Messages from Ubiquitous Messengers. *Mol. Cell. Biol.* **19**, 2435–2444 (1999).

300. Abraham, D. *et al.* Raf-1-associated protein phosphatase 2A as a positive regulator of kinase activation. *J. Biol. Chem.* **275**, 22300–22304 (2000).

301. Pattingre, S., Bauvy, C. & Codogno, P. Amino acids interfere with the ERK1/2-dependent control of macroautophagy by controlling the activation of Raf-1 in human colon cancer HT-29 cells. *J. Biol. Chem.* **278**, 16667–16674 (2003).

302. Schönwasser, D. C., Marais, R. M., Marshall, C. J. & Parker, P. J. Activation of the Mitogen-Activated Protein Kinase/Extracellular Signal-Regulated Kinase Pathway

by Conventional, Novel, and Atypical Protein Kinase C Isotypes. *Mol. Cell. Biol.* **18**, 790–798 (1998).

303. Kolch, W. *et al.* Protein kinase C alpha activates RAF-1 by direct phosphorylation. *Nature* **364**, 249–252 (1993).
304. Corbit, K. C. *et al.* Activation of Raf-1 Signaling by Protein Kinase C through a Mechanism Involving Raf Kinase Inhibitory Protein. *J. Biol. Chem.* **278**, 13061–13068 (2003).
305. Wen-Sheng, W. Protein kinase C alpha trigger Ras and Raf-independent MEK/ERK activation for TPA-induced growth inhibition of human hepatoma cell HepG2. *Cancer Lett.* **239**, 27–35 (2006).
306. Wen-Sheng, W. & Jun-Ming, H. Activation of protein kinase C alpha is required for TPA-triggered ERK (MAPK) signaling and growth inhibition of human hepatoma cell HepG2. *J. Biomed. Sci.* **12**, 289–296 (2005).
307. Lee, Y.-H., Park, J.-W. & Bae, Y.-S. Regulation of protein kinase CK2 catalytic activity by protein kinase C and phospholipase D2. *Biochimie* **121**, 131–139 (2016).
308. Schönwasser, D. C., Marais, R. M., Marshall, C. J. & Parker, P. J. Activation of the mitogen-activated protein kinase/extracellular signal-regulated kinase pathway by conventional, novel, and atypical protein kinase C isotypes. *Mol. Cell. Biol.* **18**, 790–798 (1998).

Appendix A

A

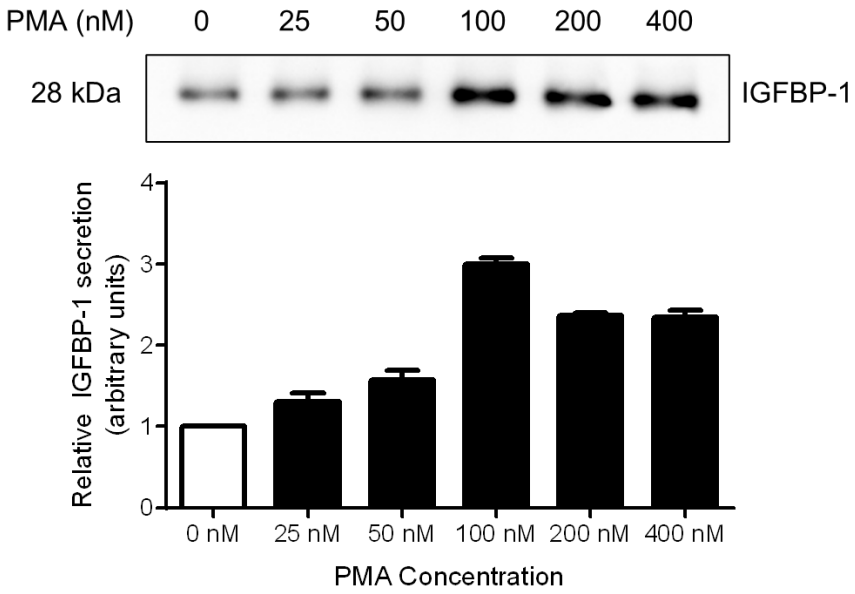

B

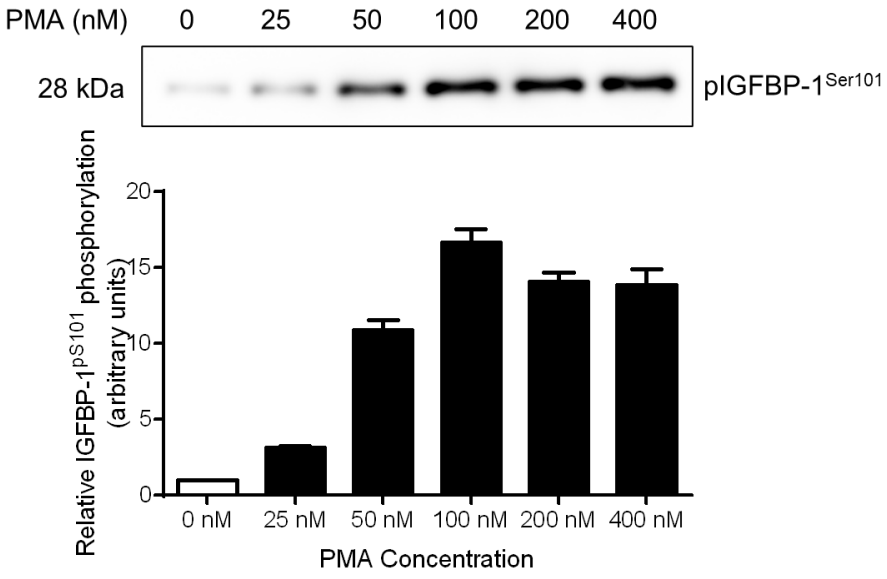

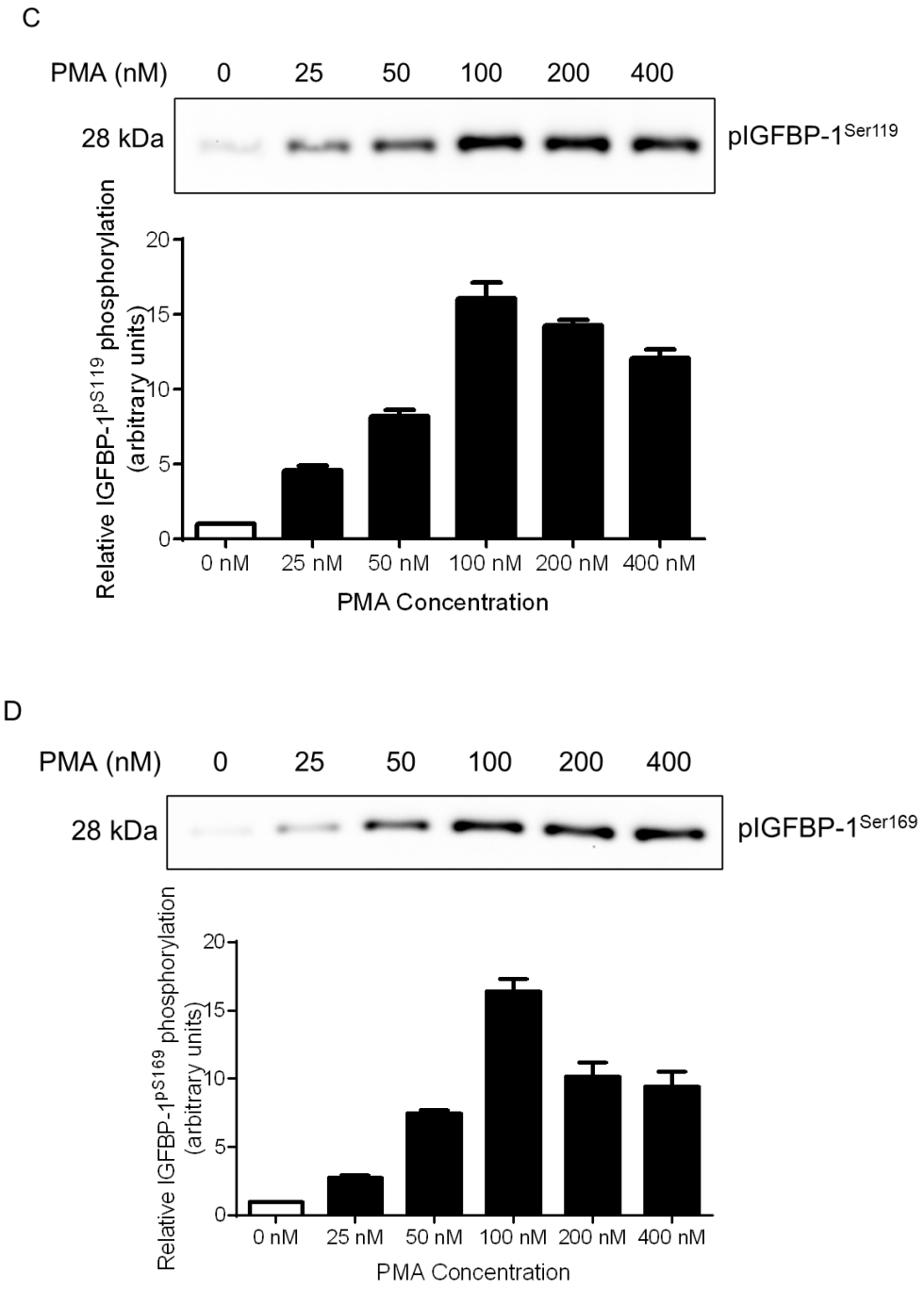

Figure A 1. The effect of increasing PMA concentration on IGFBP-1 secretion and phosphorylation. HepG2 cells were treated with increasing doses of PMA (0–400 nM) to determine optimal PMA concentrations for total IGFBP-1 secretion and IGFBP-1 phosphorylation. Representative western blots of conditioned HepG2 CM indicating (A)

total IGFBP-1 and IGFBP-1 phosphorylation at (B) Ser101, (C) Ser119 and (D) Ser169. Values are displayed as mean + SEM.

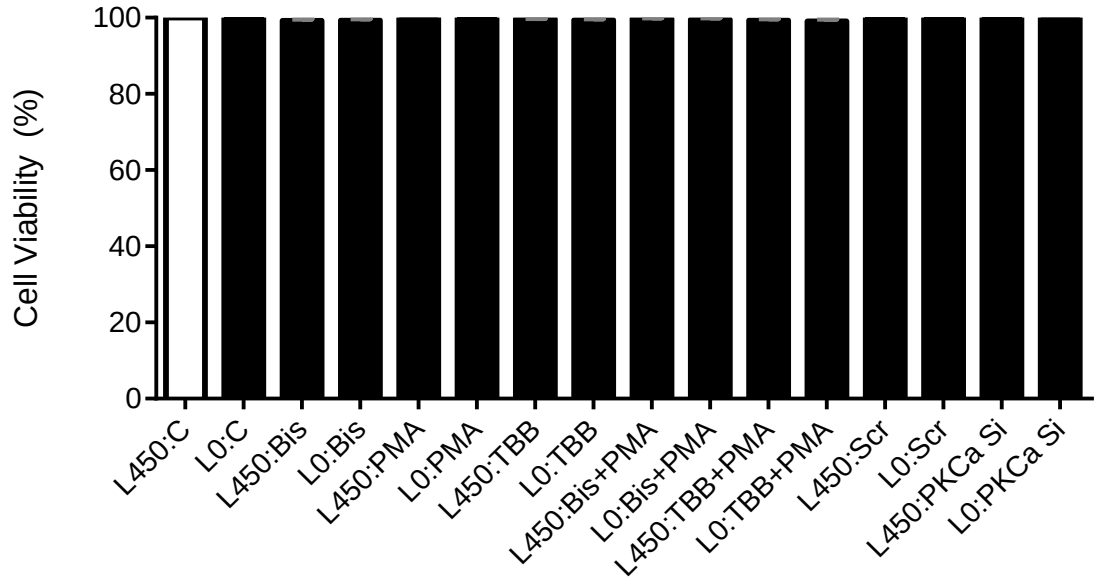

Figure A 2. Cell viability assay for all cell treatments. HepG2 cell viability after 24 hours of treatments with L0, Bis, PMA, TBB, scrambled siRNA and PKCα siRNA as determined by trypan blue exclusion assay. Cell viability was determined as percentage of measured live/total cells. All treatments demonstrated nearly identical cell viability. Values are displayed as mean + SEM. *p< 0.05, **p= 0.001-0.05, ***p < 0.0001 versus control; One-way analysis of variance; Dunnet's Multiple Comparison Test; n=10.

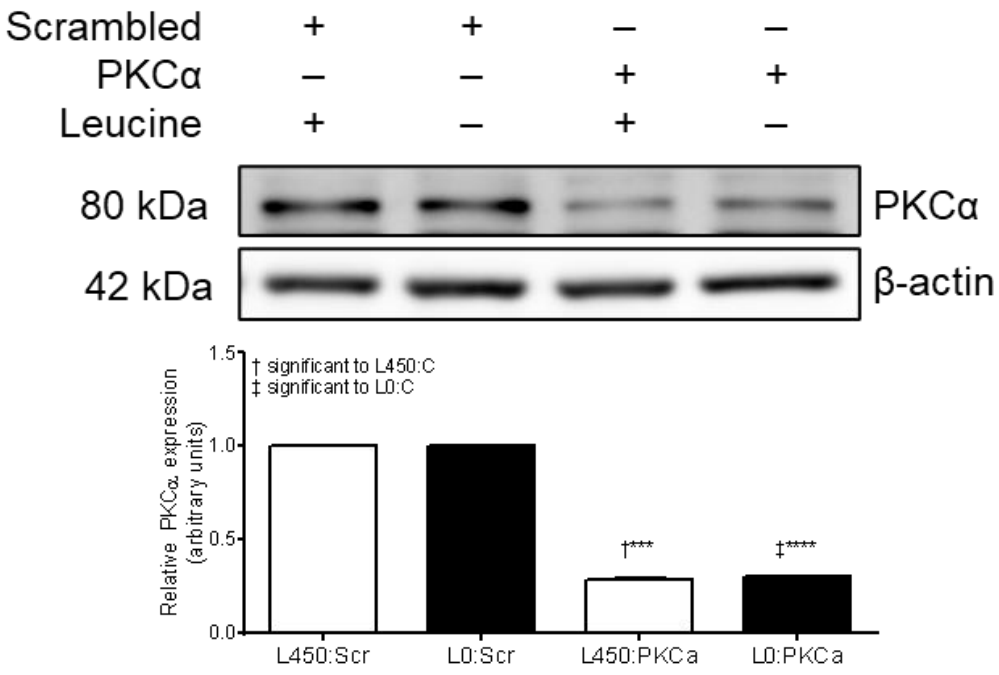

Figure A 3. PKCα silencing efficiency. Representative immunoblots of siRNA-mediated silencing efficiency for PKCα in HepG2 cells. Cells were transfected with 80 nM PRKCA siRNA for 24 hours in serum-free media, followed by L450 or L0 treatment for an additional 48 hours. Values are displayed as mean + SEM. *p< 0.05, **p= 0.001-0.05, ***p < 0.0001 versus control; One-way analysis of variance; Dunnet's Multiple Comparison Test; n=3.

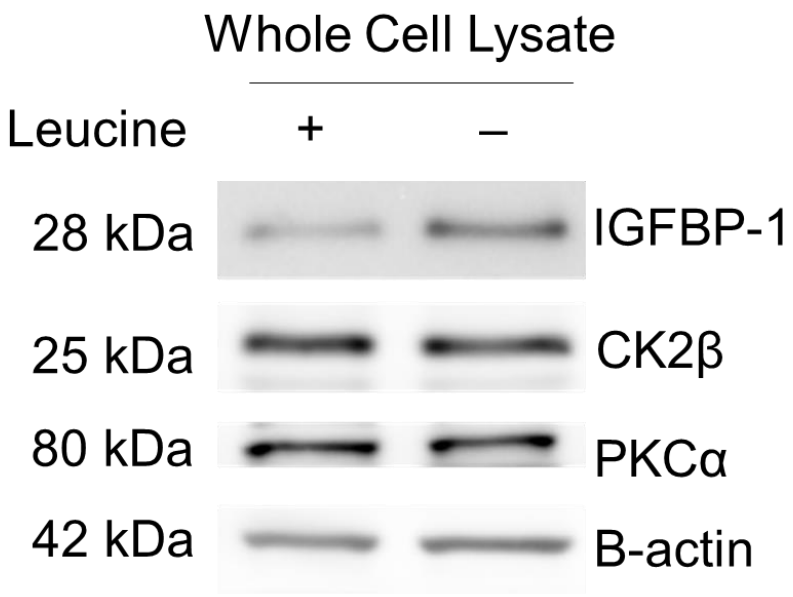

Figure A 4. Effect of leucine deprivation on IGFBP-1, CK2β and PKCα expression. Immunoblots for IGFBP-1, CK2β and PKCα in HepG2 cells cultured with and without leucine**.**

Curriculum Vitae

Name: Allan W. Chen

Post-secondary Education and Degrees:
University of Western Ontario
London, Ontario, Canada
2014-2018 BSc.

Honours and Awards:
Department of Paediatrics Graduate Studentship
2018-2019

Children's Health Research Institute (CHRI) Trainee Award
2019-2020

Children's Health Research Institution (CHRI) Travel Award
2019

Department of Paediatrics Travel Award
2019

Publications:
Chen, A.W., Biggar, K., Nygard, K., Singal, S.S., Zhao, T., Li, C., Nathanielsz, P.W., Jansson, T., Gupta M.B., (2021) IGFBP-1 hyperphosphorylation in response to nutrient deprivation is mediated by activation of protein kinase Cα (PKCα). *Mol Cell Endo*, 536, 111400. https://doi.org/10.1016/j.mce.2021.111400.

Kakadia, J., Biggar, K., Jain, B., **Chen, A.W.**, Nygard, K., Li, C., Nathanielsz, P.W., Jansson, .T, Gupta, M.B., Mechanisms linking hypoxia to phosphorylation of insulin-like growth factor binding protein-1 in baboon fetuses with intrauterine growth restriction and in cell culture. *FASEB J*. 2021 Sep;35(9):e21788. doi: 10.1096/fj.202100397R. PMID: 34425031.

Chen, A. W., Jayasinghe, M. I., Chung, C. Z., Rao, B. S., Kenana, R., Heinemann, I. U., and Jackman, J. E. (2019) The role of 3' to 5' reverse RNA polymerization in tRNA fidelity and repair. *Genes*. *10*(3), 250; https://doi.org/10.3390/genes10030250

Desai, R., Kim, K., Büchsenschütz, H. C., **Chen, A. W.,** Bi, Y., Mann, M. R., Turk, M. A., Chung, C. Z., and Heinemann, I. U. (2017) Minimal requirements for reverse polymerization and tRNA repair by $tRNA^{His}$ guanylyltransferase. *RNA Biol*. 10.1080/15476286.2017.1372076